AD-A155 042 FRICTION AND WEAR OF SOLID-LUBRICATED CONTACT IN GAS TURBINE ENGINE BEARINGS(U) MECHANICAL TECHNOLOGY INC LATHAM N Y S GRAY ET AL. NOV 84 MTI-84TR72 1/2

UNCLASSIFIED AFWAL-TR-84-4143 F33615-83-C-5037 F/G 11/8 NL

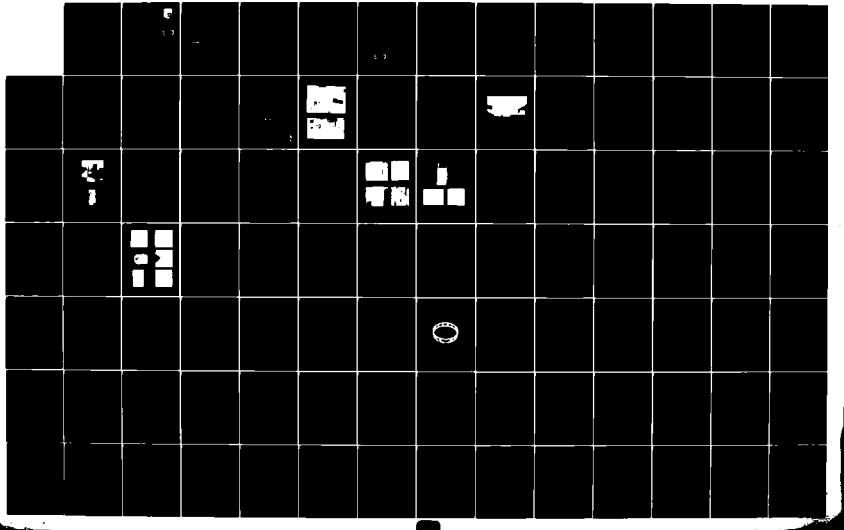

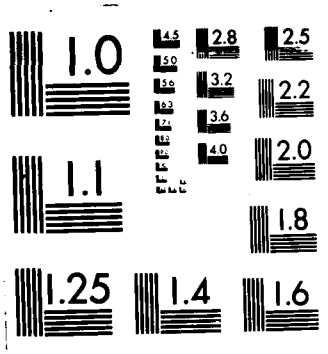

AFWAL-TR-84-4143

FRICTION AND WEAR OF SOLID-LUBRICATED CONTACT IN GAS TURBINE ENGINE BEARINGS

Stanley Gray
Pradeep K. Gupta *(Consultant)*
Mechanical Technology Incorporated
968 Albany-Shaker Road
Latham, New York 12110

November 1984

Final Report for Period April 1983 - September 1984

Approved for Public Release; Distribution Unlimited

MATERIALS LABORATORY
AIR FORCE WRIGHT AERONAUTICAL LABORATORIES
AIR FORCE SYSTEM COMMAND
UNITED STATES AIR FORCE
WRIGHT-PATTERSON AIR FORCE BASE, OHIO 45433

NOTICE

When Government drawings, specifications, or other data are used for any purpose other than in connection with a definitely related Government procurement operation, the United States Government thereby incurs no responsibility nor any obligation whatsoever; and the fact that the government may have formulated, furnished, or in any way supplied the said drawings, specifications, or other data, is not to be regarded by implication or otherwise as in any manner licensing the holder or any other person or corporation, or conveying any rights or permission to manufacture use, or sell any patented invention that may in any way be related thereto.

This report has been reviewed by the Office of Public Affairs (ASD/PA) and is releasable to the National Technical Informaion Service (NTIS). At NTIS, it will be available to the general public, inluding foreign nations.

This technical report has been reviewed and is approved for publication.

Howard E Bandow

DR HOWARD BANDOW, Project Engineer

B. D. McConnell

B. D. McCONNELL, Chief
Nonstructural Materials Branch
Nonmetallic Materials Division

FOR THE COMMANDER

F. D. Cherry

F. D. CHERRY, Chief
Nonmetallic Materials Division

"If your address has changed, if you wish to be removed from our mailing list, or if the addressee is no longer employed by your organization please notify AFWAL/MLBT, W-PAFB, OH 45433 to help us maintain a current mailing list".

Copies of this report should not be returned unless return is required by security considerations, contractual obligations, or notice on a specific document.

UNCLASSIFIED

SECURITY CLASSIFICATION OF THIS PAGE (When Data Entered)

REPORT DOCUMENTATION PAGE		READ INSTRUCTIONS BEFORE COMPLETING FORM
1. REPORT NUMBER AFWAL-TR-84-4143	2. GOVT ACCESSION NO. AD-A155 042	3. RECIPIENT'S CATALOG NUMBER
4. TITLE (and Subtitle) FRICTION AND WEAR OF SOLID-LUBRICATED CONTACT IN GAS TURBINE ENGINE BEARINGS		5. TYPE OF REPORT & PERIOD COVERED Final April, 1983 - Sept. 1984
		6. PERFORMING ORG. REPORT NUMBER MTI 84TR72
7. AUTHOR(s) Stanley Gray Pradeep K. Gupta (Consultant)		8. CONTRACT OR GRANT NUMBER(s) F33615-83-C-5037
9. PERFORMING ORGANIZATION NAME AND ADDRESS Mechanical Technology Incorporated 968 Albany-Shaker Road Latham, New York 12110		10. PROGRAM ELEMENT, PROJECT, TASK AREA & WORK UNIT NUMBERS 35760004 62102F
11. CONTROLLING OFFICE NAME AND ADDRESS Air Force Wright Aeronautical Laboratories Materials Laboratory, Air Force Systems Command Wright-Patterson AFB, Ohio 45433		12. REPORT DATE November 1984 13. NUMBER OF PAGES 105
14. MONITORING AGENCY NAME & ADDRESS(if different from Controlling Office)		15. SECURITY CLASS. (of this report) UNCLASSIFIED 15a. DECLASSIFICATION/DOWNGRADING SCHEDULE

16. DISTRIBUTION STATEMENT (of this Report)

Approval for public release, distribution unlimited.

17. DISTRIBUTION STATEMENT (of the abstract entered in Block 20, if different from Report)

18. SUPPLEMENTARY NOTES

19. KEY WORDS (Continue on reverse side if necessary and identify by block number)

Rolling Element Bearings
Solid Lubricant Composites
High Temperature Ceramics
Friction and Wear
Computer Performance Analysis

20. ABSTRACT (Continue on reverse side if necessary and identify by block number)

A combined experimental materials and computer simulation study was performed for a high temperature solid lubricated ball bearing under conditions representative of a gas turbine engine. The performance predictions were compared to the experimental test behavior of complete ball bearings and showed good correlation.

continued.....

DD FORM 1 JAN 73 1473 EDITION OF 1 NOV 65 IS OBSOLETE

UNCLASSIFIED

SECURITY CLASSIFICATION OF THIS PAGE (When Data Entered)

In the pin on disc type material sliding tests, the friction and wear performance of M-50, NC-132, and alpha silicon carbide pairs with HAC-1 type lubricant composite were determined. In the first test mode --

In the first mode of testing to simulate the interactions between the cage material and other bearing elements, the pairing of HAC-1 with M-50 and NC-132 at conditions up to 30,000 rpm and 316° C ~~(600° F)~~ showed that the HAC-1 and NC-132 pair gave the lowest friction and wear and more stable temperatures.

In the second, test mode -- ~~mode of testing~~ to simulate low speed skidding which occurs between the ball and race materials, rapid wear was found and friction was high.

This test data was used to prepare traction coefficient models as input to the ADORE computer program for bearing performance simulation. The analysis predicted that due to the high traction coefficients, the interactive forces are quite large, erratic, and inducive to cage wear and breakage.

The good agreement with full scale testing of bearings demonstrated the significance of this combined material evaluation/computer modeling technique.

Keywords: Solid lubricant composites; High temperature ceramics.

A

PREFACE

This report was prepared by Mechanical Technology Incorporated, Research and Development Division, under Contract F33615-83-C-5037 and Task No. 35760004 for the Air Force Wright Aeronautical Laboratories, Wright-Patterson Air Force Base, Ohio, 45433. Dr. H. Bandow administered the program for the Air Force. The principal investigator at Mechanical Technology Incorporated was Stanley Gray; the computer modeling and analysis was performed by Dr. Pradeep K. Gupta of PKG Pradeep K. Gupta Inc., a consultant on the program.

Mechanical Technology Incorporated modified and used a company owned high temperature friction and wear tester in the experimental evaluations.

TABLE OF CONTENTS

SECTION		PAGE
I	INTRODUCTION	1
II	TECHNICAL DISCUSSION	2
	1. Program Approach	2
	2. Experimental Program	2
	A. Test Specimen Materials and Specifications	2
	B. Friction and Wear Test Apparatus and Specimen Mounting	4
	C. Test Procedures	13
	D. Experimental Results and Data Reduction	16
	3. Analytical Program	36
	A. The Test Bearing	36
	B. Traction-Slip Model	36
	C. Computer Simulation of Bearing Performance	37
	D. Comparison of Computer Predictions with Experimental Full Bearing Data	47
III	CONCLUSIONS	53
IV	RECOMMENDATIONS	55
	REFERENCES	57
	APPENDIX A - COMPUTER OUTPUT	58
	APPENDIX B - NOMENCLATURE USED IN COMPUTER OUTPUT	96

LIST OF ILLUSTRATIONS

FIGURE		PAGE
1	Schematic Overview of the Program Approach	3
2	Continuous Sliding Ball on Disc Material Tester	7
3	Overall View of Rig and Instrumentation	8
4	Close Up of Specimens in Rig	8
5	Mounting Method for Ceramic Discs on Metal Shafting	9
6	Static Ball Specimen Mounting System	9
7	Mounting Method for Static Lubricant Material Blocks (inverted view)	11
8	High Speed Data HAC-1/T50 F1 vs. M50 at Room Temperature	17
9	M-50 Disc and HAC-1/T50 F1 Specimen after 30,000 RPM Test at Room Temperature	18
10	High Speed Data HAC-1/T50 F1 vs. M-50 Disc at 204° C (400° F) Ambient	20
11	High Speed Data HAC-1A/T300 F1 vs. NC-132 at Room Temperature	21
12	Conditions of HAC-1A/T300 F1 and NC-132 Specimens after 20,000 RPM Test at Room Temperature	23
13	Refinished HAC-1A/T300 F1 after 30,000 RPM Test at Room Temperature	24
14	High Speed Tests HAC-1A/T300 F1 vs. NC-132 at 204° C (400° F) and 316° C (600° F) Ambient	25
15	Slow Speed Sliding Tests NC-132 Ball vs. M-50 Disc	28
16	Typical Friction Force Traces	30
17	Slow Speed Sliding Tests NC-132 Ball and Disc	31
18	Typical Wear Traces on Ceramic Specimens	33
19	Slow Speed Sliding Tests Alpha Silicon Carbide Ball and Disc	34
20	The Traction Model for the Ball/Cage Interface	38
21	Ball/Race Contact Load Variation	39

LIST OF ILLUSTRATIONS (CONTD)

FIGURE		PAGE
22	The Variation in Slip and Heat Generation at the Ball/Race Contact	40
23	Typical Ball/Cage Interaction	42
24	Ball/Cage Collision Forces in Pockets 1 to 3	43
25	Ball/Cage Collision Forces in Pockets 4 to 6	44
26	Typical Interaction at the Cage/Race Interface	45
27	The Variation in Cage Mass Center Whirl and Angular Velocities	46
28	Cage Mass Center Whirl Orbit	48
29	Total Power Loss in the Bearing as a Function of Time	49
30	Simulated Wear Rates of the Bearing Elements	50
31	Self-Lubricating Composite Cage After Full Bearing Testing	52

LIST OF TABLES

TABLE		PAGE
1	Typical Physical and Thermal Properties of Ball and Disc Materials	5
2	Test Instrumentation and Drive	12
3	Summary of Test Pairs and Operating Parameters	15

SUMMARY

A combined experimental materials and computer simulation study was performed for a high temperature solid lubricated ball bearing under conditions representative of a gas turbine engine. The performance predictions were compared to the experimental test behavior of complete ball bearings and showed good correlation.

In the pin on disc type material sliding tests, the friction and wear performance of M-50, NC-132 and alpha silicon carbide pairs with HAC-1 type lubricant composite were determined.

In the first mode of testing to simulate the interactions between the cage material and other bearing elements, the pairing of HAC-1 with M-50 and NC-132 at conditions up to 30,000 rpm and 316° C (600° F) showed that the HAC-1 and NC-132 pair gave the lowest friction and wear and more stable temperatures.

In the second mode of testing to simulate low speed skidding which occurs between the ball and race materials at conditions of up to 15 cm/s, high Hertzian stress, and 427° C (800° F), the static specimens showed rapid wear. Friction coefficients were high, being in the range 0.4 to 0.8 for M-50 and NC-132 pairs and higher with Alpha Silicon Carbide pairs.

This test data was used to prepare traction coefficient models as input to the ADORE[1] computer program for bearing performance simulation. The analysis predicted that due to the high traction coefficients, the interactive forces are quite large and erratic with collisions occurring between he balls and cage pockets and between the cage and race; these conditions are inducive to cage wear and breakage.

The study results showed good agreement with full scale testing of bearings of these materials and demonstrated the significance of this combined material evaluation - computer modeling approach to future bearing design and development.

SECTION I
INTRODUCTION

Rolling element bearings are being developed for advanced applications such as high performance cruise missile engines. The temperatures experienced in such applications are beyond the capability of liquid lubricants, therefore solid lubricated bearings are being evaluated for these applications. In order to develop the optimum lubricant materials, a better understanding of the relationship between the wear and friction properties of lubricant, bearing materials and bearing performance is needed.

The objectives of this effort were to study selected solid lubricant and bearing materials, and develop experiment based friction and wear models suitable for incorporation in traction models for the dynamic simulation of the performance of rolling element bearings. The results of the subsequent computer analysis could then be compared to experimental results already available from the testing of complete ball bearings. In this way the value of this combined experimental material test and analytical approach during the design work for future solid lubricated rolling element bearings could be demonstrated.

SECTION II
TECHNICAL DISCUSSION

1. Program Approach

The program approach followed in the present investigation is schematically described in Figure 1. For the selected bearing materials the fundamental friction and wear experiments were first conducted over the expected range of operating conditions, and the friction or traction behavior at the ball/race, ball/cage and cage/race interfaces in the bearing modeled. These traction models were then used as input to the bearing dynamics computer program ADORE (Advanced Dynamics of Rolling Element). The bearing performance simulations were then generated over the expected conditions of operation. The computer predictions so obtained were compared to actual bearing performance data to establish the validity of the modeling procedure and prove the overall feasibility of the development approach.

2. Experimental Programs

A. Test Specimen Materials and Specifications

Ball and Disc Materials

The three basic materials used in the study were of types considered to be suitable for high temperature rolling element bearings; discs and balls were procured from all three materials. One material was a steel and the other two ceramics. Details of the materials, their properties and configurations used in the program are detailed below:

- M-50 tool steel CEVM heat treated to R_C 63. Balls from Winsted Precision Ball Corp. to specification Grade 10.

- NC-132 hot pressed silicon nitride. Base material provided by Norton Corp. Test ball of NC-132 were provided by WPAFB from a group manufactured by SKF Industries, Inc.

taking point. A new contact position was used at the start of each temperature level test for each materials pair. In the testing of the materials pair, NC-132 vs. NC-132, particular emphasis was put on obtaining friction data in the 0 to 10 rpm range.

D. Experimental Results and Data Reduction

(1) Lubricant Block vs. Disc Experiments

- HAC-1/T50 F1 vs. M-50 Disc at Room Temperature

The results of the frictional tests performed at four speed levels, at room temperature and with increasing loads are shown plotted in Figure 8. The maximum test loading at any disc speed was limited when drive spindle speed or frictional torque became erratic or if specimen temperatures became excessive.

The data indicated that under these conditions of test the lubricant block material would not sustain as high as loading as about 3.4 MPa (500 psi) in the 5,000 - 10,000 rpm speed range, or about 0.34 MPa (50 psi) at 30,000 rpm corresponding to a maximum PV of 27.5 MPa x m/s (785,000 psi x fpm) at the higher speed and considerably higher at the lower speeds; this, of course, is not very surprising.

The friction trend showed an increase as a function of speed level from typically a coefficient of 0.3 at 5,000 rpm to 0.6 or 0.8 at 30,000 rpm and became increasingly erratic as a function of increasing speed.

The maximum temperature reached at the end of the 30,000 rpm test was 166° C (330° F) as measured on the static specimen mounting block, and examination of the disc indicated a blueing of the material. Figure 9 shows the surface condition of the disc and specimen at the end of these tests, with grid-like lines caused by the structural fibers in the lubricant material showing on the disc surface, indicating evidence of composite material transfer.

TABLE 3

SUMMARY OF TEST PAIRS AND OPERATING PARAMETERS

TEST PARAMETERS	MATERIAL TEST - PAIRS				
	M-50 Steel vs. HAC-1(1)	Silicon Nitride NC-132 vs. HAC-1(1)	M-50 Disc vs. Silicon Nitride NC-132(2)	Alpha Silicon Carbide vs. Self (2)	Silicon Nitride NC-132 vs. Self(2)
SPEED RPM	0 - 30,000	0 - 30,000	0 - 50	0 - 50	0 - 50
SPEED cm/sec.	-----	-----	0 - 13.3	0 - 13.3	0 - 13.3
AMBIENT TEMPERATURE °C	204	204, 316	204	316, 427	316, 427
AMBIENT TEMPERATURE °F	R.T., 400(3)	R.T.,400,600	R.T., 600	R.T., 600, 800	R.T., 600, 800
CONTACT STRESS MPa	0.69 to 20.7	0.69 to 20.7	690 to 1725	690 to 1725	690 to 1725
CONTACT STRESS KPSI	0.1 to 3	0.1 to 3	100 - 250 (4)	100 - 250(4)	100 - 250(4)

FOOTNOTES: (1) HAC-1/T50 F1 and HAC-1A/T300 F1.

(2) Lubricated by stick lubricant transfer.

(3) Temperature limited because of bond to metal strength of HAC materials.

(4) Initial contact stresses.

ing additional tests at other positions on a test specimen, or by refinishing the specimens. The test materials, combinations and operating conditions used in the evaluations are summarized in Table 3. The detailed test procedures used are discussed in the following paragraphs.

- Detailed Procedure - Lubricant Block against Disc

The initial evaluations were performed with the M-50 disc material, in combination with the lubricant block specimens. A series of constant speed tests with increasing unit loading was performed at room temperature ambient; test speeds were 5,000, 10,000, 20,000 and 30,000 rpm. Termination of operation at each speed level was based on smoothness of torque reading, self-generated temperature rise and wear rate. Typical test times were in the range of 4 to 8 minutes at each speed level.

The elevated temperature test procedure with the same specimens used a loading based on experience in the room temperature ambient tests, but with the temperature limited initially to a 204° C (400° F) maximum because of concern with the strength of the epoxy bond between the lubricant material and its mounting block. It was decided that the best method of testing the available specimens was to make a continuous, but slow, sweep through the speed range up to 30,000 rpm over a few minutes period and take friction and temperature data during a short dwell interval at selected speed levels.

- Detailed Test Procedure - Ball on Disc

The test procedure for the three material pairs was performed in a similar manner in the speed range of 0 to 50 rpm (13 cm/sec max.) which was representative of the sliding velocities in a ball bearing and at temperatures of R.T., 316° C (600° F) and 427° C (800° F). The 427° C test was omitted for the M-50 tool steel. All tests were provided with lubrication by transfer stick.

Tests were performed in a series of constant load levels through the speed range, following prelubrication of the disc by stick transfer for one hour. The test time was approximately one minute at each speed data

C. Test Procedures

- General

Prior to performing friction and wear tests, the disc specimen was mounted onto the spindle sleeve and checked for radial runout using a dial indicator to ensure that the runout was within 7.6 μm (0.0003") TIR or less. The spindle system was then taken up to 30,000 rpm at room temperature to check disc integrity and runout and the tightness of the tie bolt nut was rechecked. The spindle was then raised to the maximum test temperature and the above procedure repeated. The static test specimen, either a ball or a solid lubricant block, was mounted on the loader arm and the arm or the static specimen was adjusted to be at the desired contact plane on the disc rim. The contact was carefully aligned.

The ball type specimen had the inherent advantage of self-alignment but as discussed later, gave a rapid reduction in contact stress as ball wear occurred.

The torque measuring system was statically calibrated before and after tests by lifting the loader arm on a thin thread just enough to achieve contact separation from the disc and then a series of increasing loads were applied at the specimen mounting position with a precision Fisher scale. This generated a stepped calibration plot on the moving tape in the Sanborn recorder.

In order to determine wear of compliant static specimens, these were dimensionally measured using a precision micrometer before and at the end of each test and the dimensional difference calculated. The static ball specimens were measured for diameter of wear spot using an optical micrometer attachment on a microscope. This also permitted determination of final contact stress. Disc wear conditions were determined by observation or measurement with a Talysurf. Because of the limited availability of disc, ball and solid lubricant specimens, the test program was planned in the most meaningful manner and sometimes necessitated the continued usage of the same specimen pairs during a series of load or speed changes. This problem was alleviated somewhat due to the ability of perform-

TABLE 2

TEST INSTRUMENTATION AND DRIVE

Temperatures	Chromel-Alumel thermocouples. Omega Engineering Model 250 KFI Digital Readout Honeywell Electronik #111 Strip Chart Recorder
Speed	MTI Fotonic Fiber-Optic Sensor Model KD-A5. Frequency Counter HP 5381A. 80 MHZ. Textronix Oscilloscope Type 502. Stop Watch.
Friction Torque	Statham Load Cell #9016 Model G1-80-350 (± 80 Ozs.). Sanborn Model #321 Dual Channel Amplifier Recorder
Low Speed Motor -Speed Reducer and Controller	Baldor Industrial Motor Frame No. 74JKO. Cat. No. GP7402 1/8 HP. 75 in. lb., 33/1 Ratio. Boehm Controller Serial No. V-15133 SPN No. BC-115

Figure 7 Mounting Method for Static Lubricant Material Blocks (inverted view)

The two different types of static specimens required different mounting systems. The ceramic or steel balls were held on the loading arm using the system shown on Figure 6 where the elasticity of a steel spring cup held the ball into a conical collet type of seat. No difficulty was experienced due to ball movement and the ball could easily be rotationally repositioned for additional test zones. In a similar manner, the axial location of the loader arm and its support could be changed relative to the mounting plate by shims to provide up to three test band positions on the disc rim.

The solid lubricant impregnated test specimens were mounted on a simple bracket as shown on Figure 7; this bracket replacing the ball type mounting assembly on the load arm. Alignment of the compliant specimen to the disc surface was achieved by adjustment to the loader arm's universal joint on the mounting plate. Two test positions were possible on the surface of the disc rim.

To provide a lubricant transfer to the ball-disc contact, a block or stick of the solid lubricant impregnated cage materials was mounted in the carrier mechanism previously illustrated on Figure 2 and visible on Figure 4. The lubricating block was guided and dead weight loaded against the disc rim surface and could be conveniently disengaged by removing the loading weight external to the hot test environment. A load of 13 N (3 lb.) was used in all tests giving contact pressure of the order of 0.5 MPa (70 psi).

The test instrumentation used in the program is illustrated on Figure 3. This figure also shows the low speed electric motor with its speed controller coupled to the rear end of the spindle and the turbine multiple air line connections.

Details of the test instrumentation are summarized on Table 2 and consist of chromel-alumel thermocouples mounted on the static specimen spring cup or specimen block and in the furnace, with the outputs displayed on a strip chart and digital readout for temperature measurements, a fiber-optical speed readout picking up a black and white segmented target on the turbine wheel or electric motor shaft and a digital display on a frequency counter, a stop watch for setting and measuring the electric motor drive speed at the low end of the speed range; and a strain gage load cell and a strip chart recorder for frictional torque measurements.

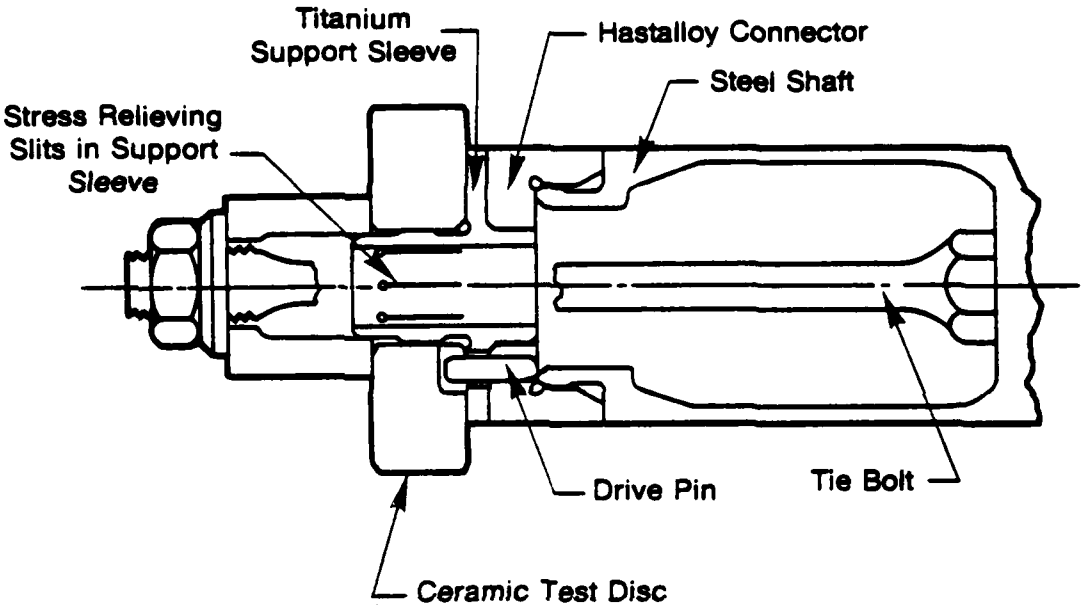

Figure 5 Mounting Method for Ceramic Discs on Metal Shafting

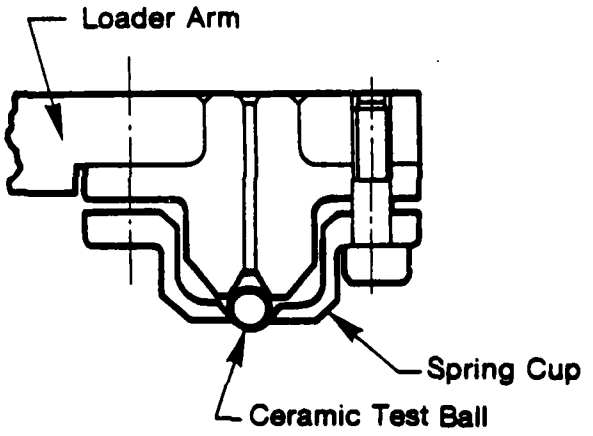

Figure 6 Static Ball Specimen Mounting System

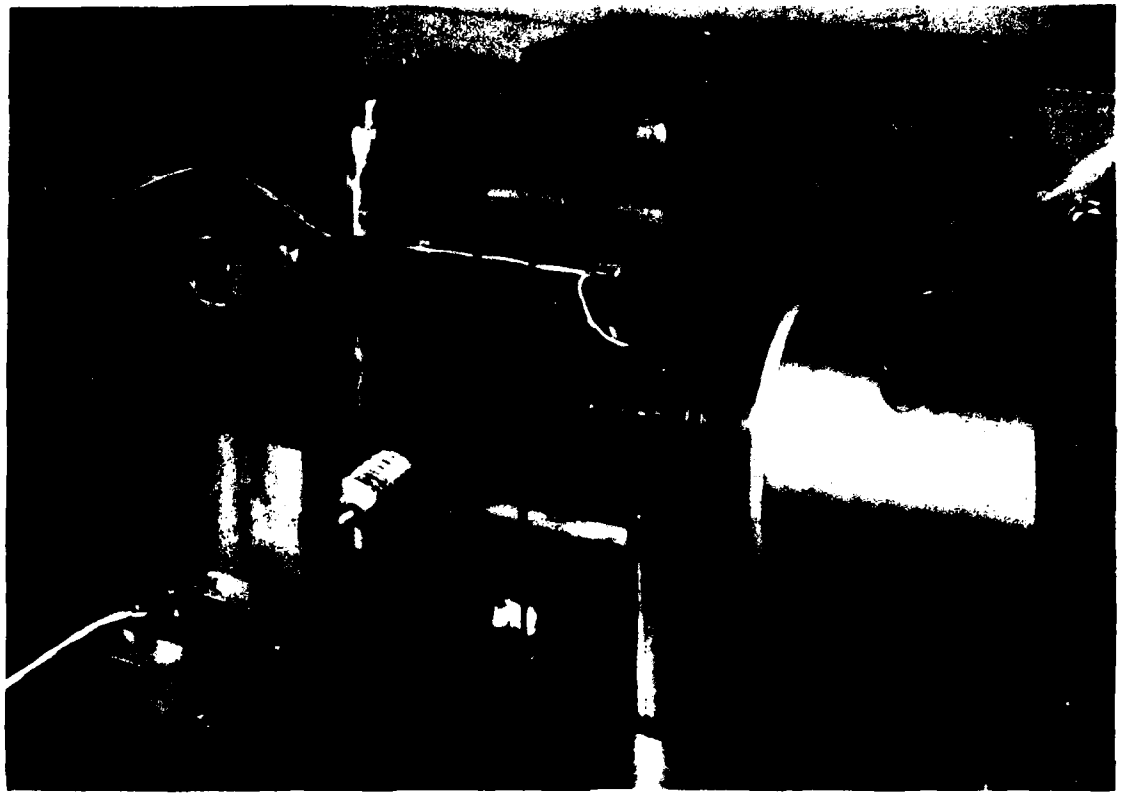

Figure 4 Close Up of Specimens in Rig

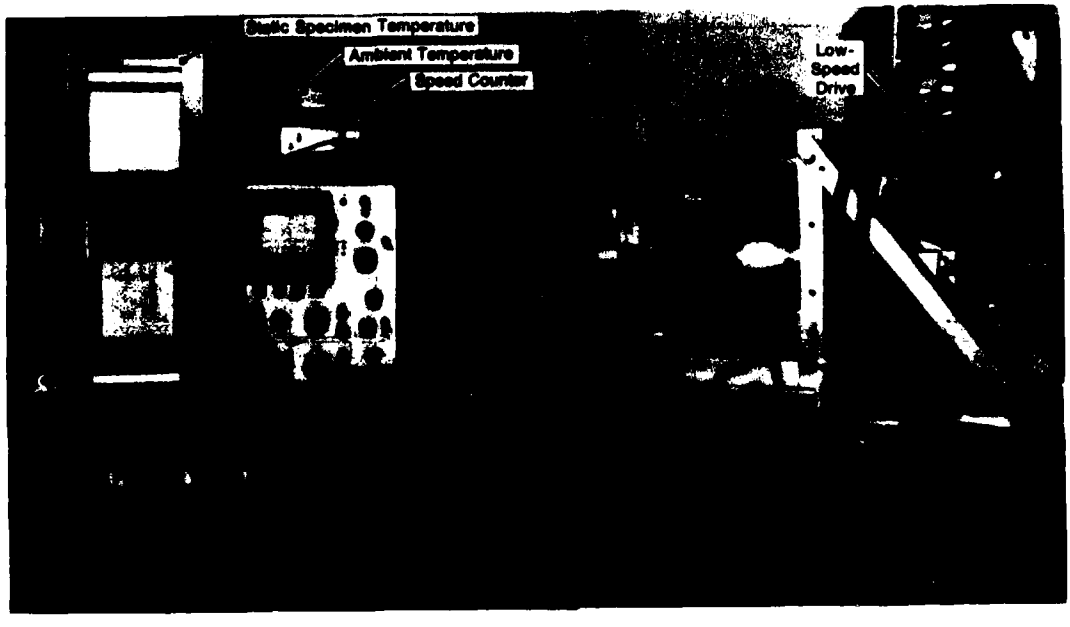

Figure 3 Overall View of Rig and Instrumentation

650°C BALL-ON-DISC FRICTION AND WEAR TESTER

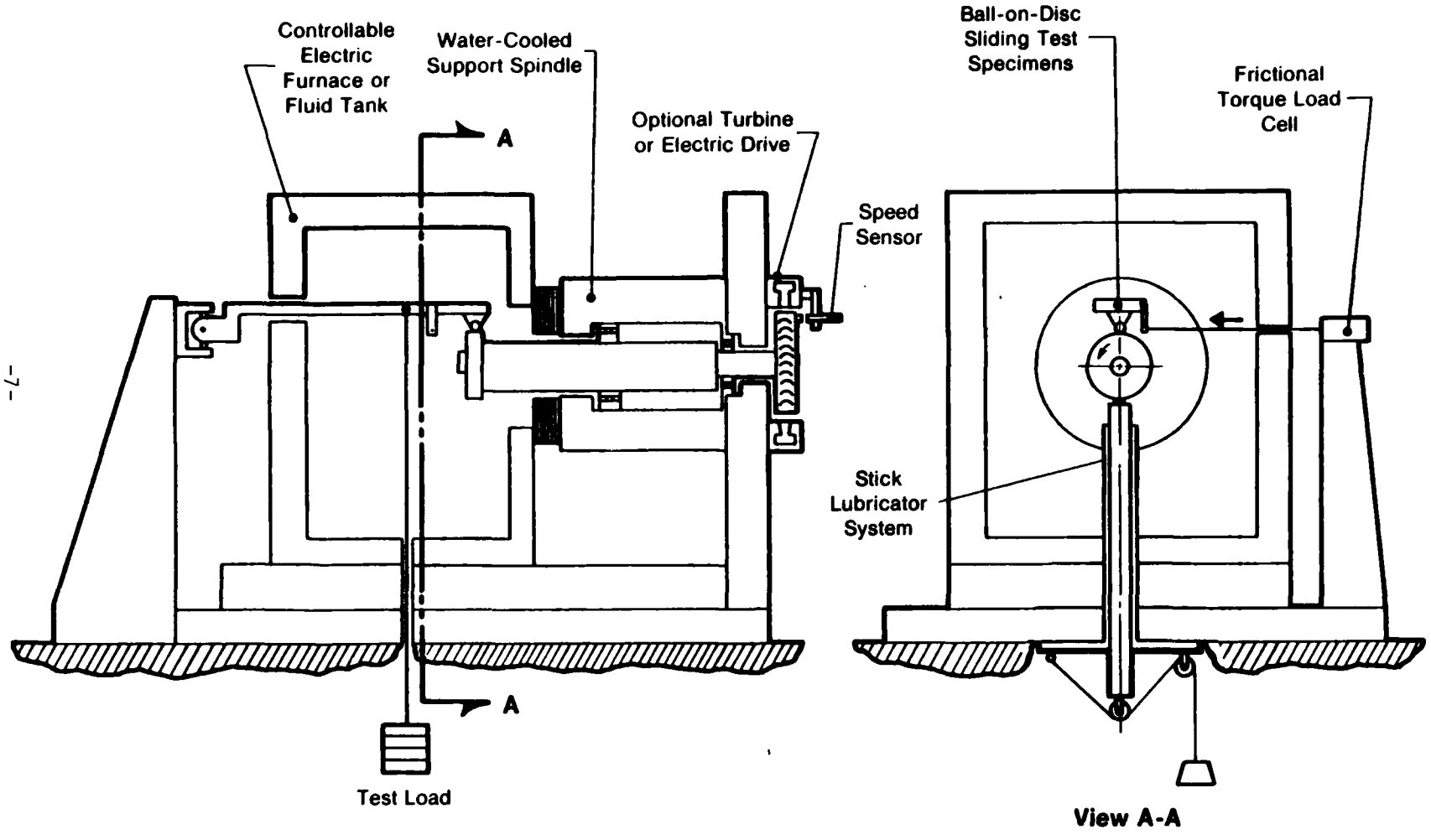

Figure 2 Continuous Sliding Ball on Disc Material Tester

illustrated schematically on Figure 2 and photographically on Figure 3 consists of a horizontally mounted precision spindle with oil lubricated ball bearings which can be driven at the remote end by an integral air turbine for high speed operation, or by an electric motor for low speed operation. For convenience, the electric drive can be coupled to the spindle without removing the turbine. The front end of the spindle is water cooled to protect the support ball bearing from the hot test environment.

The front end of the spindle with the rotating test disc shown on Figure 4 is surrounded by a clam shell type electric furnace which has an array of quartz heater rods for generating the required test temperatures. The furnace will provide test temperatures up to 700° C (1300° F).

The static test specimen is mounted at the end of the loader arm and makes sliding contact with the periphery of the test disc. The other end of the loader arm is mounted on a simple universal joint built with small instrument size ball bearings which have negligible friction compared with that experienced at the mating test specimens.

Loading is by dead weight, and specimen friction is measured with a strain gage type load cell connected to the loader arm through the furnace wall by a rigid, but self-aligning, linkage.

Particular care was used in designing the mounting systems for the test specimens for the different test modes. The rotating test disc must maintain precise concentricity while operating up to speeds of 30,000 rpm in the temperature range from room temperature up to 427° C (800° F). One of the difficulties in achieving this is the range of the coefficients of expansion of the disc materials which significantly affected the bore fit on the spindle mounting sleeve. This problem was solved as illustrated on Figure 5 by utilizing transition components between the steel spindle and the test disc made from materials of decreasing coefficients of expansion to match the bore size of the lower expansion rate discs. Additional features of the mounting system were to use stress relieving slits in the disc support sleeve and select the bore diameter to give the best fit over the operating temperature range. The thermal mismatches in the axial direction were handled with the flexibility of a tie bolt. No problems of loss of concentricity or cracking of the ceramic discs were experienced.

TABLE 1

TYPICAL PHYSICAL AND THERMAL PROPERTIES OF BALL AND DISC MATERIALS[2]

Material	Hardness at 20°C Rc	Elastic Modulus at 20°C GPa(10^6 PSI)	Thermal Conductivity Cal/s m °C		Coefficient of Thermal Expansion 10^{-6}/°C 0-800°C
			20°C	800°C	
M-50 Steel	64	190 (28)	13.4	-----	12.3 (300°C)
Silicon Nitride	78	310 (45)	7.3	4.7	2.9
Silicon Carbide	90	410 (59)	35.0	12.0	5.0

- Alpha Silicon Carbide - sintered. Base material and machined parts provided by Carborundum, Hexalloy Div.

Some typical physical and thermal properties of these materials are given in Table 1.

Balls were 5.56 mm (7/32") diameter and ground to precision bearing tolerances and finishes. The test discs were 50.8 mm (2") diameter X 12.7 mm (1/2") wide with a 15.24 mm (0.6") bore for mounting purposes; roundness, squareness, concentricity and flatness tolerances were within 5.0 μm (.0002") TIR and the cylindrical outer diameter test surface was within 0.1 μm (4 microinch) finish.

Lubricant Test Materials

The graphite fiber strengthened lubricant composite test pieces were provided by WPAFB from an earlier development program[3] where these dry lubricant containing materials had been developed for use in cages in ball bearings operating at high temperatures. These materials had the following compositions:

- HAC-1*/T50 F1 consisting of 50.1%+ woven graphite fiber; 41.3% polyimide, 2.2% "Westinghouse compound" composed of gallium, indium and tungsten diselenide, 1.4% $(NH_4)_2HPO_4$ and 4% voids.

- HAC-1A/T300 F1 similar to the above, but with approximately double the percentage of "Westinghouse compound".

The second of these materials was introduced into the test program because of limited quantities of specimens of the first material. Lubricant specimens were machined to give 1/4" x 1/4" or 40.3 mm^2 projected wear surface.

B. Friction and Wear Test Apparatus and Specimen Mounting

The experimental friction and wear studies were performed in a pin on disc type rig owned and modified by MTI for the program requirements. The basic rig,

*HAC = Hughes Aircraft Corp. + volume percentage

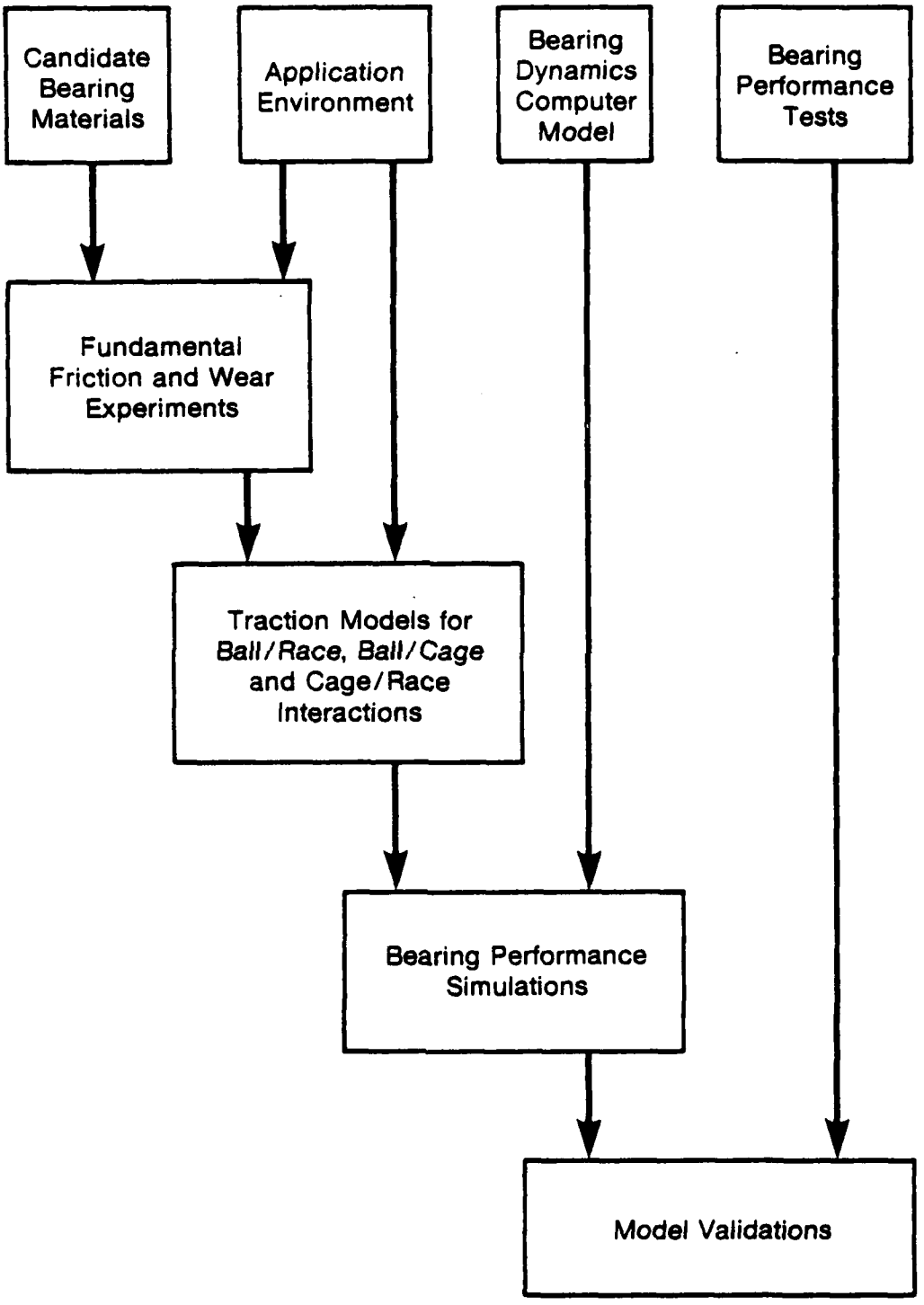

Figure 1 Schematic Overview of the Program Approach

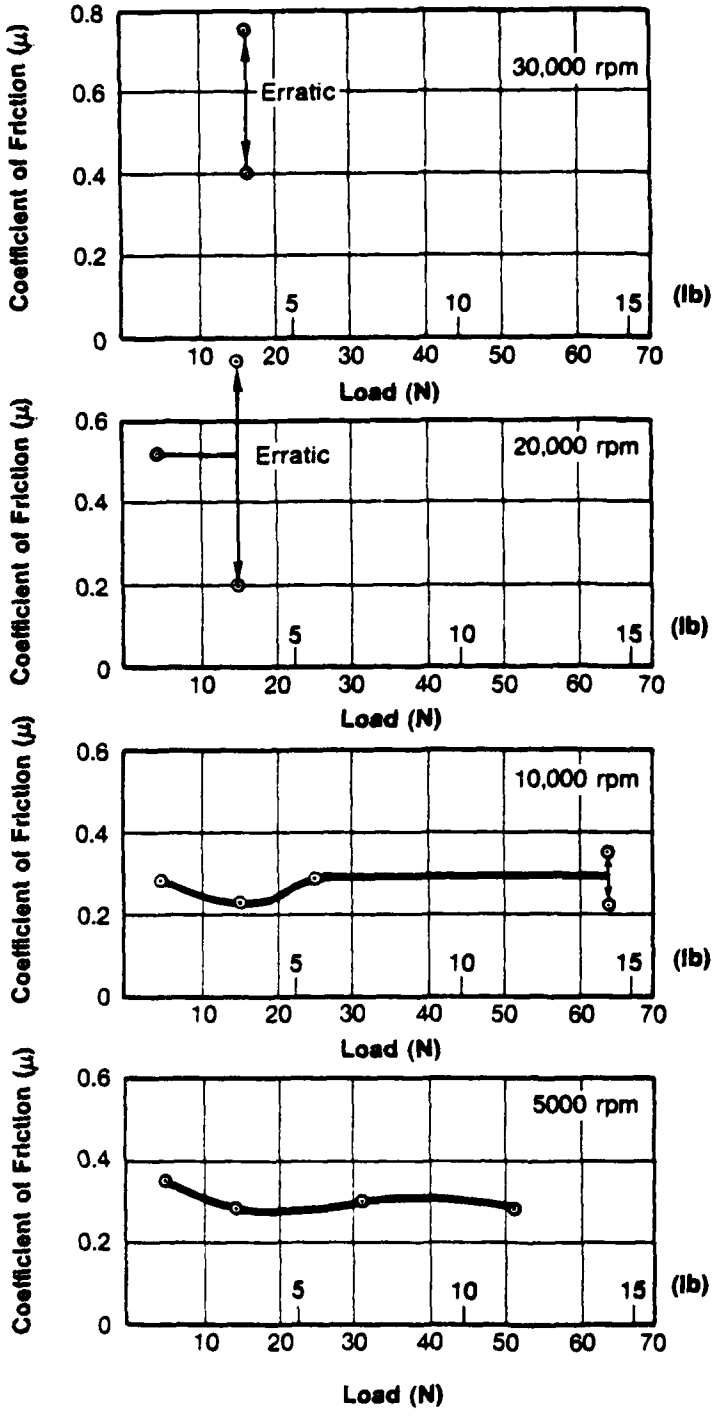

End of Test Conditions		
Temperature °C (°F)	Load* MPa (psi)	Total Test Time min.
166 (330)	0.34 (50)	4
Disc Blue		
121 (250)	0.90 (130)	5
116 (240)	3.24 (470)	6
71 (160)	2.41 (350)	8

*Based on Wear Scar Area

Disc Spec No. 1: M-50
Cage Spec No. 1: HAC-1/T50F1

Figure 8 High Speed Data HAC-1/T50 F1 vs. M50 at Room Temperature

842538

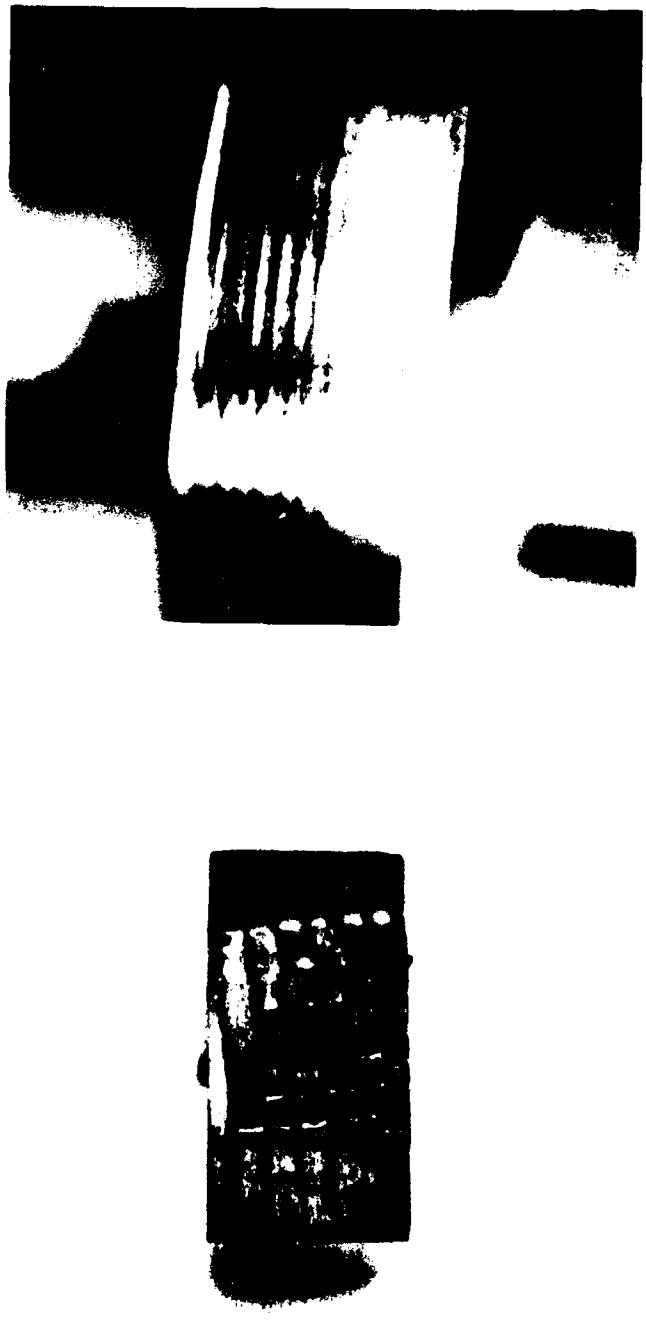

Figure 9 M-50 Disc and HAC-1/T50 F1 Specimen after 30,000 rpm Test at Room Temperature

During the accumulated 23 minutes of operation in these tests, the averaged wear rate of the lubricant block was calculated to be 0.49 mm^3/min. (3×10^{-5} in^3/min).

- HAC-1/T50 F1 vs. M-50 Disc at Elevated Temperatures

A second specimen block of the lubricant material was used in these tests with the previous M-50 test disc. The test disc was cleaned by lightly wiping with carbon tetrachloride fluid.

Figure 10 gives a plot of the friction data and static specimen temperature as a function of speed with the specimens in a 204° C (400° F) ambient temperature environment. Based on the findings of the previous room temperature tests, the dead weight loading was limited to 5.1 N (1.15 lbs.).

During the six minutes duration of this test, when sweeping through the speed range from 0 to 30,000 rpm, the static specimen reached 427° C (800° F) due to self-induced heating and the coefficient of friction exceeded 1.0 at 10,000 rpm and finished at 0.6 at 30,000 rpm.

After the test, the disc surface was found to be clean and smooth with no visual evidence of a lubricant transfer. The lubricant material was severely worn with evidence of delamination of the structural fibers. The calculated average wear rate for the lubricant block was 8.2 mm^3/min.(5×10^{-4} in^3/min). Due to the heavy wear of the specimen which significantly changed its effective area, the contact stress reduced from about 0.69 MPa (100 psi) at initial contact to 0.076 MPa (11 psi) at the end of the test.

- HAC-1A/T300 F1 vs. NC-132 at Room Temperature

Data from the room temperature ambient tests with this material combination given on Figure 11 showed a general similarity of performance to that of HAC-1/T50 F1 vs. M-50 except that coefficients of friction were somewhat lower being typically 0.2 at 5,000 rpm and 0.3 to 0.4 at 30,000 rpm and the data suggests that slightly higher loading levels could be

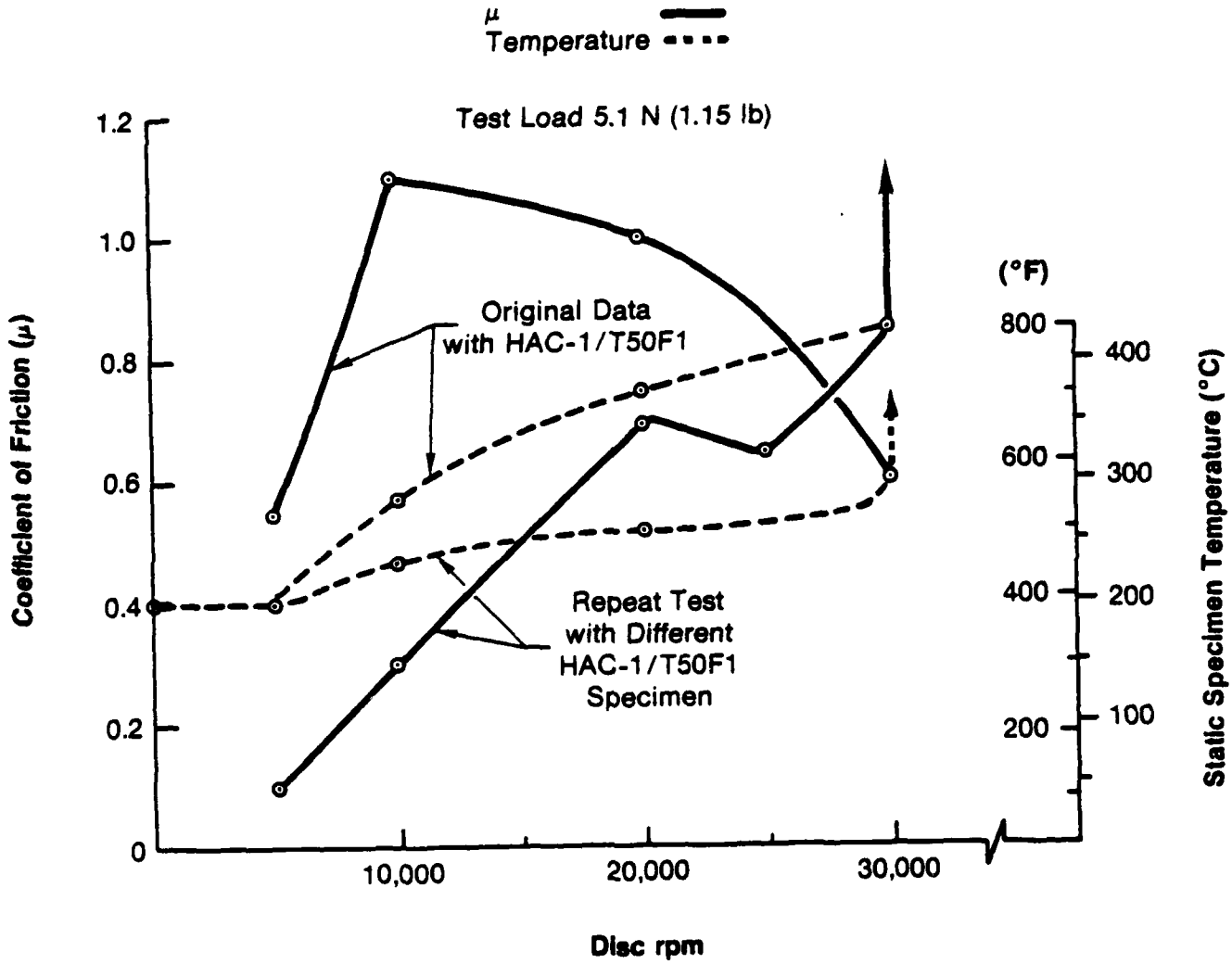

Continuous sweep through speed range for 6 and 6.8 minutes (original and repeat test respectively)

Figure 10 High Speed Data HAC-1/T50 F1 vs. M-50 Disc at 204°C (400°F) Ambient

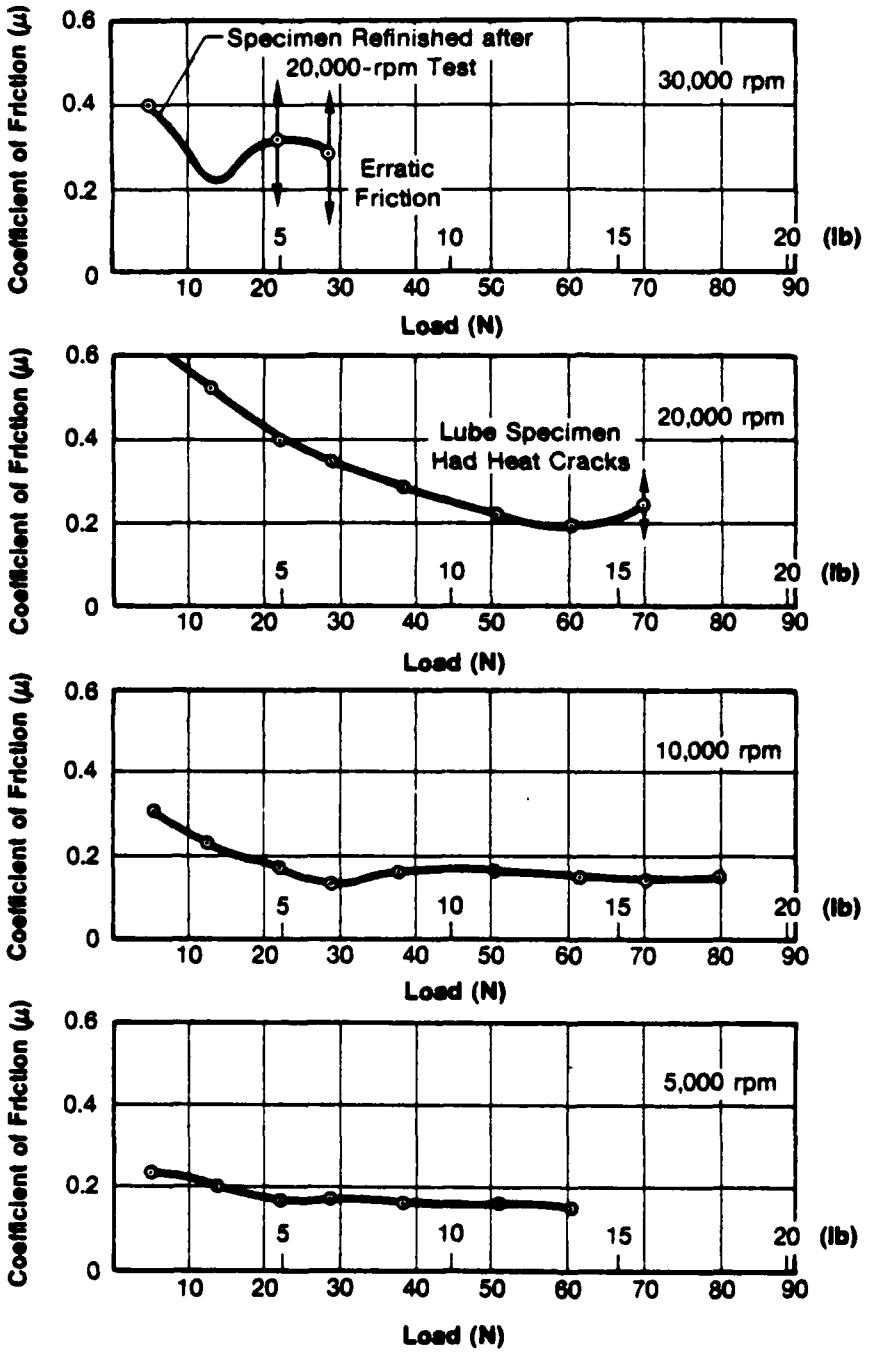

End of Test Conditions		
Temperature °C (°F)	Load* MPa (psi)	Total Test Time min
166 (330)	0.83 (120)	3
218† (425)		
174 (345)	1.72 (250)	13
293† (560)		
141 (285)	2.00 (290)	17.8
232† (450)		
66 (150)	2.41 (350)	10.5

*Based on Wear Scar Area
†Disc Temp after Rotation Stopped

Figure 11 High Speed Data HAC-1A/T300 F1 vs. NC-132 at Room Temperature

842541

sustained at higher speeds before self-generated temperatures became excessive.

As noted on Figure 11, as a result of attempting to push the material pair to higher loading at 20,000 rpm, operation became erratic; the static specimen reached 174° C (345° F) and the disc specimen as measured with a surface contact pyrometer immediately on stopping had reached over 293° C (560° F). Examination of the static lubricant specimen showed significant surface cracking. This is illustrated on Figure 12. The disc, also shown on Figure 12, looked clean and smooth.

In continuing the test program, the same lubricant specimen was refinished, the disc surface cleaned, and the mating pair run-in for 5 minutes at 10,000 rpm prior to proceeding to the 30,000 rpm speed level. At the 30,000 rpm speed, testing was stopped immediately when erratic behavior was evident to prevent specimen burn up. The good condition of the specimens after this test is shown on Figure 13.

The total test time over the full speed range and including the 5 minute run-in period was 49 minutes.

- HAC-1A/T300 F1 vs. NC-132 at Elevated Temperatures

The same specimens used in the previous test were cleaned or refinished and a similar test procedure of sweeping through the speed range up to 30,000 rpm at an ambient temperature of 204° C (400° F) was used as had been described for the HAC-1/T50 F1 vs. M-50 test combination.

The results shown on Figure 14 are significantly different to the HAC-1/T50 F1 vs. M-50 tests previously illustrated on Figure 10, showing a stabilized temperature and friction level over the speed range with a friction coefficient of about 0.15 as compared to almost run away temperature and very high coefficients for the previous combination. This confirmed the trend apparent in the room temperature tests and indicates that the lubricant composite performs better with NC-132.

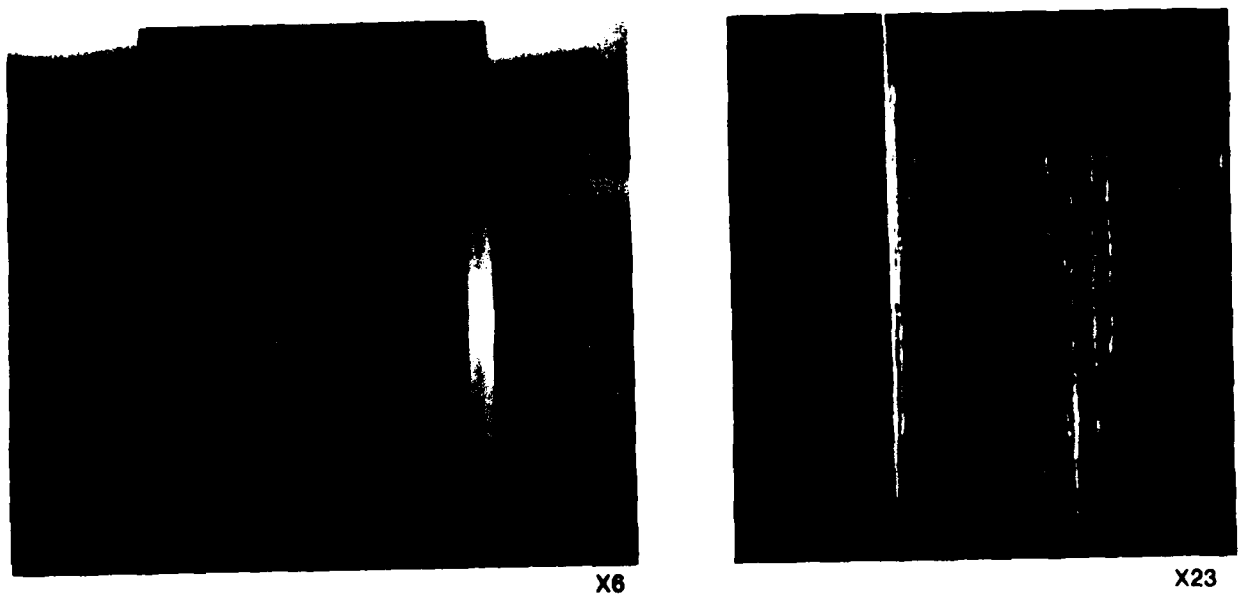

NC-132 Disc

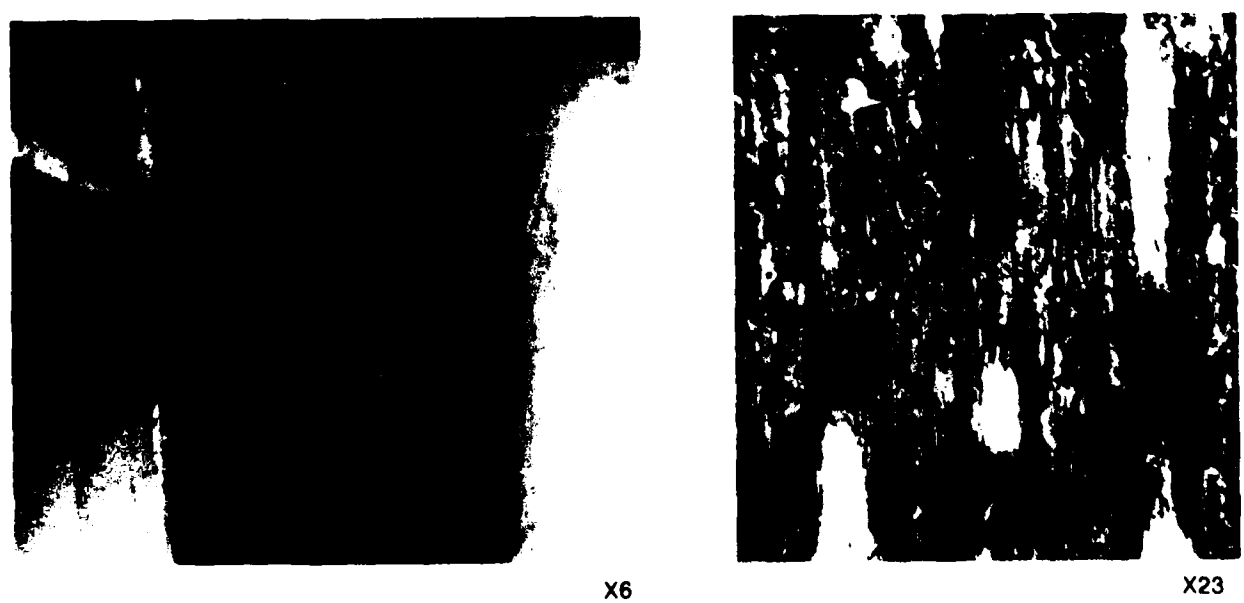

HAC-1A/T300F1 Lubricant Block

Figure 12 Condition of HAC-1A/T300 F1 and NC-132 Specimens after 20,000 rpm Test at Room Temperature

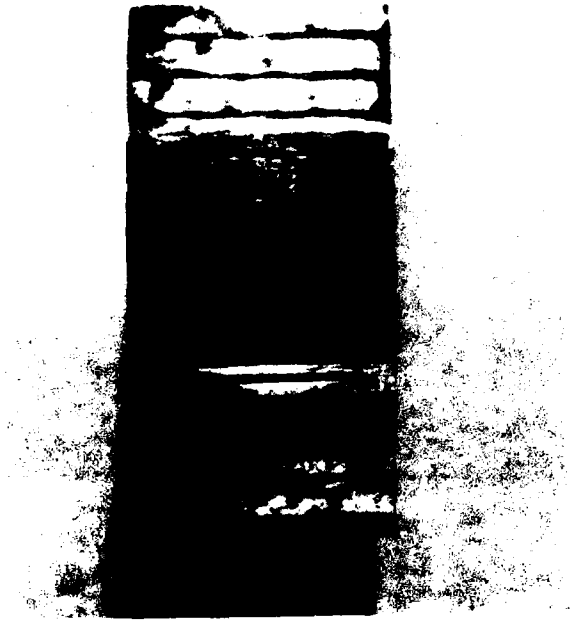

X6

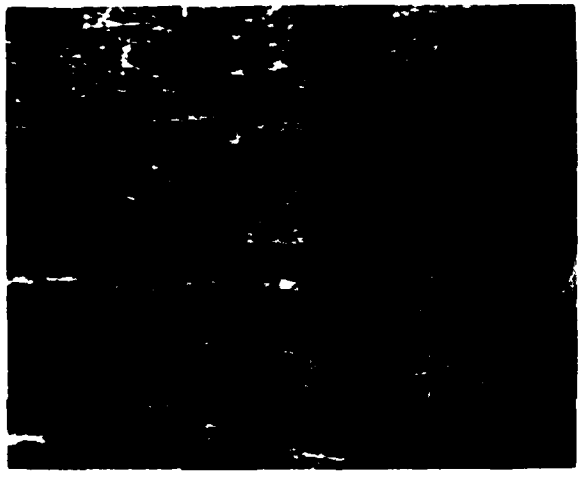

X23

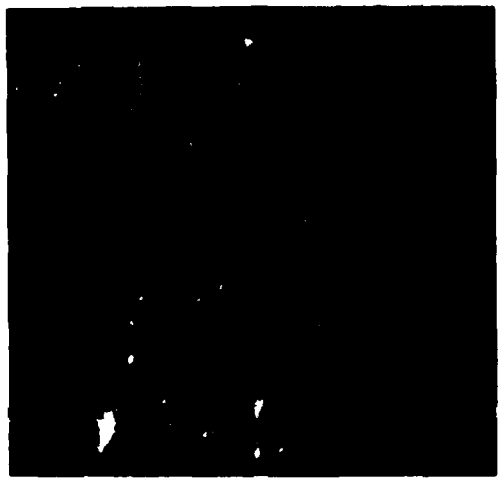

X54

Figure 13 Refinished HAC-1A/T300 F1 after 30,000 rpm Test at Room Temperature

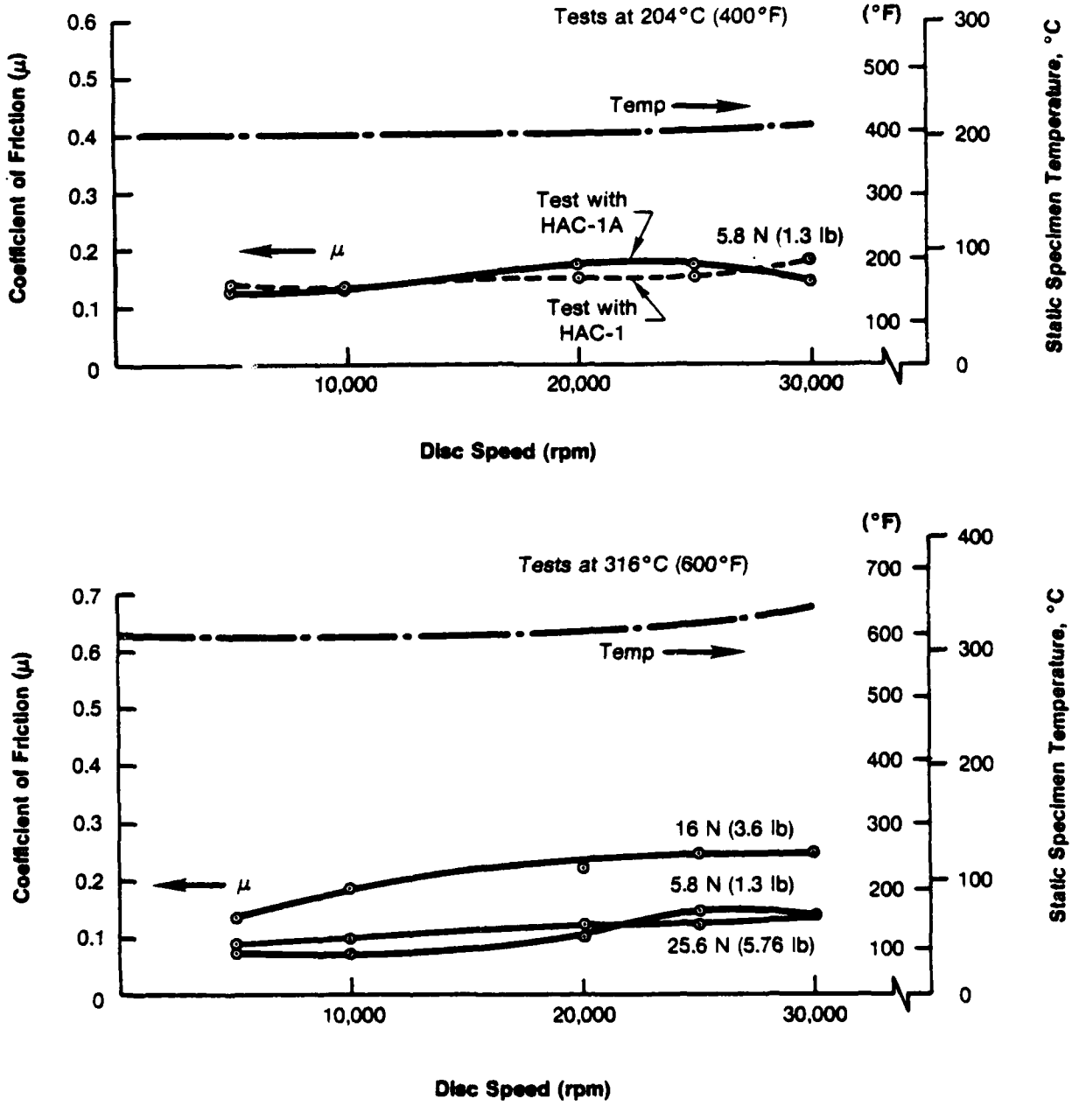

Figure 14 High Speed Tests HAC-1A/T300 F1 vs NC-132 at 204°C (400°F) and 316°C (600°F) Ambient

842539

In the next tests, the evaluation of the same HAC-1A/T300 F1 vs. NC-132 specimens were continued in a 316° C (600° F) temperature environment and as shown on Figure 14 stable temperatures and friction levels were evident over the speed range with the friction coefficients in the same general levels as in the 204° C ambient tests. In these tests, a range of increasing levels of test loadings was evaluated.

The total operating time at the 204° C and 316° C temperature levels was 58.4 minutes and the total averaged wear rate was 0.28 mm^3/min. (1.7 x 10^{-5} in^3/min) which was about 1/30 of that measured in the HAC-1/T50 F1 vs. M-50 tested only at 204° C and under light load. The condition of the lubricant block after test was good and the disc surface was clean, and did not show visual evidence of lubricant composite transfer.

Because of this interesting result and to evaluate the effect of the lubricant differences, the last test was repeated at the 204° C ambient temperature substituting the HAC-1/T50 F1 for the HAC-1A/T300 F1 material. The results of this test are shown in Figure 14 for comparison purposes. The friction results were very similar, indicating no apparent difference with NC-132 related to the two lubricant composites.

- Repeat of HAC-1/T50 F1 vs. M-50 Elevated Temperature Test

Because of the poor performance previously discussed with this material combination at 204° C (400° F), it was decided to repeat the evaluation.

A plot of this repeat test using a different HAC-1/T50 F1 specimen, but the original M-50 disc has been added to Figure 10 for comparison with the original test data. This indicates similar high levels of friction and temperature increases and confirmed again the better performance of the lubricant composite materials with the NC-132 disc material.

(2) Ball vs. Disc - Low Speed Sliding Experiments with Stick Transfer Lubrication

- NC-132 Ball vs. M-50 Disc with HAC-1/T50 F1 Lubrication

This combination was of particular interest because of the correlation possible in the computer modeling with data from actual bearing tests. Evaluations were made at room temperature and 316° C (600° F). The disc was prelubricated in these as in all subsequent test by running the transfer lubricant stick against the disc at the proposed test temperature for one hour at about 100 rpm. Because of program limitations, the same ball and disc contact zones were used during each series of tests at a given temperature level with the contact loading starting as the minimum value and then increasing in steps. The dwell time to get data at any particular load and speed point was approximatly one minute.

Figure 15 shows the friction vs. speed curves at three levels of loading for this first material combination. The friction data showed some sensitivity to speed in the 0-5 cm/sec. range but less above this range. The data showed some sensitivity of friction to load and also apparently to elapsed time in the room temperature tests, but considerably less sensitivity to load in the 316° C (600° F) tests. This reduced sensitivity to load at elevated temperature was probably due to the formation of beneficial oxides on the M-50 steel and to better lubricant performance.

The total elapsed test time for each temperature level is also given on Figure 15. The tests started at Hertzian contact stress levels of 1,324 MPa (192,000 psi), and as indicated in Figure 15, these rapidly decreased during a test due to ball wear. Ball wear reached a scar diameter of 0.61 mm in a total test time of 20 minutes at room temperature and 0.33 mm in a test time of 18 minutes at 316° C.

As a final test with this material combination, the loading at the end of the 316° C test was increased to raise the contact stress to 690 MPa (100,000 psi) and a single low speed test point was taken as shown on Figure 15. In 10 minutes of operation, the contact stress had decreased to 315.8 MPa (45,800 psi) due to ball wear, but the friction coefficient associated with higher direct load fell to 0.15.

The condition of the specimens at the end of the room temperature test showed that the ball had some brownish-red debris around the edge of the

New Ball and Track Contact at Start of Each Set of Tests
at Each Temperature: Ball 5.56 mm (7/32 in.) dia.; Disc 50.8 mm (2 in.) dia.
Contact Lubricated by HAC-1/T50F1 by Stick Transfer.

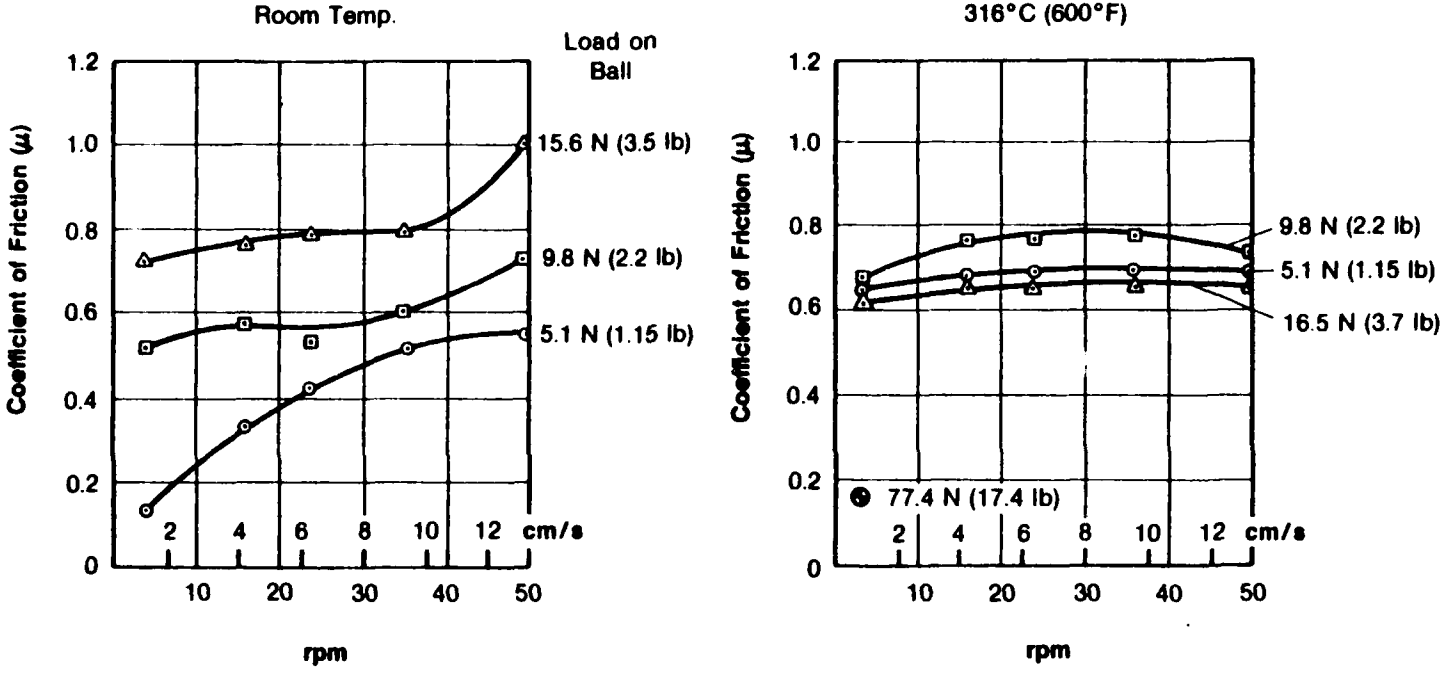

Total Test Time, min.	20	18	10
Final Ball Wear Dia., mm (in.)	0.61 (0.024)	0.33 (0.013)	0.56 (0.022)
Final Stress, MPa (lb/in.²)	53.1 (7700)	193.1 (28,000)	315.8 (45,800)
			Continuation of Test for 77.4 N Load Point

Figure 15 Slow Speed Sliding Tests NC-132 Ball vs. M-50 Disc

842336

contact zone and the disc had two sharp scratches. At the end of the elevated temperature test, a light surface band was evident on the disc.

During all testing, somewhat random, high pitched screeching occurred. This was more frequent at lower loads or higher sliding speeds.

Typical torque force traces from these and other material pair tests are shown on Figure 16 for both room temperature and elevated temperature tests and various loads and speeds. For the NC-132 and M-50 combination the traces show the expected increase in chatter related to higher loadings and speeds. There was no apparent correlation with audible noise which in any case would be above the frequency response of the chart recorder pen mechanism.

- NC-132 Ball vs. NC-132 Disc with HAC-1A/T300 F1 Lubricant

Figure 17 shows the friction coefficient plots for this ceramic combination derived at room temperature, 316° C (600° F) and 427° C (800° F). In these tests, particular effort was made to obtain data at the lower end of the speed range and this did show a trend of increasing friction with speed. The frictional test results also showed some load dependency, particularly at higher speeds. Friction levels at room temperature and 316° C were of the same order as the NC-132 vs. M-50 tests at those temperatures, but the NC-132 material pairs showed lower levels of friction when the ambient test temperature was raised to 427° C.

These frictional coefficients were higher than usually found in the literature and are believed to be the result of the high contact stress causing rough operation during the rapid ball wear process.

From an initial Hertzian contact stress of 1,580 MPa (229,000 psi), the results again showed the rapid reduction in contact stress due to ball wear with the ball scar diameters reaching 0.71 mm in 21 minutes at room temperature, 1.12 mm in 19 minutes at 316° C and 0.91 mm in 16 minutes at 427° C respectively.

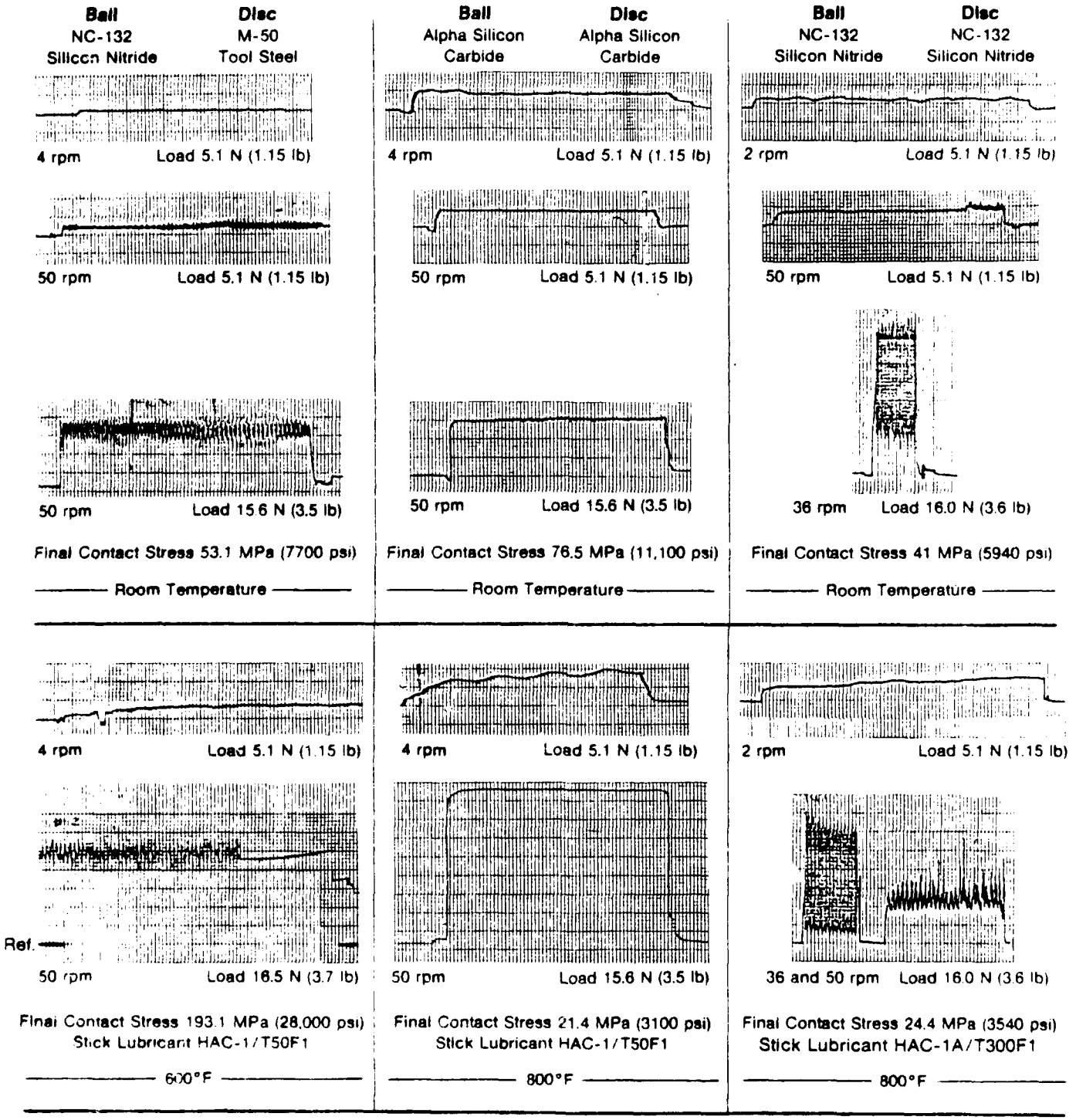

New Contact Pair Used at Start of Each Temperature Level.
Ball Diameter 5.56 mm (7/32 in.) Disc Diameter 50.8 mm (2 in.)
Horizontal Scale — 1 minor div/sec

Figure 16 Typical Friction Force Traces

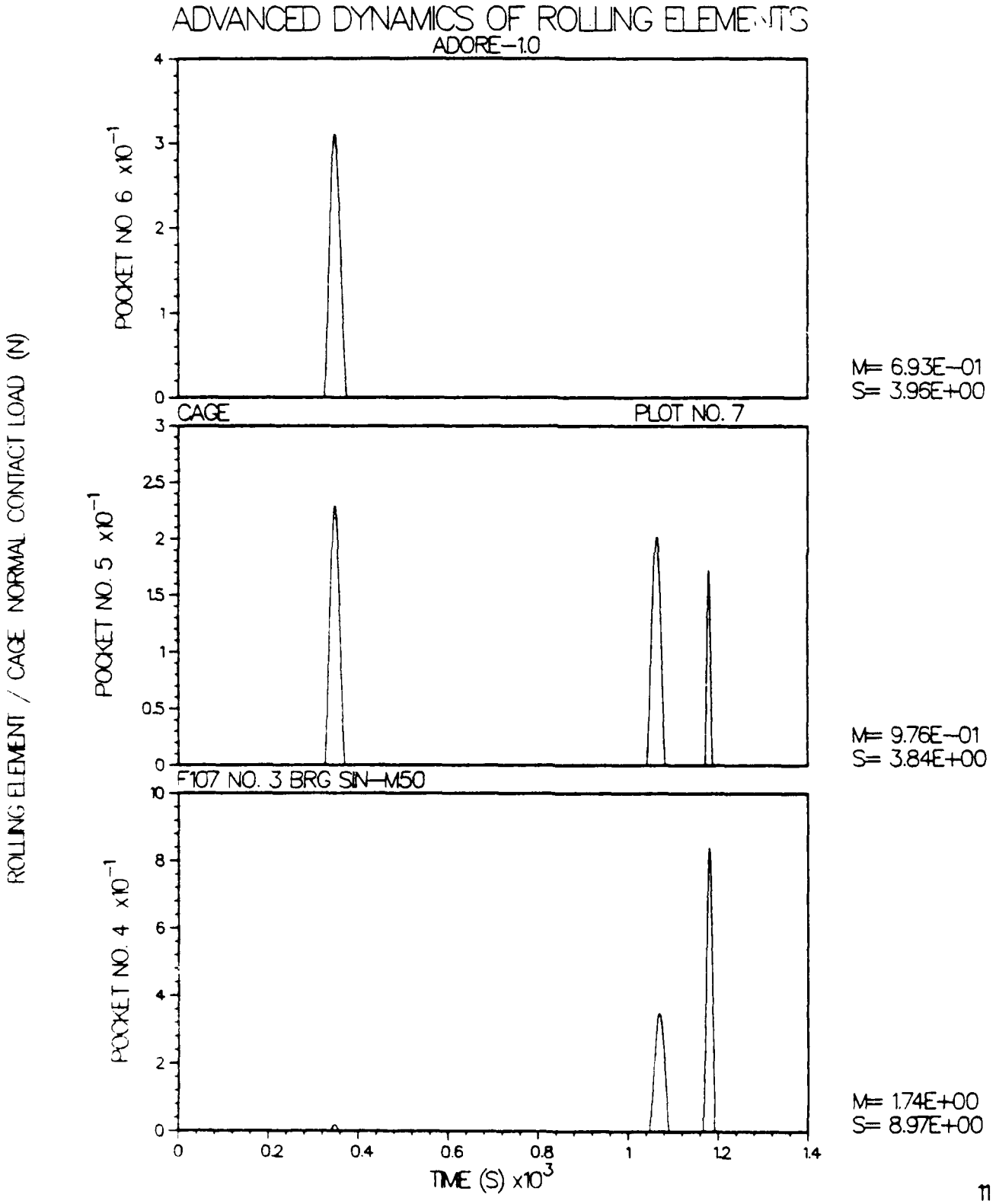

Figure 25 Ball/Cage Collision Forces in Pockets 4 to 6

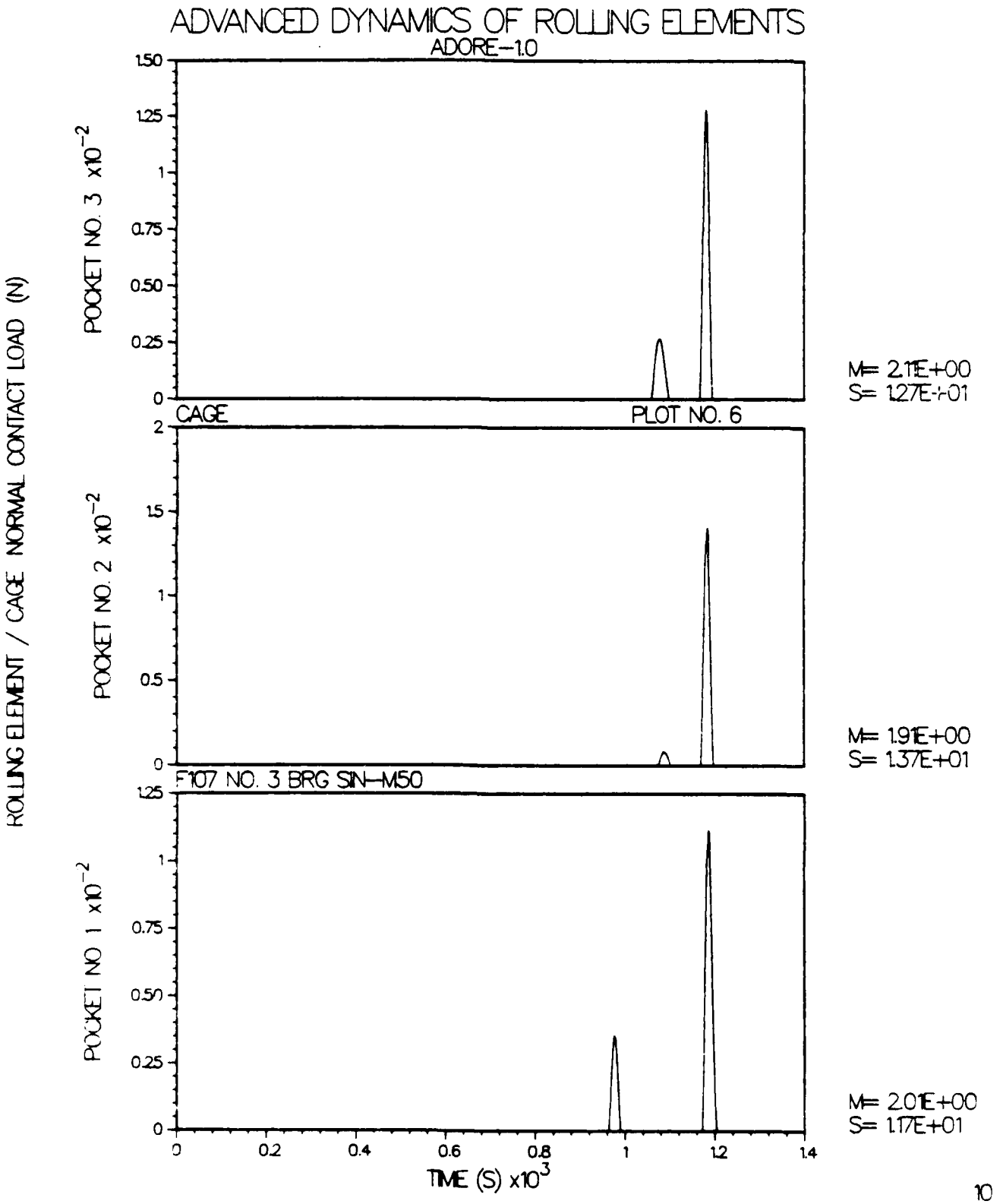

Figure 26 Ball/Cage Collision Forces in Pockets 1 to 3

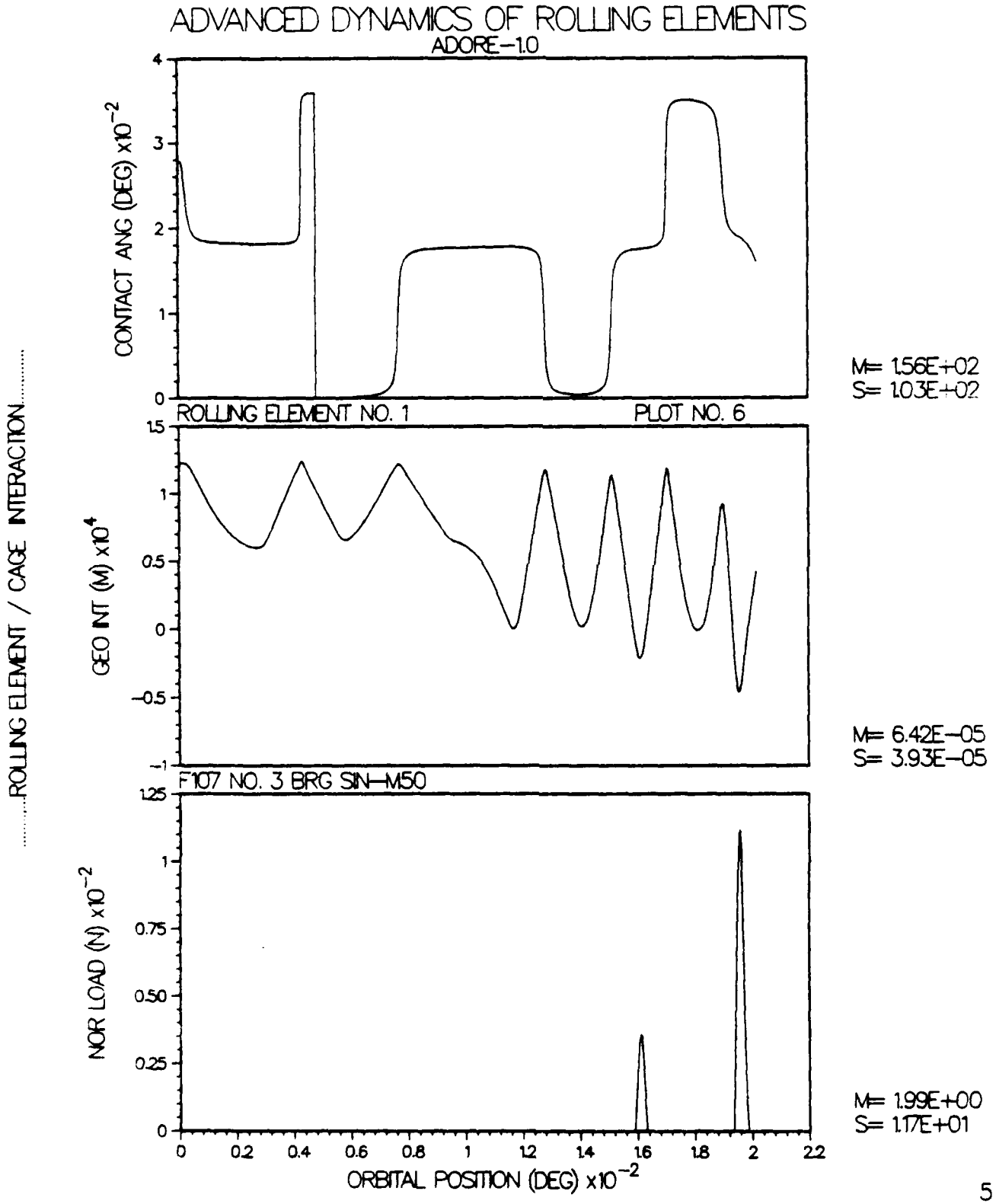

Figure 23 Typical Ball/Cage Interaction

generation return to their nominal values. This indicates a fairly stable motion of the balls which is free of excessive skidding.

Typical interaction in the ball pocket is shown on Figure 23. The periodic variation in the geometric interaction indicates the normal cyclic excursion of the ball in the cage pocket. The contact angle of 0° represents a configuration where the cage drives the ball, while the contact angle is 180° when the ball drives the cage. Note that at the time of both collisions on Figure 23, the contact angle was close to 180°, meaning that the ball is trying to drive the cage; this results in a slight reduction in the ball orbital velocity, as seen earlier in Figure 21.

The magnitude of the ball/cage collision force (of the order of 100 N) is typical. Figures 24 and 25 plot the collision forces for several balls in the bearing. Aside from the rather large magnitude of the collision forces, the collisions in pockets 1 to 5 are taking place almost simultaneously. This may lead to a situation where several adjacent pockets may be torn, i.e., the wall separating the two pockets may fracture, which could lead to a rather catastrophic failure.

As a result of the large pocket forces, the interaction at the cage guide land is also relatively severe. Note that the magnitude of the cage/race contact force, on Figure 26, is gradually increasing, which indicates some form of instability. Also, the reduction in time between collisions indicates increased cage/race interaction as a function of time. The heat generation at the cage/race interface may also be significant in the sense that a higher temperature at the cage surface may lead to a reduced guide clearance due to the differential thermal expansion of the cage and the guiding race. The reduced guide clearance may result in further increase in the cage/race interaction which may rapidly lead to a rather catastrophic cage failure. However, in order to confirm such a behavior, it will be necessary to obtain the computer simulations as a function of the cage/race guide clearance.

The overall motion of the cage may be understood in terms of the mass center whirl and the angular velocity variation plotted on Figure 27. Note that the cage angular velocity does go through a cyclic variation due to the various collisions in the pocket and at the guide lands. The angles THETA and PHI, shown

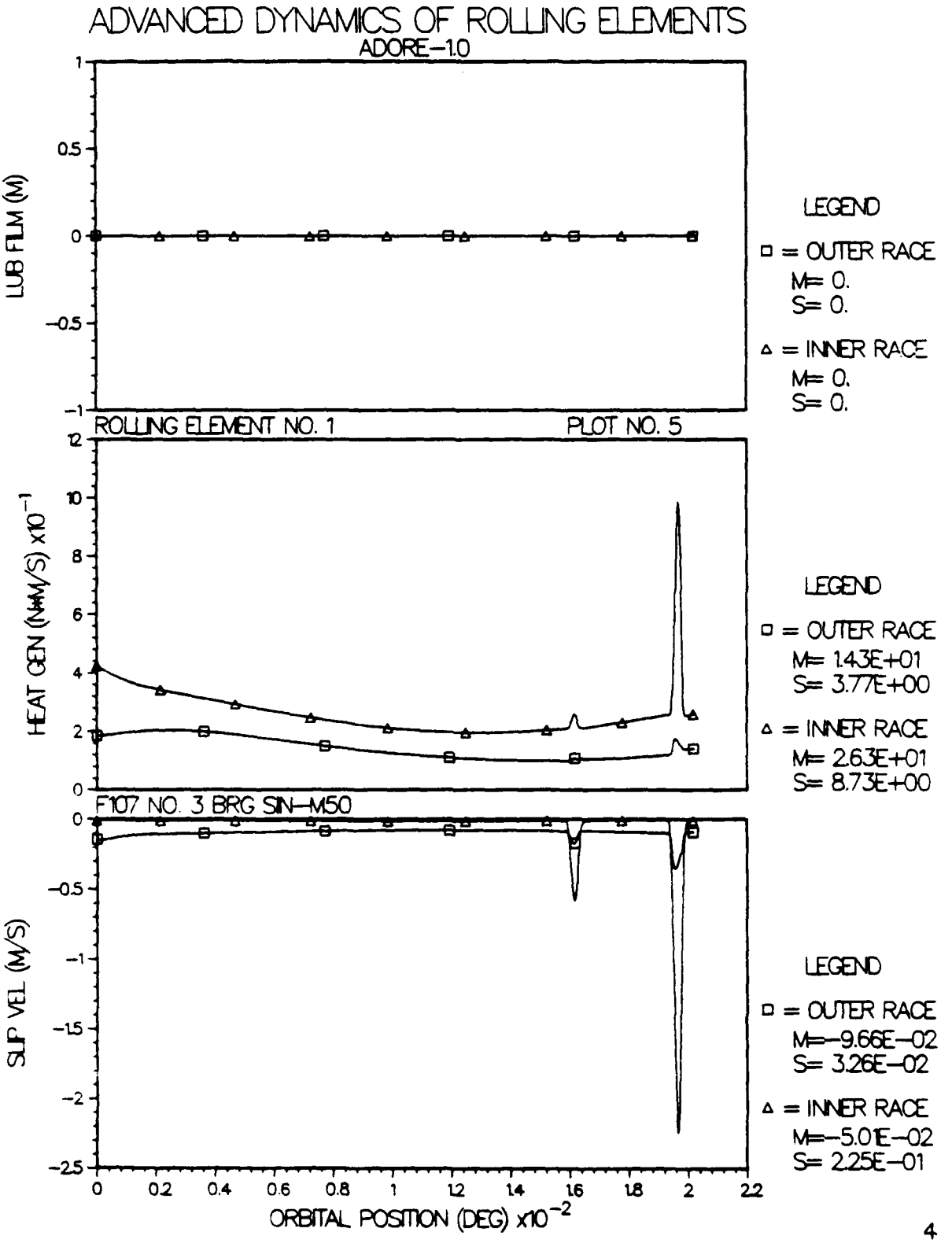

Figure 22 The Variation in Slip and Heat Generation at the Ball/Race Contact

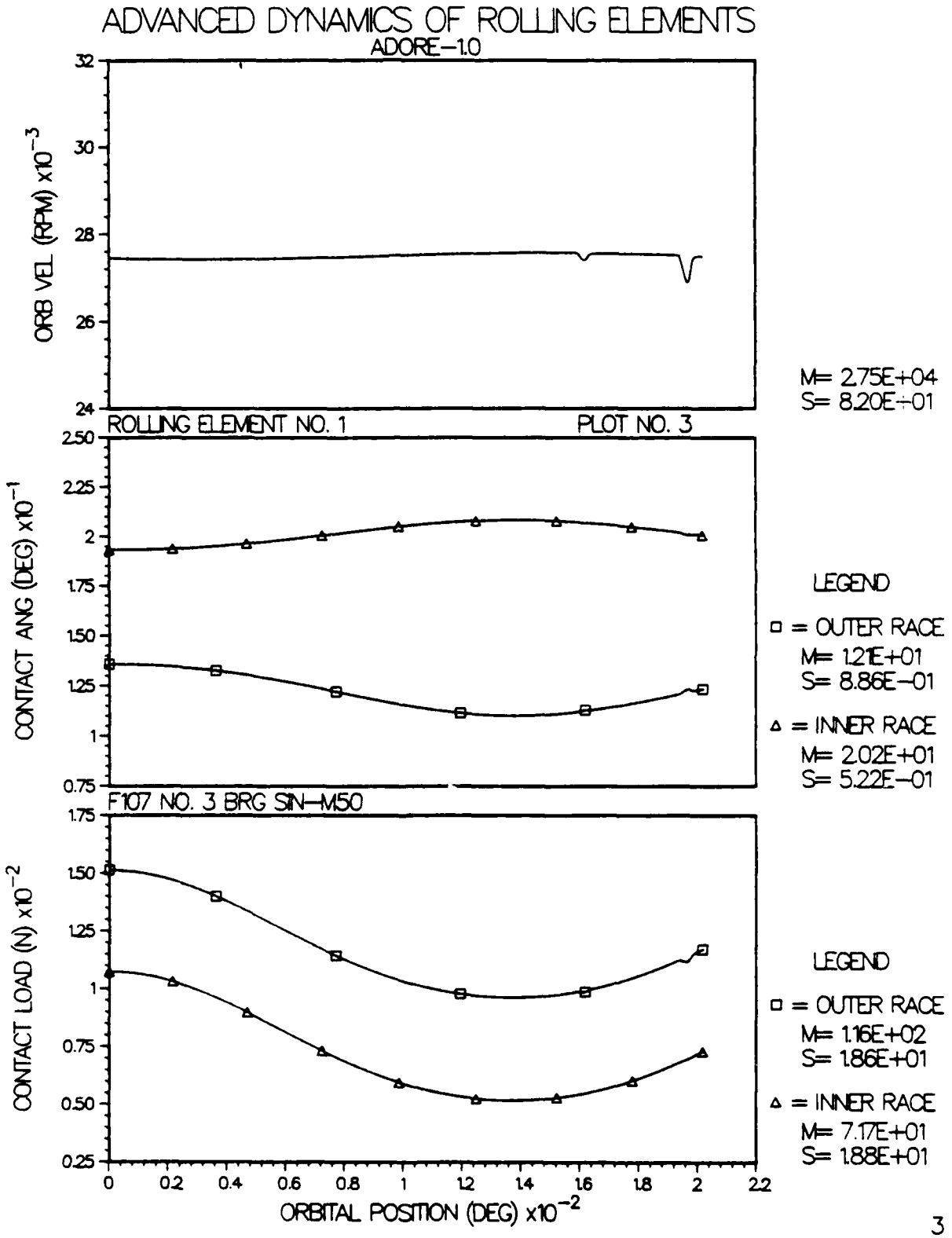

Figure 21 Ball/Race Contact Load Variation

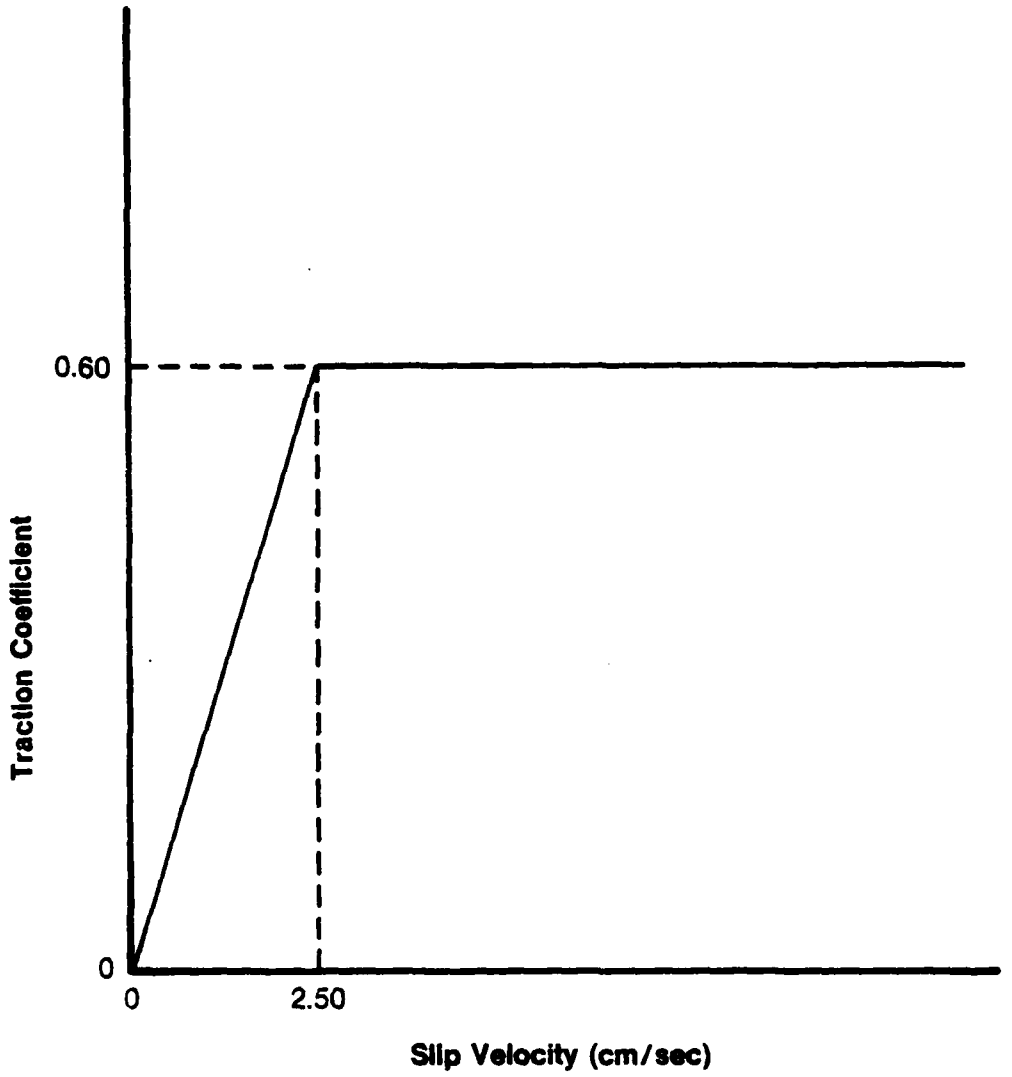

Figure 20 The Traction Model for The Ball/Cage Interface

842556

The behavior between the silicon nitride ball and M-50 races was simulated by taking a linear variation in traction as a function of slip until a maximum traction coefficient of 0.60 was reached at a slip velocity of 2.5 cm/sec. The relationship is shown schematically on Figure 20. This model simulates the observed friction behavior with the M-50 disc and silicon nitride ball, as shown earlier on Figure 15.

Again, based on the experimental results obtained with the silicon nitride disc against HAC-1 composite, shown earlier on Figure 14, the friction coefficient at the ball/cage interface was assumed to be constant at 0.10.

For the cage/race interface a constant friction coefficient of 0.60 is assumed. This is based on the HAC-1 vs. M-50 friction tests, shown on Figure 10.

C. Computer Simulation of Bearing Performance

Using the advanced computer model ADORE (Advanced Dynamics of Rolling Elements), the performance of the F107 #3 position bearing was simulated over approximately 475° rotation of the shaft. The initial print output, containing the geometry and operating conditions is presented in Appendix A along with the graphic output obtained near the end of the simulation. Appendix B gives the nomenclature used in the analytical data.

As discussed, the bearing is subjected to a thrust load of 450 N and a rotating radial load of 225 N, with the shaft speed of 63,500 rpm. The rotating radial load results in a sinusoidal variation in the ball/race contact loads and angles as shown on Figure 21. The ball orbital velocity also has a sinusoidal component, however, since the peak variation is quite small compared to the average velocity, this variation is not seen on Figure 21. The small "bumps" in the orbital velocity are due to the ball/cage collisions.

The slip velocities in the center of the ball/race contact zone are in the range of about 5 to 10 cm/sec. and the corresponding heat generation at a typical ball/race contact varied between 10 and 30 watts. However, for the small time duration of ball/cage collision, the slip velocity may greatly increase as seen on Figure 22. Note that after the collision, both the slip velocity and the heat

Problems could occur due to hard metal or ceramic wear debris being picked up on the lubricant stick to create a lapping or cutting action. This may have occurred at one time in the NC-132 vs. M-50 tests and would explain the sharp scratches found on the disc.

The third factor which was not studied in these evaluations, is establishing the optimum stick contact pressure as a function of other operating parameters which will give the minimum controlled feed rate for the stick for effective lubrication.

3. Analytical Program

The analytical effort in the present program consisted of modeling the friction behavior at the ball/race, ball/cage and cage/race interfaces, the computer simulation of the bearing performance, and then comparison of the computer predictions with actual bearing tests.

A. The Test Bearing

In order to demonstrate the significance of the friction experiments undertaken during the present investigation, the #3 position ball bearing in the Williams International F107 cruise missile engine was selected as the candidate bearing and the influence of the observed friction behavior on the overall bearing performance was investigated. The geometry of the bearing and the operating conditions are detailed in the typical computer output given in Appendix A. The operating speed of 63,500 rpm, thrust load of 450 N and a rotating radial load of 225 N selected are typical of actual application.

B. Traction-Slip Model

Based on the experimental data reported in the preceding sections, the traction-slip models for the various interactions in the bearing were established using the following materials:

Bearing Races:	M-50 Steel
Balls:	Silicon Nitride
Cage:	Hughes HAC-1 Composite

Another difference compared to both of the other material pairs was the smooth, albeit high friction force traces, shown on Figure 16. This was coupled with little audible noise during the testing of this material pair.

Relative Wear Performance

An evaluation of the relative wear rates of the balls was made based on calculating the total ball wear volume loss in the total elapsed time of each series of tests at the various loads and at a given temperature level. This showed the following trends:

- At room temperature and 316° C, the M-50 ball wear rate in the NC-132 vs. M-50 pair was lower than that of any other pair.

- At 316° C and 427° C, the NC-132 ball wear rate in the NC-132 vs. NC-132 pair was lower than for the Alpha Silicon Carbide vs. Alpha Silicon Carbide combination.

In terms of disc wear at the two elevated temperature levels, the NC-132 vs. NC-132 combination was slightly greater than Alpha Silicon Carbide vs. Alpha Silicon Carbide.

Experience and Comments on Stick Lubricant Transfer System

While it was not an objective to study the lubricant transfer mechanism, lubricant transfer was effective and sometimes visually evident in some of the testing. Some of the factors which should be considered in applying this technique to machinery include the following:

There can be difficulties related to keeping the lubricant stick aligned to ensure that the actual disc/ball contact track is receiving lubricant. This problem would be influenced by any thermal distortions of mechanical components affecting alignment. The more compliant the stick material is at the rotating contact surface, the better the transfer should be. This compliancy should be helped by higher operating temperatures.

New Ball and Track Contact at Start of Each Set of Tests
at Each Temperature: Ball 5.56 mm (7/32 in.) dia.; Disc 50.8 mm (2 in.) dia.
Contact Lubricated by HAC-1/T50F1 by Stick Transfer.

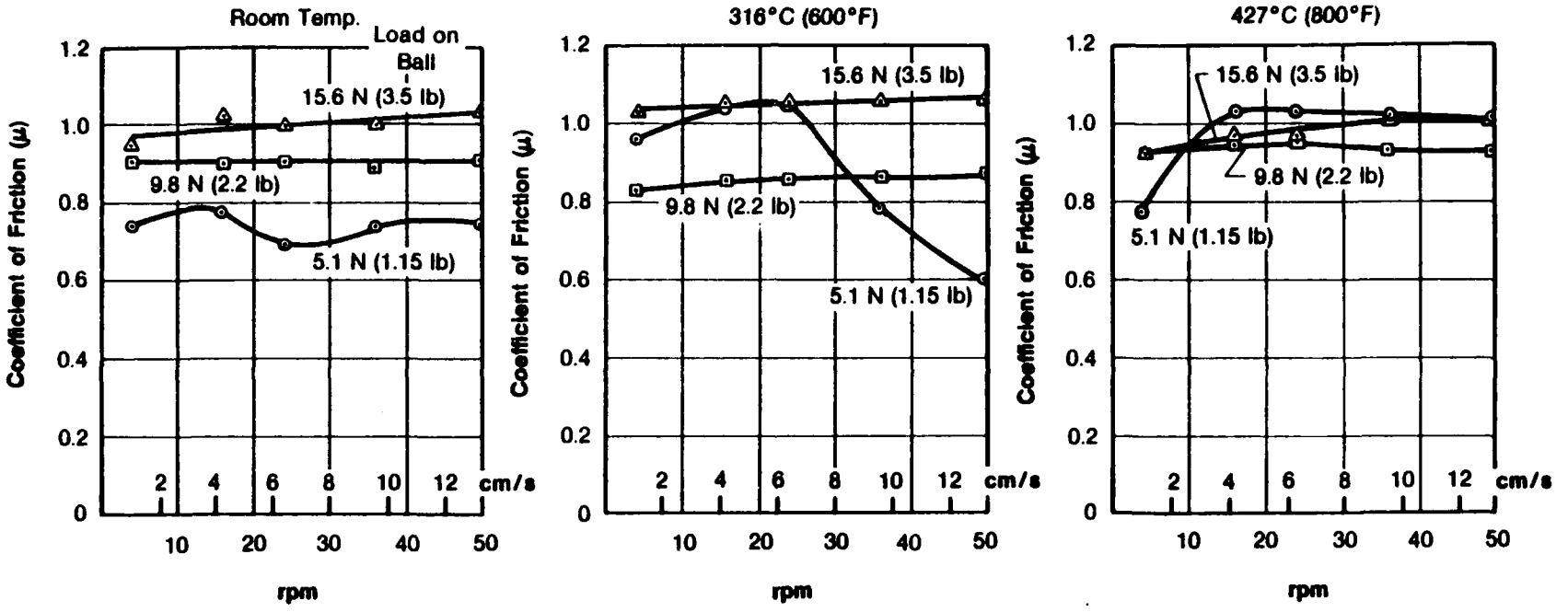

Total Test Time, min.	16	15	17
Final Ball Wear Dia., mm (in.)	0.50 (0.020)	1.19 (0.047)	0.99 (0.039)
Final Stress, MPa (lb/in.²)	76.5 (11,100)	14.2 (2060)	21.4 (3100)

Figure 19 Slow Speed Sliding Tests Alpha-Silicon Carbide Ball and Disc

842335

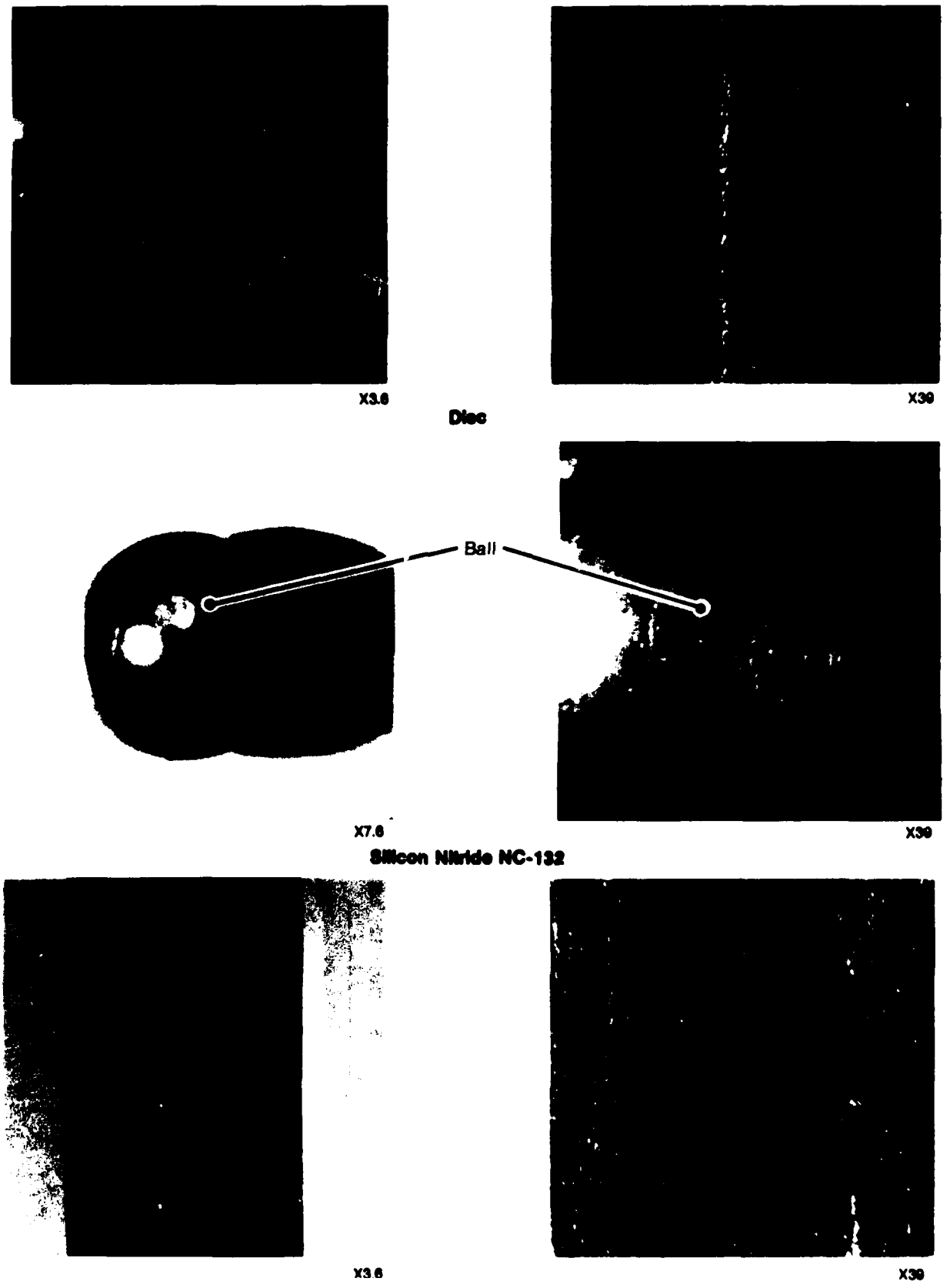

Figure 18 Typical Wear Traces on Ceramic Specimens

The wear surfaces on the ball and disc after test are shown on Figure 18. Examination of the tracks on the disc revealed light polishing in the track for room temperature tests, but surface material disturbance spikes of the order of ±19 μm (±80 microinches) in the track for the 316° C test temperature wear track and slightly less in the 427° C wear track with clear indication of some lubricant transfer in the track roughness in both high temperature tests.

The random high frequency contact audible noise, which was uncomfortably powerful at times, occurred in both room temperature and 316° C testing, but was not evident at 427° C. In addition, a low frequency noise similar to a cutting action was heard in the elevated temperature tests.

Sample traces from the torque force measurements shown on Figure 16 for this material combination taken at room temperature and 427° C show the same trends relative to load and speed noted with the NC-132 vs. M-50 combination, but with significantly greater excitation amplitude at the high load, high speed combination of operating conditions.

- Alpha Silicon Carbide vs. Alpha Silicon Carbide with HAC-1-T50 F1 Lubricant

These test specimens were made from a material with the highest Young's Modulus of Elasticity of all the materials tested; the results of the friction testing are shown on Figure 19. There was no particular sensitivity to sliding speed, but the frictional coefficient levels were significantly higher than the other two material pairs reach μ= 1.0 or higher in some tests and at all temperature levels.

Starting with an initially high Hertzian contact stress of 1,696 MPa (246,000 psi), related to the higher modulus of elasticity, the same rapid drop with ball wear was again evident with the ball scar diameter being 0.50 mm in 16 minutes at room temperature, 1.19 mm in 15 minutes at 316° C and 0.99 mm in 17 minutes at 427° C respectively. Unlike the NC-132 vs. NC-132 tests and as shown on Figure 18, all the wear was concentrated on the ball with only light polishing and lubricant transfer evident on the disc tracks.

New Ball and Track Contact at Start of Each Set of Tests
at Each Temperature: Ball 5.56 mm (7/32 in.) dia.; Disc 50.8 mm (2 in.) dia.
Contact Lubricated by HAC-1A/T300F1 by Stick Transfer.

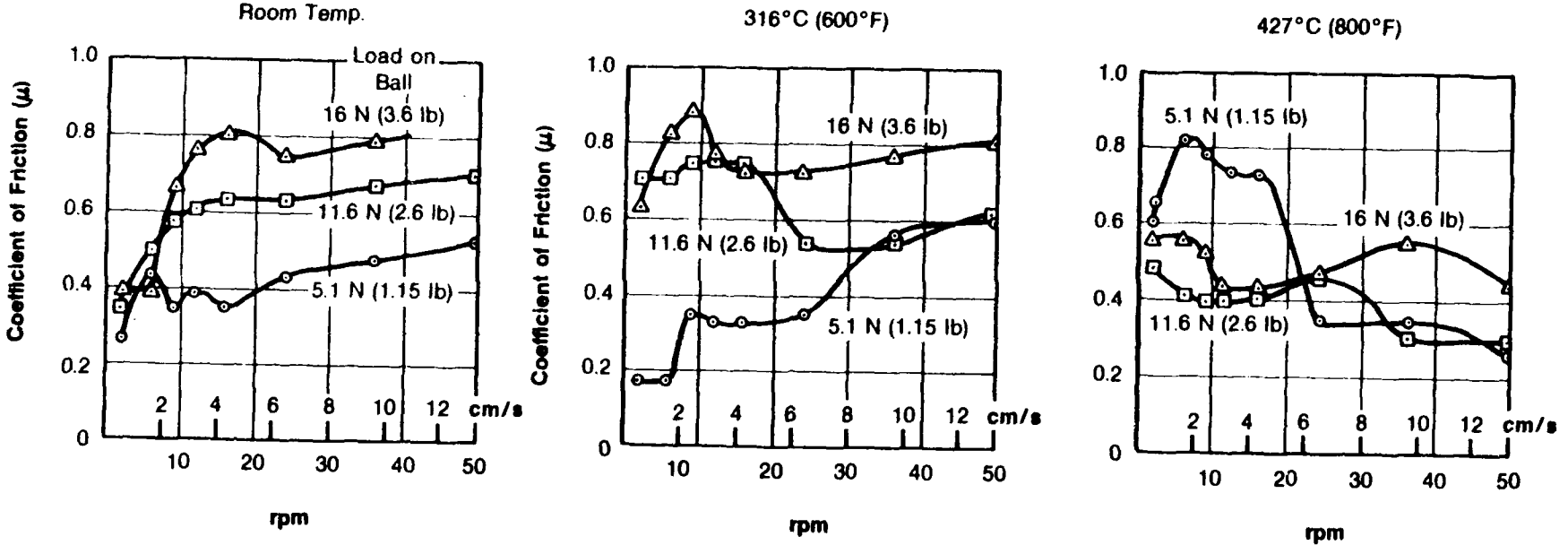

Total Test Time, min.	21	19	16
Final Ball Wear Dia., mm (in.)	0.71 (0.028)	1.12 (0.041) (at 2.6 lb)	0.91 (0.036)
Final Stress, MPa (lb/in.²)	41 (5940)	13.6 (1970)	24.4 (3540)

Figure 17 Slow Speed Sliding Tests NC-132 Ball and Disc

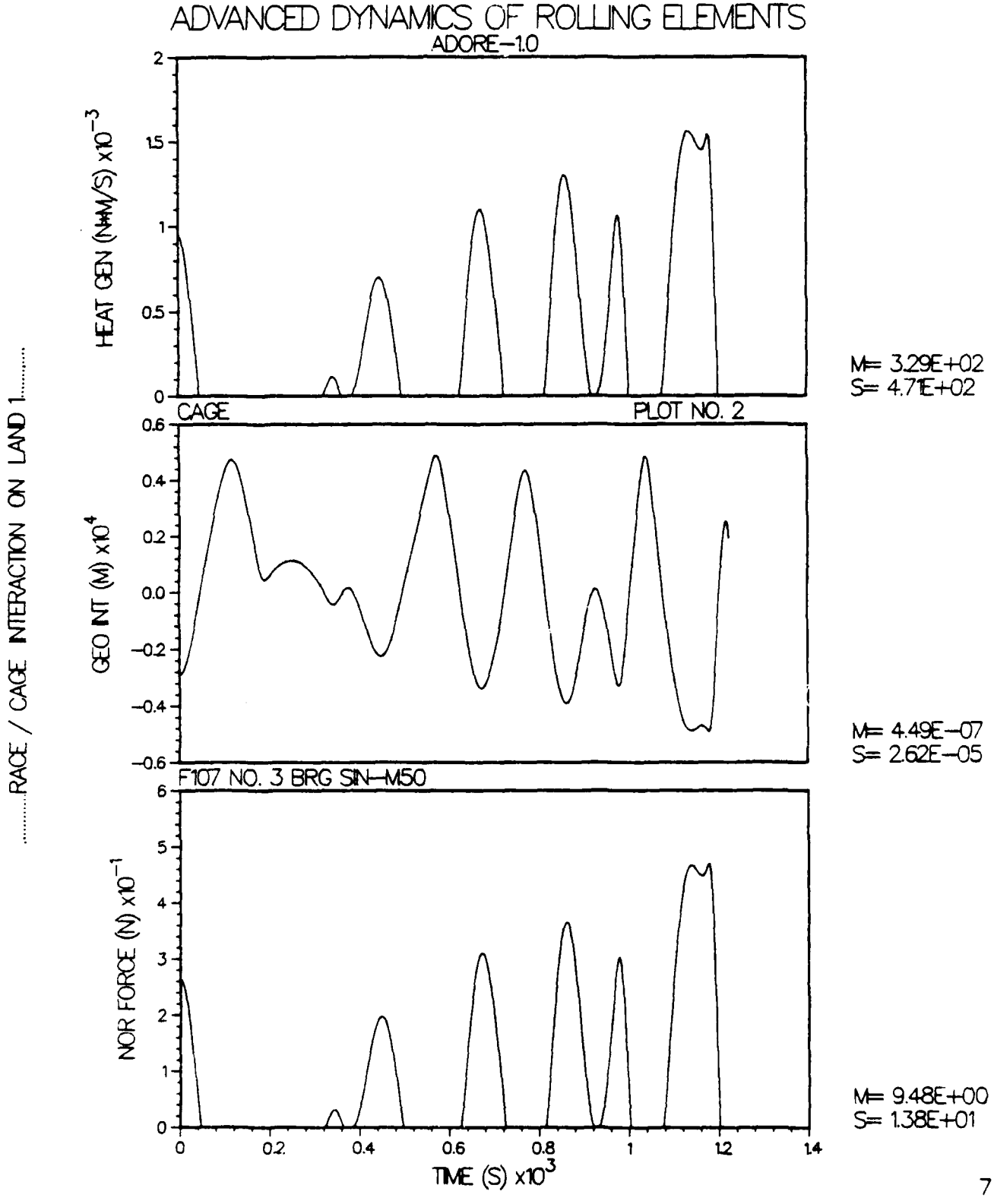

Figure 26 Typical Interaction at the Cage/Race Interface

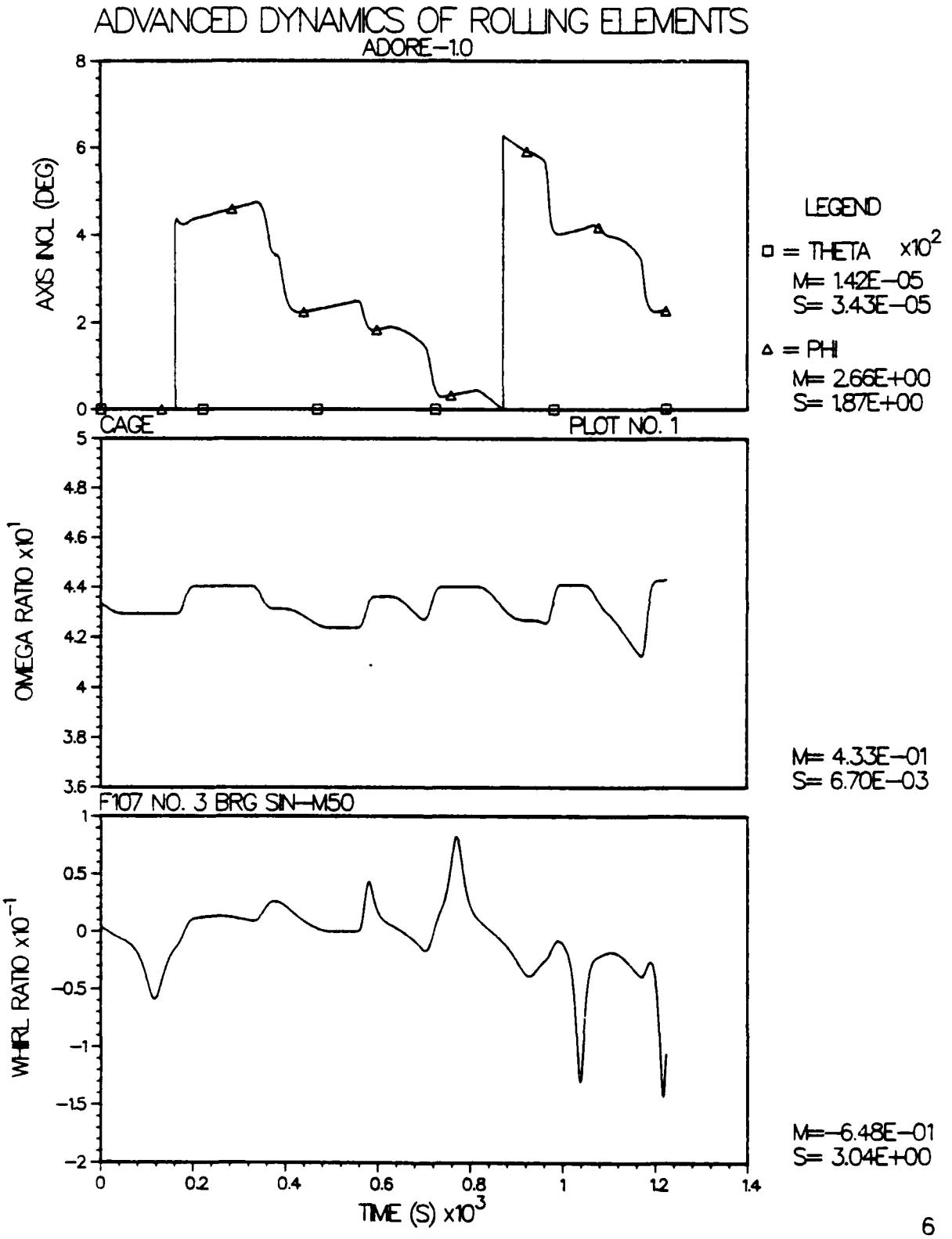

Figure 27 The Variation in Cage Mass Center Whirl and Angular Velocities

on Figure 27, denote the orientation of the cage angular velocity vector; THETA, being essentially zero, indicates no significant coning motion of the cage. The variations in the mass center whirl velocity are quite erratic on Figure 27. This implies no significant whirl orbit and the cage essentially moves around between the guide lands in an erratic fashion. This is confirmed by plotting the mass center orbit, as shown on Figure 28.

The variation in the total power loss in the bearing is shown on Figure 29. Note the increasing peaks in the power loss represent the increasing cage interactions. Over the time of simulation the average power loss, as indicated on Figure 29, is about 1.5 kilowatts. This is primarily due to the high traction coefficient at the ball/race and cage/race contacts and excessive cage interactions.

Based on the Archard's wear equation, the time average wear rates of the various bearing elements are shown on Figure 30. Although the absolute values of these rates are subject to the validity of the wear coefficients assumed, as indicated in the print output in Appendix A, at the various interactions, certain trends in the wear rates are significant. The wear rate of the ball will essentially go through a cyclic variation, due to the rotating radial load on the bearing, and it will eventually stabilize to a certain steady-state value. The wear rates of the outer and inner races have already stabilized over the range of simulation shown on Figure 30. This essentially means that the ball/race interactions are dynamically stable and these contacts will have their normal wear life. The wear of the cage, however, continues to increase as a function of time; this is due to the increasing interactions at the ball/cage and cage/race interactions. Such an increasing wear rate represents a possible instability as discussed earlier.

D. Comparison of Computer Predictions with Experimental Full Bearing Data

Experimental data on the performance of the bearing under consideration was recently obtained by Meeks and Eusepi[4]. The bearing materials and the operating conditions were similar to those assumed in the present investigation. The duration of tests in the bearing program was quite limited, being dominated by cage failures, in some cases the cage was completely destroyed while in other cases the two rims of the cage were separated due to the fractured pockets.

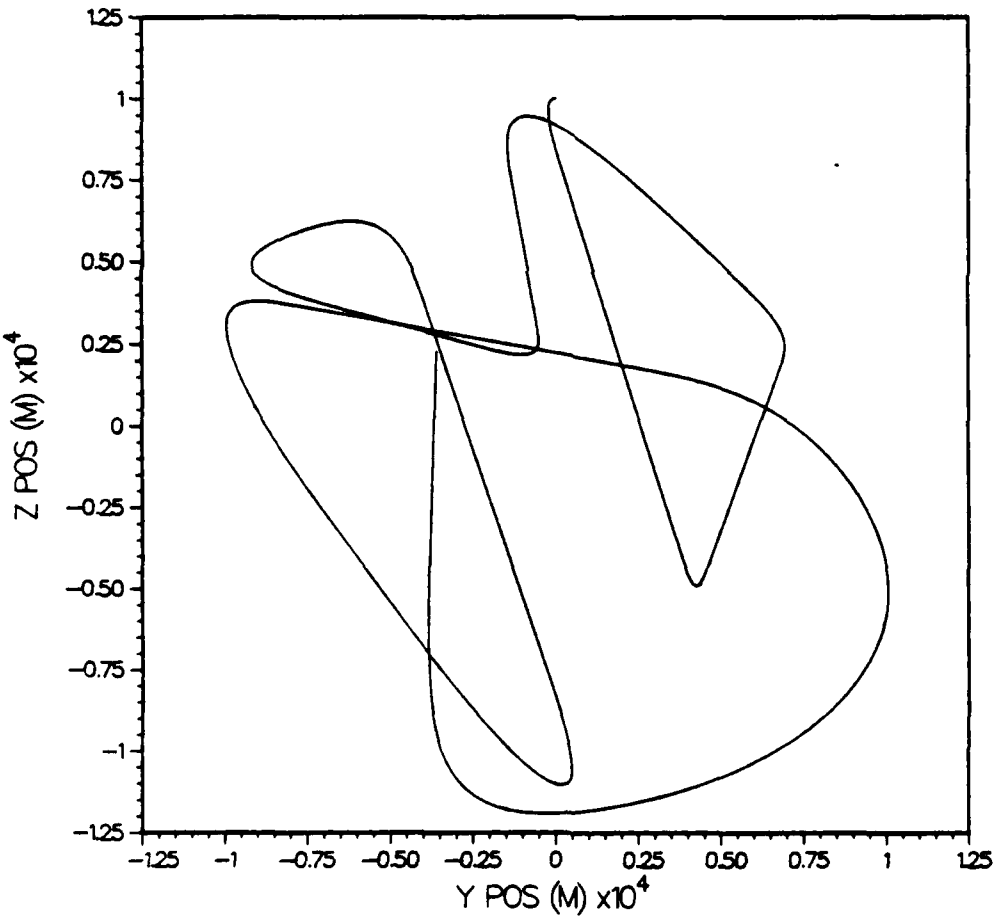

9

Figure 28 Cage Mass Center Whirl Orbit

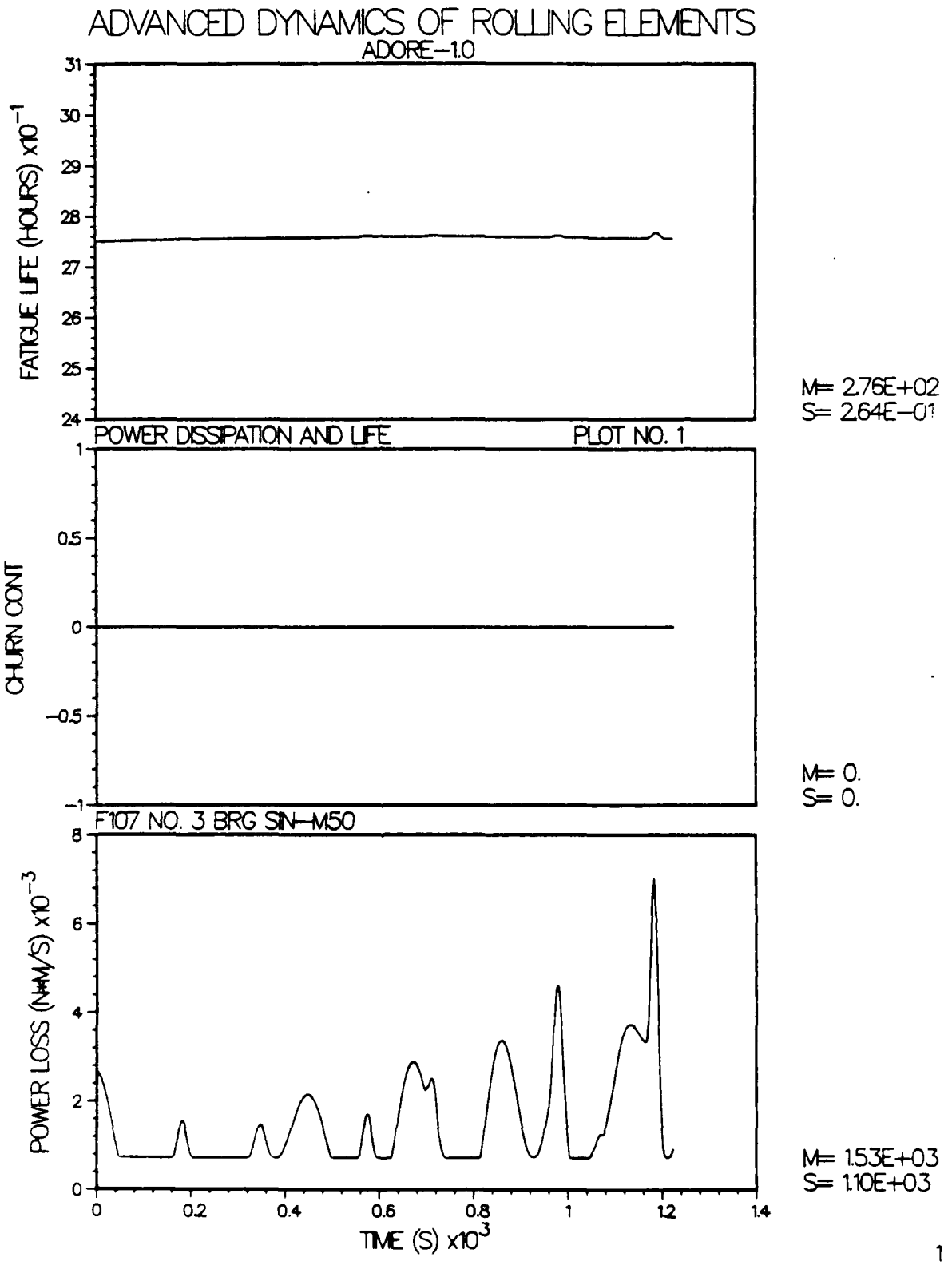

Figure 29 Total Power Loss in the Bearing as a Function of Time

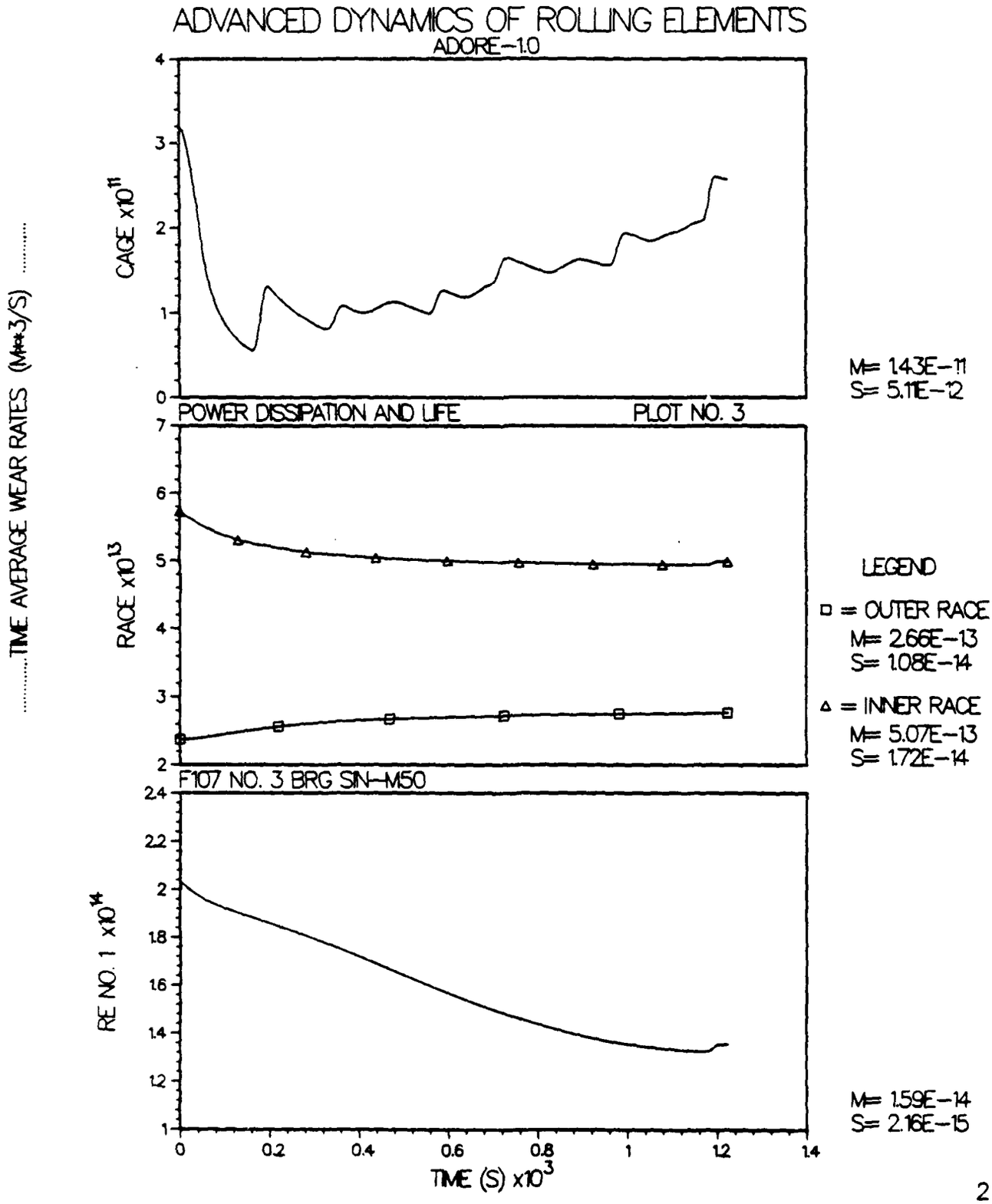

Figure 30 Simulated Wear Rates of the Bearing Elements

Figure 31 shows a typical cage after failure. The balls and races, however, were free of any substantial damage in most cases. These observations are, clearly, in extremely good agreement with the computer predictions discussed above. Thus the modeling techniques used in the present investigation are proven to be reasonably sound. This validation also establishes the significance of the fundamental friction experiments for deriving the friction behavior in the bearing.

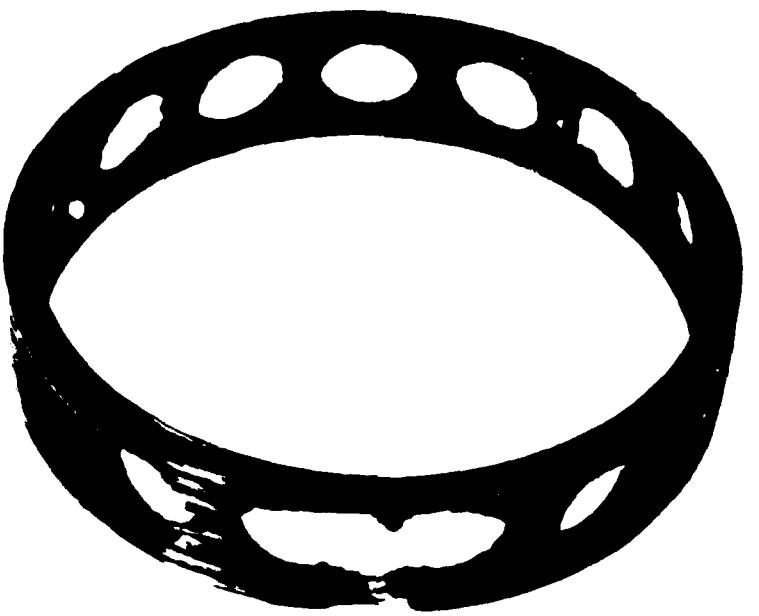

Figure 31 Self-Lubricating Composite Cage after Full Bearing Testing

SECTION III
CONCLUSIONS

The computer simulation of a high temperature engine ball bearing operating with solid lubrication was successfully completed. To achieve this, the study utilized experimental friction and wear data which was modeled and used as input to the advanced bearing dynamics computer program ADORE.

Three materials considered suitable for high temperature operation, namely M-50 tool steel, NC-132 silicon nitride and Alpha Silicon Carbide, were experimentally evaluated in a pin on disc type tester to obtain friction and wear data. Two variations of HAC-1 material containing "Westinghouse Compound" lubricant in a composite structure were utilized in these experiments.

In the first series of tests, the friction, wear and lubricating behavior of HAC-1 against M-50 and NC-132 discs was determined at sliding contact speeds up to 30,000 rpm, and ambient temperatures up to 316° C (600° F) and over a range of loads, conditions which were considered to be representative of cage operation in the high speed bearing. These tests showed superior performance of the HAC-1 vs. NC-132 pair compared to HAC-1 vs. M-50 in terms of stable temperatures, higher load capacity, lower coefficients of friction and lower wear rates of the lubricant composite. This data was used in establishing a model for the computer program input.

This result suggests that applying a coating of silicon nitride onto M-50 bearing races in the areas of cage contact might be beneficial in future bearing designs.

In the second series of experimental tests, the low speed skidding or sliding velocities occurring between balls and races during normal operation were simulated by sliding a ball against a disc. All three bearing materials were used at sliding speed of 0 to 15 cm/s and at temperatures up to 427° C (800° F). The sliding contact received lubrication by rubbing a stick of the HAC-1 material against the disc to achieve transfer to the contact zone. The initial Hertzian contact stress between the ball and disc was typically around 1,550 MPa (225,000 psi).

This testing showed that the contact stresses reduced rapidly due to ball wear with all material combinations. Coefficients of friction were high in the upper parts of the test speed range, being in the range of 0.4 to 0.8 for the NC-132 vs. M-50 and NC-132 vs. NC-132 pairs and even higher for the Alpha Silicon Carbide vs. itself and the sliding contacts at times generated significant audible noise. These friction levels are somewhat higher than those found in the literature[2,5]; this is believed to be due to the high contact stresses causing rapid wear and related surface roughness. Data from the NC-132 vs. M-50 tests were used to establish a model for the computer program input.

The F107 #3 bearing, comprised of M-50 races, silicon nitride balls and the HAC-1 composite cage, was modeled, the traction coefficient at the ball/race contacts determined, and the dynamic performance of the bearing was simulated.

The computer results demonstrated that due to high traction coefficients at the ball/race interface, the ball/cage forces are quite large and the collision in the cage pockets and at the cage/race interface are quite severe and rather erratic. Furthermore, the dynamic simulations indicate that the cage interactions gradually increase as a function of time leading to increasing loads and, therefore, increasing wear rates of the cage. This mode of instability led to a situation where severe ball/cage collisions occurred simultaneously in several adjacent pockets. The rather large magnitude of these collision forces simulates a potential cage failure. These results agree with actual bearing tests, carried out earlier, where cage failures resulting in torn pockets were observed.

The good agreement between the computer predictions achieved with the ADORE computer program and the experimentally observed bearing behavior demonstrates the significance of the computer modeling approach through fundamental experiments which define the friction behavior in the bearing, such as those undertaken in the present investigation, for actual bearing design and materials development for advanced bearing applications, such as the cruise missile engine.

SECTION IV
RECOMMENDATIONS

Based on the feasibility of the modeling approach established during the present investigation, it is recommended that with the objective of developing a solid lubricated ball bearing for the cruise missile type application the research and development effort must be directed towards five principal areas:

1. The development of materials and lubricants is probably the most significant area. The close coupling between the materials behavior and the bearing performance demands that this development effort be carried out with very close coordination with friction tests and the computer modeling of bearing performance discussed below.

2. Modeling of the friction behavior of the candidate materials is perhaps the most important task in the bearing design process. It is recommended that fundamental friction experiments of the type undertaken during the present investigation be performed using a larger number of test specimens which will permit greater separation of test conditions and the repeating of data points to model the friction characteristics at the various interactions in the bearing. In addition to supplying the necessary inputs for bearing design, these experiments will provide efficient screening of candidate materials.

3. The design of a lubricant transport system which ensures the presence of the lubricant at the various interactions in the bearing is crucial to acceptable bearing performance. For example, whether the lubricant should be impregnated in the cage, supplied as fine powder particles in a gaseous carrier, or supplied in the form of a sputtered, vacuum deposited or ion-implanted coating, must be investigated in parallel with the materials development effort.

4. Computer modeling of bearing performance provides the principal coordination between the materials behavior and the bearing performance. The computer simulations are extremely effective and efficient, as

demonstrated in the present investigation, in both the design of bearings and in defining the range of acceptable materials behavior to meet the bearing performance specification. It is essential that the available computer models be used in close conjunction with the materials development and the friction experiments proposed above.

5. Finally, the actual bearing tests which will demonstrate acceptable bearing performance for the candidate designs, derived from the above development steps, will be essential. In addition to establishing the overall significance of the above development effort, such test will continually strengthen the computer modeling and design techniques for rolling element bearings.

REFERENCES

1. Gupta, P.K., "Advanced Dynamics of Rolling Elements", published by Springer-Verlag, 1984.

2. Bhushan, B., Sibley, L.B., "Silicon Nitride Rolling Bearings for Extreme Operating Conditions", ASLE Preprint 81-LC-4C-1, October 5, 1981.

3. Gardos, M.N., "Solid Lubricated Rolling Element Bearings Final Report", AFWAL-TR-83-4129, February 1984.

4. Meeks, C. R., Eusepi, M. W., "Solid Lubricated Rolling Element Bearings - Part V: Development of High Speed, High Temperature Bearings for Turbine Engines", Third International Solid Lubricants Conferences, Denver, CO., August 5, 1984.

5. Kyoto Ceramic Company Ltd., Catalog Test Data for Silicon Carbide, 1980.

APPENDIX A

COMPUTER OUTPUT

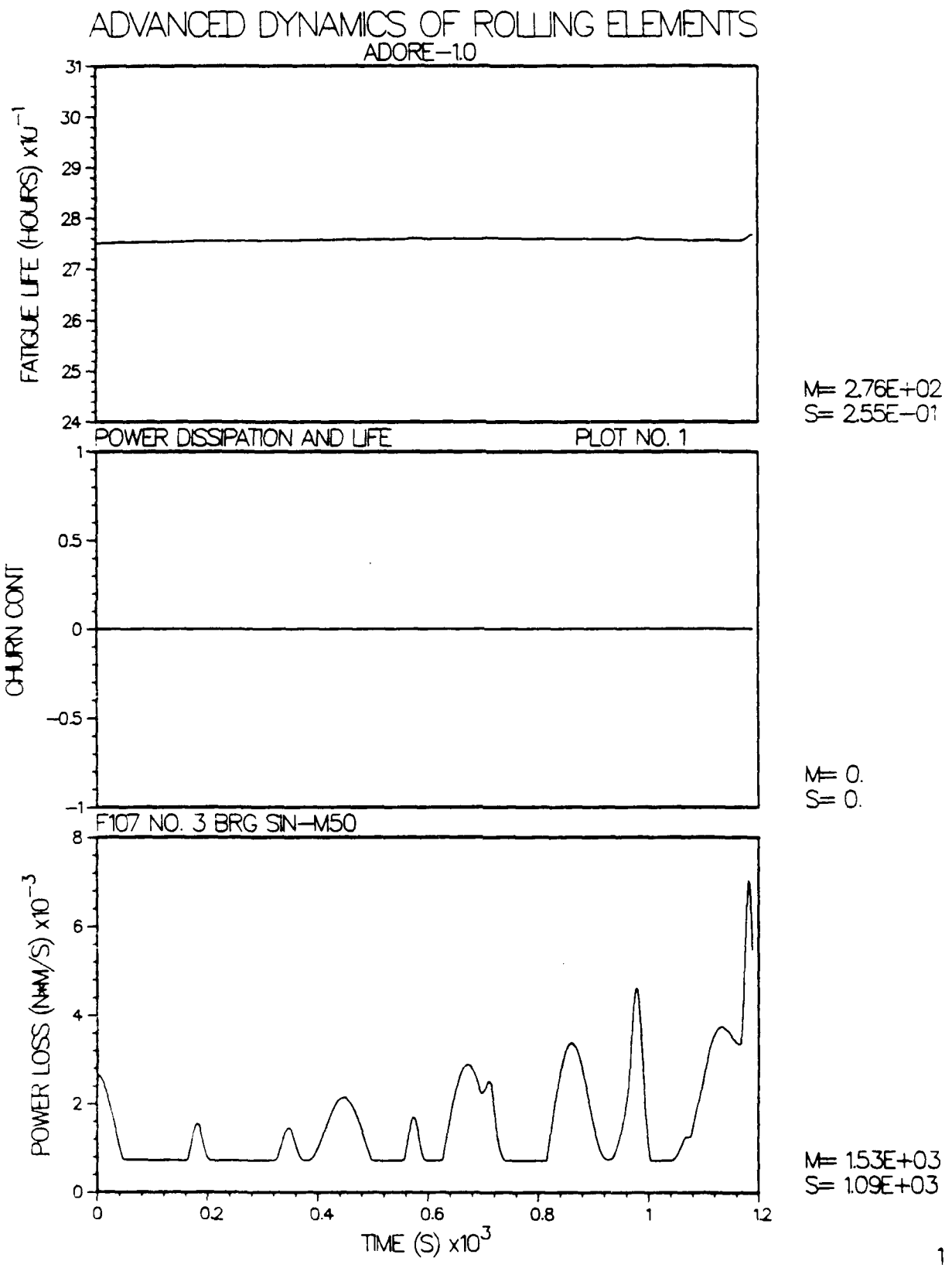
ADVANCED DYNAMICS OF ROLLING ELEMENTS
ADORE-1.0
FATIGUE LIFE (HOURS) X10^{-1}
31
30
29
28
27
26
25
24
M= 2.76E+02
S= 2.55E-01
POWER DISSIPATION AND LIFE
PLOT NO. 1
CHURN CONT
1
0.5
0
-0.5
-1
M= 0.
S= 0.
F107 NO. 3 BRG SIN-M50
POWER LOSS (N*M/S) X10^{-3}
8
6
4
2
0
0
0.2
0.4
0.6
0.8
1
1.2
TIME (S) X10^{3}
M= 1.53E+03
S= 1.09E+03
1

STEP NO	TAU	TIME (S)	OUTER RACE ROT (DEG)	INNER RACE ROT (DEG)	
160	1.239E+00	5.220E-05	0.	1.989E+01	F107 NO. 3 BRG SIN-M50

3. APPLIED PARAMETERS

	APPLIED FORCES (N) COMP-X	(N) COMP-Y	(N) COMP-Z	APPLIED MOMENTS (N*M) COMP-X	(N*M) COMP-Y	(N*M) COMP-Z
CAGE	0.	0.	1.584E-02	0.	0.	0.
ORACE	5.098E+02	-7.516E+01	2.073E+02	1.093E-01	1.350E+00	5.217E-01
IRACE	-4.594E+02	7.741E+01	-2.116E+02	-7.047E-02	-1.445E+00	-1.737E-03

BASIC FATIGUE LIFE	(HOURS)	2.753E+02
INTERNAL CLEARANCE	(M)	-2.195E-05
OUTER RACE FIT	(M)	0.
INNER RACE FIT	(M)	-5.063E-06
TOTAL POWER LOSS	(N*M/S)	7.327E+02
CHURNING LOSS FRACTION		0.

4. TIME STEP SUMMARY

STEP NO	TIME (S)	OUTER RACE ROTATION (DEG)	INNER RACE ROTATION (DEG)	TIME AVERAGE PARAMETERS: FATIGUE LIFE (HOURS)	POWER LOSS (N*M/S)	RE ORBITAL VEL RATIO	CAGE OMEGA RATIO	CAGE WHIRL RATIO	CAGE WEAR RATE (M**3/S)
160	5.220E-05	0.	1.989E+01	2.752E+02	1.774E+03	4.335E-01	4.307E-01	-2.332E-01	1.715E-11

EXECUTION COMPLETED
EXIT FROM -ADORE- DUE TO MAXIMUM STEP COUNT

STATISTICS OF THIS RUN

MINIMUM STEP SIZE	=	5.00000E-04
MAXIMUM STEP SIZE	=	8.22345E-03
LAST STEP SIZE	=	8.22345E-03
MAX AVE TRUNCATION	=	3.71528E-06
TOTAL DERIVATIVE CALLS	=	1309

STEP NO	TAU	TIME (S)	OUTER RACE ROT (DEG)	INNER RACE ROT (DEG)	
160	1.239E+00	5.220E-05	0.	1.989E+01	F107 NO. 3 BRG SIN-M50

2. RACE AND CAGE PARAMETERS

RE NO	RE/CAGE INTERACTION GEO INT (M)	CONTACT FORCE (N)	CONTACT ANGLE (DEG)	CONTACT LOSS (N*M/S)	TIME AVE WEAR RATE (M**3/S)
1	9.942E-05	0.	1.854E+02	0.	0.
2	7.664E-05	0.	1.829E+02	0.	0.
3	5.810E-05	0.	1.819E+02	0.	0.
4	4.613E-05	0.	1.812E+02	0.	0.
5	4.207E-05	0.	1.806E+02	0.	0.
6	4.626E-05	0.	1.800E+02	0.	0.
7	5.811E-05	0.	1.791E+02	0.	0.
8	7.626E-05	0.	1.778E+02	0.	0.
9	9.853E-05	0.	1.745E+02	0.	0.
10	1.212E-04	0.	1.333E+02	0.	0.
11	1.054E-04	0.	7.454E+00	0.	0.
12	8.854E-05	0.	3.060E+00	0.	0.
13	7.916E-05	0.	1.350E+00	0.	0.
14	7.886E-05	0.	1.216E-01	0.	0.
15	8.772E-05	0.	3.587E+02	0.	0.
16	1.043E-04	0.	3.555E+02	0.	0.
17	1.225E-04	0.	2.371E+02	0.	0.

LAND NO	RACE/CAGE FORCES (N) NORMAL	(N) TRACTION	(DEG) CON ANGLE	(DEG) ATT ANGLE	RACE/CAGE GEO INT (M)	RACE/CAGE SLIP VEL (M/S)	EFFECTIVE DIA PLAY (M)	CONTACT LOSS (N*M/S)	TIME AVE WEAR RATE (M**3/S)
1	0.	0.	8.567E+00	-1.800E+02	5.069E-06	0.	1.444E-04	0.	8.576E-12
2	0.	0.	8.567E+00	-1.800E+02	5.069E-06	0.	1.444E-04	0.	8.576E-12

	MASS CENTER POSITION AXIAL (M)	RADIAL (M)	ORBITAL (DEG)	ORBITAL VELOCITY (RPM)	ANGULAR VELOCITY AMPLITUDE (RPM)	THETA (DEG)	PHI (DEG)	ANG POSITION THETA (DEG)	PHI (DEG)	HOOP STRESS (PA)	TIME AVE WEAR RATE (M**3/S)
CAGE	-1.100E-05	6.711E-05	3.554E+02	-5.087E+04	2.726E+04	0.	0.	0.	0.	5.032E+06	0.
ORACE	0.	0.	0.	0.	0.	0.	0.	0.	0.	0.	2.402E-13
IRACE	-4.839E-06	1.456E-06	1.989E+01	6.350E+04	6.350E+04	0.	0.	0.	0.	8.951E+07	5.515E-13

RE NO	....SLIP VELOCITY.... (M/S)		.....TRAC COEFF.....		....ISO LUB FILM..... (M)		...THERMAL RED FAC...		.....DRAG (N)	..CHUR MOM (N*M)	..NET LOSS (N*M/S) (DRAG+CHUR)
	OUTER RACE	INNER RACE	OUTER RACE	INNER RACE	OUTER RACE	INNER RACE	OUTER RACE	INNER RACE			
1	-1.246E-01	-1.048E-02	-5.995E-01	-2.516E-01							
2	-1.270E-01	-1.002E-02	-5.995E-01	-2.405E-01							
3	-1.276E-01	-9.408E-03	-5.994E-01	-2.258E-01							
4	-1.279E-01	-8.328E-03	-5.993E-01	-1.999E-01							
5	-1.259E-01	-6.933E-03	-5.992E-01	-1.664E-01							
6	-1.221E-01	-5.431E-03	-5.990E-01	-1.303E-01							
7	-1.173E-01	-4.272E-03	-5.989E-01	-1.025E-01							
8	-1.129E-01	-4.004E-03	-5.989E-01	-9.609E-02							
9	-1.095E-01	-4.857E-03	-5.989E-01	-1.166E-01							
10	-1.071E-01	-6.586E-03	-5.989E-01	-1.581E-01							
11	-1.057E-01	-8.476E-03	-5.990E-01	-2.034E-01							
12	-1.055E-01	-9.850E-03	-5.990E-01	-2.364E-01							
13	-1.067E-01	-1.053E-02	-5.991E-01	-2.526E-01							
14	-1.097E-01	-1.061E-02	-5.992E-01	-2.546E-01							
15	-1.136E-01	-1.065E-02	-5.993E-01	-2.557E-01							
16	-1.177E-01	-1.067E-02	-5.994E-01	-2.560E-01							
17	-1.215E-01	-1.064E-02	-5.994E-01	-2.554E-01							

STEP NO	TAU	TIME (S)	OUTER RACE ROT (DEG)	INNER RACE ROT (DEG)	
160	1.239E+00	5.220E-05	0.	1.989E+01	F107 NO. 3 BRG SIN-M50

1. ROLLING ELEMENT PARAMETERS

RE NO	...ORBITAL POSITION (DEG)	....CONTACT ANGLE.... (DEG)		....CONTACT LOAD..... (N)		...CONTACT STRESS.... (PA)		..MAJOR HALF WIDTH... (M)		..MINOR HALF WIDTH... (M)	
		OUTER RACE	INNER RACE	OUTER RACE	INNER RACE	OUTER RACE	INNER RACE	OUTER RACE	INNER RACE	OUTER RACE	INNER RACE
1	8.597E+00	1.358E+01	1.934E+01	1.506E+02	1.067E+02	1.610E+09	1.875E+09	5.793E-04	4.021E-04	7.712E-05	6.759E-05
2	2.977E+01	1.358E+01	1.934E+01	1.508E+02	1.069E+02	1.610E+09	1.876E+09	5.795E-04	4.023E-04	7.715E-05	6.762E-05
3	5.095E+01	1.346E+01	1.942E+01	1.463E+02	1.024E+02	1.594E+09	1.850E+09	5.738E-04	3.966E-04	7.639E-05	6.667E-05
4	7.214E+01	1.320E+01	1.957E+01	1.383E+02	9.427E+01	1.564E+09	1.799E+09	5.630E-04	3.858E-04	7.496E-05	6.485E-05
5	9.332E+01	1.283E+01	1.980E+01	1.281E+02	8.403E+01	1.525E+09	1.731E+09	5.489E-04	3.712E-04	7.309E-05	6.242E-05
6	1.145E+02	1.237E+01	2.007E+01	1.178E+02	7.355E+01	1.483E+09	1.656E+09	5.337E-04	3.551E-04	7.108E-05	5.972E-05
7	1.357E+02	1.188E+01	2.036E+01	1.088E+02	6.438E+01	1.444E+09	1.584E+09	5.198E-04	3.397E-04	6.923E-05	5.714E-05
8	1.569E+02	1.144E+01	2.061E+01	1.021E+02	5.750E+01	1.413E+09	1.525E+09	5.088E-04	3.271E-04	6.778E-05	5.503E-05
9	1.781E+02	1.113E+01	2.079E+01	9.796E+01	5.329E+01	1.394E+09	1.487E+09	5.019E-04	3.189E-04	6.686E-05	5.366E-05
10	1.992E+02	1.102E+01	2.085E+01	9.652E+01	5.183E+01	1.387E+09	1.473E+09	4.994E-04	3.160E-04	6.654E-05	5.317E-05
11	2.204E+02	1.112E+01	2.079E+01	9.776E+01	5.311E+01	1.393E+09	1.485E+09	5.016E-04	3.186E-04	6.682E-05	5.360E-05
12	2.416E+02	1.142E+01	2.062E+01	1.017E+02	5.715E+01	1.411E+09	1.522E+09	5.082E-04	3.265E-04	6.769E-05	5.492E-05
13	2.627E+02	1.185E+01	2.037E+01	1.082E+02	6.387E+01	1.441E+09	1.580E+09	5.189E-04	3.388E-04	6.911E-05	5.699E-05
14	2.839E+02	1.234E+01	2.008E+01	1.171E+02	7.290E+01	1.480E+09	1.651E+09	5.327E-04	3.541E-04	7.094E-05	5.955E-05
15	3.051E+02	1.281E+01	1.981E+01	1.274E+02	8.333E+01	1.522E+09	1.726E+09	5.479E-04	3.702E-04	7.295E-05	6.225E-05
16	3.263E+02	1.318E+01	1.958E+01	1.376E+02	9.364E+01	1.562E+09	1.795E+09	5.621E-04	3.849E-04	7.485E-05	6.471E-05
17	3.474E+02	1.344E+01	1.942E+01	1.459E+02	1.020E+02	1.592E+09	1.847E+09	5.732E-04	3.960E-04	7.631E-05	6.657E-05

RE NO	...ORBITAL VELOCITY (RPM)	.....ANGULAR VELOCITY..... AMPLITUDE (RPM)	THETA (DEG)	PHI (DEG)	...RE ANG POSITION... THETA (DEG)	PHI (DEG)	.....SPIN/ROLL.....		....CONTACT LOSS..... (N*M/S)		..TIME AVE WEAR RATE (M**3/S)
							OUTER RACE	INNER RACE	OUTER RACE	INNER RACE	
1	2.744E+04	2.174E+05	-1.299E+01	3.600E+02	1.121E+01	1.765E+02	-2.214E-02	1.439E-01	1.936E+01	3.781E+01	1.961E-14
2	2.744E+04	2.174E+05	-1.294E+01	3.600E+02	1.115E+01	1.765E+02	-2.104E-02	1.447E-01	1.930E+01	3.808E+01	1.944E-14
3	2.745E+04	2.175E+05	-1.272E+01	3.600E+02	1.098E+01	1.764E+02	-1.884E-02	1.494E-01	1.822E+01	3.713E+01	1.852E-14
4	2.746E+04	2.177E+05	-1.235E+01	3.600E+02	1.069E+01	1.761E+02	-1.583E-02	1.578E-01	1.640E+01	3.510E+01	1.703E-14
5	2.749E+04	2.179E+05	-1.186E+01	3.600E+02	1.032E+01	1.758E+02	-1.256E-02	1.693E-01	1.432E+01	3.228E+01	1.527E-14
6	2.752E+04	2.182E+05	-1.131E+01	3.600E+02	9.895E+00	1.755E+02	-9.707E-03	1.827E-01	1.237E+01	2.912E+01	1.354E-14
7	2.756E+04	2.186E+05	-1.079E+01	3.600E+02	9.486E+00	1.752E+02	-7.849E-03	1.960E-01	1.080E+01	2.613E+01	1.207E-14
8	2.760E+04	2.189E+05	-1.037E+01	3.600E+02	9.162E+00	1.750E+02	-7.265E-03	2.070E-01	9.713E+00	2.372E+01	1.100E-14
9	2.762E+04	2.191E+05	-1.013E+01	3.600E+02	8.982E+00	1.749E+02	-7.874E-03	2.140E-01	9.090E+00	2.213E+01	1.038E-14
10	2.762E+04	2.191E+05	-1.011E+01	3.600E+02	8.980E+00	1.748E+02	-9.380E-03	2.155E-01	8.905E+00	2.148E+01	1.024E-14
11	2.761E+04	2.190E+05	-1.030E+01	3.600E+02	9.155E+00	1.748E+02	-1.143E-02	2.114E-01	9.148E+00	2.178E+01	1.057E-14
12	2.758E+04	2.187E+05	-1.067E+01	3.600E+02	9.474E+00	1.750E+02	-1.369E-02	2.025E-01	9.834E+00	2.302E+01	1.136E-14
13	2.755E+04	2.184E+05	-1.117E+01	3.600E+02	9.880E+00	1.752E+02	-1.592E-02	1.903E-01	1.099E+01	2.512E+01	1.260E-14
14	2.751E+04	2.181E+05	-1.170E+01	3.600E+02	1.030E+01	1.755E+02	-1.801E-02	1.769E-01	1.261E+01	2.788E+01	1.420E-14
15	2.748E+04	2.178E+05	-1.220E+01	3.600E+02	1.068E+01	1.758E+02	-1.985E-02	1.643E-01	1.458E+01	3.098E+01	1.599E-14
16	2.746E+04	2.176E+05	-1.261E+01	3.600E+02	1.096E+01	1.761E+02	-2.132E-02	1.541E-01	1.664E+01	3.397E+01	1.768E-14
17	2.744E+04	2.175E+05	-1.288E+01	3.600E+02	1.114E+01	1.764E+02	-2.217E-02	1.471E-01	1.838E+01	3.636E+01	1.898E-14

STEP NO	TAU	TIME (S)	OUTER RACE ROT (DEG)	INNER RACE ROT (DEG)	
0	0.	0.	0.	0.	F107 NO. 3 BRG SIN-M50

3. APPLIED PARAMETERS

	APPLIED FORCES (N) COMP-X	APPLIED FORCES (N) COMP-Y	APPLIED FORCES (N) COMP-Z	APPLIED MOMENTS (N*M) COMP-X	APPLIED MOMENTS (N*M) COMP-Y	APPLIED MOMENTS (N*M) COMP-Z
CAGE	0.	3.202E+01	-5.334E+01	-6.616E-01	0.	0.
ORACE	4.500E+02	-3.494E+01	2.757E+02	1.224E+00	1.392E+00	-2.848E-03
IRACE	-4.478E+02	2.031E+00	-2.251E+02	7.728E-03	-1.413E+00	-2.743E-02

BASIC FATIGUE LIFE	(HOURS)	2.884E+02
INTERNAL CLEARANCE	(M)	2.195E-05
OUTER RACE FIT	(M)	0.
INNER RACE FIT	(M)	-5.063E-06
TOTAL POWER LOSS	(N*M/S)	2.681E+03
CHURNING LOSS FRACTION		0.

4. TIME STEP SUMMARY

STEP NO	TIME (S)	OUTER RACE ROTATION (DEG)	INNER RACE ROTATION (DEG)	TIME AVERAGE PARAMETERS: FATIGUE LIFE (HOURS)	POWER LOSS (N*M/S)	RE ORBITAL VEL RATIO	CAGE OMEGA RATIO	CAGE WHIRL RATIO	CAGE WEAR RATE (M**3/S)
0	0.	0.	0.	2.884E+02	2.681E+03	4.338E-01	4.338E-01	4.338E-01	3.196E-11

***TRUNCATION CHECK AT STEP NO 1 DIMENSIONLESS TIME = 5.00000E-04 STEP SIZE = 5.00000E-04 MAX ERROR = 1.63071E-04

STEP NO	TAU	TIME (S)	OUTER RACE ROT (DEG)	INNER RACE ROT (DEG)	
0	0.	0.	0.	0.	F107 NO. 3 BRG SIN-M50

2. RACE AND CAGE PARAMETERS

RE NO	RE/CAGE INTERACTION GEO INT (M)	CONTACT FORCE (N)	CONTACT ANGLE (DEG)	CONTACT LOSS (N*M/S)	TIME AVE WEAR RATE (M**3/S)
1	1.226E-04	0.	2.700E+02	0.	0.
2	8.880E-05	0.	1.836E+02	0.	0.
3	5.760E-05	0.	1.816E+02	0.	0.
4	3.547E-05	0.	1.808E+02	0.	0.
5	2.543E-05	0.	1.802E+02	0.	0.
6	2.882E-05	0.	1.797E+02	0.	0.
7	4.518E-05	0.	1.789E+02	0.	0.
8	7.231E-05	0.	1.775E+02	0.	0.
9	1.064E-04	0.	1.716E+02	0.	0.
10	1.064E-04	0.	8.355E+00	0.	0.
11	7.231E-05	0.	2.482E+00	0.	0.
12	4.518E-05	0.	1.096E+00	0.	0.
13	2.882E-05	0.	3.438E-01	0.	0.
14	2.543E-05	0.	3.598E+02	0.	0.
15	3.547E-05	0.	3.592E+02	0.	0.
16	5.760E-05	0.	3.584E+02	0.	0.
17	8.880E-05	0.	3.564E+02	0.	0.

LAND NO	RACE/CAGE FORCES (N) NORMAL	(N) TRACTION	(DEG) CON ANGLE	(DEG) ATT ANGLE	RACE/CAGE GEO INT (M)	RACE/CAGE SLIP VEL (M/S)	EFFECTIVE DIA PLAY (M)	CONTACT LOSS (N*M/S)	TIME AVE WEAR RATE (M**3/S)
1	2.668E+01	1.601E+01	3.600E+02	-1.800E+02	-2.943E-05	5.990E+01	1.421E-04	9.589E+02	1.598E-11
2	2.668E+01	1.601E+01	3.600E+02	-1.800E+02	-2.943E-05	5.990E+01	1.421E-04	9.589E+02	1.598E-11

	MASS CENTER POSITION AXIAL (M)	RADIAL (M)	ORBITAL (DEG)	ORBITAL VELOCITY (RPM)	ANGULAR VELOCITY AMPLITUDE (RPM)	THETA (DEG)	PHI (DEG)	ANG POSITION THETA (DEG)	PHI (DEG)	HOOP STRESS (PA)	TIME AVE WEAR RATE (M**3/S)
CAGE	-1.100E-05	1.000E-04	0.	2.755E+04	2.755E+04	0.	0.	0.	0.	5.138E+06	0.
ORACE	0.	0.	0.	0.	0.	0.	0.	0.	0.	0.	2.373E-13
IRACE	-4.839E-06	1.456E-06	0.	6.350E+04	6.350E+04	0.	0.	0.	0.	8.951E+07	5.734E-13

RE NO	....SLIP VELOCITY.... (M/S)		.....TRAC COEFF.....		....ISO LUB FILM..... (M)		...THERMAL RED FAC...		.....DRAG (N)	..CHUR MOM (N*M)	..NET LOSS (N*M/S) (DRAG+CHUR)
	OUTER RACE	INNER RACE	OUTER RACE	INNER RACE	OUTER RACE	INNER RACE	OUTER RACE	INNER RACE			
1	-1.436E-01	-9.682E-03	-6.000E-01	-2.324E-01							
2	-1.421E-01	-9.028E-03	-6.000E-01	-2.167E-01							
3	-1.379E-01	-7.155E-03	-6.000E-01	-1.717E-01							
4	-1.319E-01	-4.315E-03	-6.000E-01	-1.036E-01							
5	-1.250E-01	-8.927E-04	-6.000E-01	-2.142E-02							
6	-1.184E-01	2.650E-03	-6.000E-01	6.360E-02							
7	-1.129E-01	5.835E-03	-6.000E-01	1.400E-01							
8	-1.092E-01	8.232E-03	-6.000E-01	1.976E-01							
9	-1.073E-01	9.517E-03	-6.000E-01	2.284E-01							
10	-1.073E-01	9.517E-03	-6.000E-01	2.284E-01							
11	-1.092E-01	8.232E-03	-6.000E-01	1.976E-01							
12	-1.129E-01	5.835E-03	-6.000E-01	1.400E-01							
13	-1.184E-01	2.650E-03	-6.000E-01	6.360E-02							
14	-1.250E-01	-8.927E-04	-6.000E-01	-2.142E-02							
15	-1.319E-01	-4.315E-03	-6.000E-01	-1.036E-01							
16	-1.379E-01	-7.155E-03	-6.000E-01	-1.717E-01							
17	-1.421E-01	-9.028E-03	-6.000E-01	-2.167E-01							

STEP NO	TAU	TIME (S)	OUTER RACE ROT (DEG)	INNER RACE ROT (DEG)	
0	0.	0.	0.	0.	F107 NO. 3 BRG SIN-M50

1. ROLLING ELEMENT PARAMETERS

RE NO	ORBITAL POSITION (DEG)	CONTACT ANGLE (DEG)		CONTACT LOAD (N)		CONTACT STRESS (PA)		MAJOR HALF WIDTH (M)		MINOR HALF WIDTH (M)	
		OUTER RACE	INNER RACE	OUTER RACE	INNER RACE	OUTER RACE	INNER RACE	OUTER RACE	INNER RACE	OUTER RACE	INNER RACE
1	0.	1.359E+01	1.933E+01	1.514E+02	1.074E+02	1.612E+09	1.879E+09	5.803E-04	4.029E-04	7.725E-05	6.773E-05
2	2.118E+01	1.352E+01	1.937E+01	1.490E+02	1.051E+02	1.604E+09	1.865E+09	5.773E-04	4.000E-04	7.685E-05	6.723E-05
3	4.235E+01	1.333E+01	1.949E+01	1.425E+02	9.845E+01	1.580E+09	1.825E+09	5.687E-04	3.914E-04	7.571E-05	6.580E-05
4	6.353E+01	1.301E+01	1.969E+01	1.331E+02	8.896E+01	1.544E+09	1.765E+09	5.559E-04	3.784E-04	7.402E-05	6.362E-05
5	8.471E+01	1.259E+01	1.994E+01	1.226E+02	7.837E+01	1.503E+09	1.691E+09	5.409E-04	3.627E-04	7.203E-05	6.100E-05
6	1.059E+02	1.210E+01	2.022E+01	1.128E+02	6.845E+01	1.461E+09	1.617E+09	5.262E-04	3.467E-04	7.008E-05	5.831E-05
7	1.271E+02	1.163E+01	2.050E+01	1.050E+02	6.042E+01	1.426E+09	1.550E+09	5.136E-04	3.326E-04	6.842E-05	5.594E-05
8	1.482E+02	1.125E+01	2.072E+01	9.963E+01	5.494E+01	1.402E+09	1.502E+09	5.047E-04	3.222E-04	6.724E-05	5.420E-05
9	1.694E+02	1.104E+01	2.084E+01	9.696E+01	5.219E+01	1.389E+09	1.476E+09	5.002E-04	3.167E-04	6.664E-05	5.329E-05
10	1.906E+02	1.104E+01	2.084E+01	9.696E+01	5.219E+01	1.389E+09	1.476E+09	5.002E-04	3.167E-04	6.664E-05	5.329E-05
11	2.118E+02	1.125E+01	2.072E+01	9.963E+01	5.494E+01	1.402E+09	1.502E+09	5.047E-04	3.222E-04	6.724E-05	5.420E-05
12	2.329E+02	1.163E+01	2.050E+01	1.050E+02	6.042E+01	1.426E+09	1.550E+09	5.136E-04	3.326E-04	6.842E-05	5.594E-05
13	2.541E+02	1.210E+01	2.022E+01	1.128E+02	6.845E+01	1.461E+09	1.617E+09	5.262E-04	3.467E-04	7.008E-05	5.831E-05
14	2.753E+02	1.259E+01	1.994E+01	1.226E+02	7.837E+01	1.503E+09	1.691E+09	5.409E-04	3.627E-04	7.203E-05	6.100E-05
15	2.965E+02	1.301E+01	1.969E+01	1.331E+02	8.896E+01	1.544E+09	1.765E+09	5.559E-04	3.784E-04	7.402E-05	6.362E-05
16	3.176E+02	1.333E+01	1.949E+01	1.425E+02	9.845E+01	1.580E+09	1.825E+09	5.687E-04	3.914E-04	7.571E-05	6.580E-05
17	3.388E+02	1.352E+01	1.937E+01	1.490E+02	1.051E+02	1.604E+09	1.865E+09	5.773E-04	4.000E-04	7.685E-05	6.723E-05

RE NO	ORBITAL VELOCITY (RPM)	ANGULAR VELOCITY AMPLITUDE (RPM)	THETA (DEG)	PHI (DEG)	RE ANG POSITION THETA (DEG)	PHI (DEG)	SPIN/ROLL OUTER RACE	SPIN/ROLL INNER RACE	CONTACT LOSS (N*M/S) OUTER RACE	CONTACT LOSS (N*M/S) INNER RACE	TIME AVE WEAR RATE (M**3/S)
1	2.746E+04	2.178E+05	-1.189E+01	0.	1.189E+01	1.800E+02	2.425E-14	1.606E-01	1.853E+01	4.251E+01	2.035E-14
2	2.747E+04	2.178E+05	-1.183E+01	0.	1.183E+01	1.800E+02	-1.447E-13	1.622E-01	1.805E+01	4.167E+01	1.991E-14
3	2.748E+04	2.179E+05	-1.166E+01	0.	1.166E+01	1.800E+02	1.150E-13	1.669E-01	1.675E+01	3.931E+01	1.869E-14
4	2.750E+04	2.181E+05	-1.139E+01	0.	1.139E+01	1.800E+02	-4.871E-15	1.746E-01	1.496E+01	3.591E+01	1.695E-14
5	2.753E+04	2.183E+05	-1.101E+01	0.	1.101E+01	1.800E+02	3.157E-15	1.849E-01	1.306E+01	3.208E+01	1.505E-14
6	2.756E+04	2.186E+05	-1.059E+01	0.	1.059E+01	1.800E+02	-6.911E-14	1.967E-01	1.138E+01	2.845E+01	1.328E-14
7	2.760E+04	2.189E+05	-1.017E+01	0.	1.017E+01	1.800E+02	-1.837E-15	2.081E-01	1.010E+01	2.547E+01	1.186E-14
8	2.763E+04	2.192E+05	-9.840E+00	0.	9.840E+00	1.800E+02	1.219E-14	2.173E-01	9.264E+00	2.341E+01	1.089E-14
9	2.765E+04	2.193E+05	-9.655E+00	0.	9.655E+00	1.800E+02	7.075E-15	2.224E-01	8.858E+00	2.236E+01	1.041E-14
10	2.765E+04	2.193E+05	-9.655E+00	0.	9.655E+00	1.800E+02	7.075E-15	2.224E-01	8.858E+00	2.236E+01	1.041E-14
11	2.763E+04	2.192E+05	-9.840E+00	0.	9.840E+00	1.800E+02	1.219E-14	2.173E-01	9.264E+00	2.341E+01	1.089E-14
12	2.760E+04	2.189E+05	-1.017E+01	0.	1.017E+01	1.800E+02	-1.837E-15	2.081E-01	1.010E+01	2.547E+01	1.186E-14
13	2.756E+04	2.186E+05	-1.059E+01	0.	1.059E+01	1.800E+02	-6.911E-14	1.967E-01	1.138E+01	2.845E+01	1.328E-14
14	2.753E+04	2.183E+05	-1.101E+01	0.	1.101E+01	1.800E+02	3.157E-15	1.849E-01	1.306E+01	3.208E+01	1.505E-14
15	2.750E+04	2.181E+05	-1.139E+01	0.	1.139E+01	1.800E+02	-4.871E-15	1.746E-01	1.496E+01	3.591E+01	1.695E-14
16	2.748E+04	2.179E+05	-1.166E+01	0.	1.166E+01	1.800E+02	1.150E-13	1.669E-01	1.675E+01	3.931E+01	1.869E-14
17	2.747E+04	2.178E+05	-1.183E+01	0.	1.183E+01	1.800E+02	-1.447E-13	1.622E-01	1.805E+01	4.167E+01	1.991E-14

INITIAL OPERATING CONDITIONS

APPL AXIAL LOAD	(N)	4.50000E+02
APPL RADIAL LOAD	(N)	2.25000E+02
SHAFT TEMP	(K)	2.95000E+02
HOUSING TEMP	(K)	2.95000E+02
ROLL ELE TEMP	(K)	2.95000E+02
ROOM TEMP	(K)	2.95000E+02
CAGE POS...AXIAL	(M)	0.
...RADIAL	(M)	1.00000E-04
..ANGULAR	(RAD)	0.

		OUTER RACE	INNER RACE	
ANGULAR VELOCITY	(RPM)	0.	6.35000E+04	
TEMPERATURE	(K)	2.95000E+02	2.95000E+02	
MISALIGNMENT-Y	(RAD)	0.	0.	
MISALIGNMENT-Z	(RAD)	0.	0.	
TRANSLATIONAL CONSTRAINTS		1 1 1	1 1 1	
ROTATIONAL CONSTRAINTS		1	1	
GRAVITY VECTOR	(M/S**2)	0.	0.	9.81000E+00
CAGE TEMPERATURE	(K)	2.95000E+02		

SCALE FACTORS AND OUTPUT CONTROLS

.....SCALE FACTORS.....		
LENGTH	(M)	2.77800E-03
LOAD	(N)	4.50000E+02
TIME	(S)	4.21189E-05

.....STEP SIZE INFO.....	
MINIMUM	5.00000E-04
MAXIMUM	1.00000E+00
INITIAL	5.00000E-03

NO OF STEPS	160		
DATA CONTROL	1	160	
AUTO PLOTS	1	18	0
	0	0	0
INT METHOD	5		

OUTPUT FROM USER ACCESSIBLE ROUTINES ---
****

INERTIAL PARAMETERS

	.....MASS (KGM)	.....MOMENT OF INERTIA..... (KGM*M**2)			.....MASS TO GEO CENTER..... (M)		
		X-COMP	Y-COMP	Z-COMP	X-COMP	Y-COMP	Z-COMP
RE	2.87366E-04	8.87074E-10	8.87074E-10	8.87074E-10	0.	0.	0.
CAGE	1.61468E-03	6.25153E-07	3.21604E-07	3.21604E-07	0.	0.	0.

LUBRICATION PARAMETERS

	CRITICAL FILM (M)	TRAC COEFF AT ZERO SLIP	MAXIMUM TRAC COEFF	TRAC COEFF AT INF SLIP	SLIP AT MAX TRACTION (M/S)	COEFFICIENT A	COEFFICIENT B (S/M)	COEFFICIENT C (S/M)	COEFFICIENT D
RE/RACE	0.					0.	2.40000E+01	0.	-6.00000E-01
RE/CAGE	5.00000E-07					1.00000E-01	0.	0.	-1.00000E-01
CAGE/RACE	5.00000E-07					6.00000E-01	0.	0.	-6.00000E-01

LUBRICANT CODE..... 0 HYPOTHETICAL MODEL

```
 AAAAAAAAA   DDDDDDDDDD    OOOOOOOOO   RRRRRRRRR   EEEEEEEEEE
AAAAAAAAAAA  DDDDDDDDDDD  OOOOOOOOOOO  RRRRRRRRRR  EEEEEEEEEE
AA       AA    DD     DD  OO       OO    RR     RR  EE
AA       AA    DD     DD  OO       OO    RR     RR  EE
AA       AA    DD     DD  OO       OO    RRRRRRRRR  EEEEEEE
AA       AA    DD     DD  OO       OO    RRRRRRRRR  EEEEEEE
AAAAAAAAAAA    DD     DD  OO       OO    RR  RR     EE
AAAAAAAAAAA    DD     DD  OO       OO    RR   RR    EE
AA       AA    DD     DD  OO       OO    RR    RR   EEEEEEEEEE
AA       AA    DDDDDDDDDD  OOOOOOOOOOO   RR     RR  EEEEEEEEEE
AA       AA    DDDDDDDDD    OOOOOOOOO    RR      RR EEEEEEEEEE

ADVANCED        DYNAMICS       OF       ROLLING        ELEMENTS
========        ========       ==       =======        ========
```

-A REAL TIME SIMULATION OF ROLLING BEARING PERFORMANCE-
(VERSION ADORE-1.0)

BY
PRADEEP K. GUPTA

****

* BEARING TYPE = BALL PROGRAM MODE = 1 SPEC CODE = F107 NO. 3 BRG SIN-M50 *

****

BEARING GEOMETRY

NO OF BALLS	17	OUTER CUR FAC	5.20000E-01	OUTER FIT	(M) 0.	SHAFT OD	(M) 2.95420E-02
BALL DIA	(M) 5.55600E-03	INNER CUR FAC	5.40000E-01	INNER FIT	(M) 0.	SHAFT ID	(M) 1.00000E-02
PITCH DIA	(M) 3.85100E-02	DIA PLAY	(M) 3.48238E-05			BEARING OD	(M) 4.70000E-02
CON ANGLE	(DEG) 1.86000E+01	END PLAY	(M) 2.12657E-04			HOUSING OD	(M) 6.00000E-02
CAGE OD	(M) 4.12240E-02	CAGE WIDTH	(M) 8.19100E-03	LAND DIA	(M) 4.12240E-02	LAND WIDTH	(M) 1.00000E-03
CAGE ID	(M) 3.73890E-02	POC DIA CL	(M) 2.50000E-04		4.12240E-02		1.00000E-03
OUTER CLS	(M) 2.50000E-04	GUIDE LAND TYPE	1 1	LAND CLS	(M) 2.50000E-04	LAND POS	(M) 4.09550E-03
INNER CLS	(M) 1.00000E-03				2.50000E-04		4.09550E-03

MATERIAL PROPERTIES

	DENSITY (KGM/M**3)	ELASTIC MODULUS (PA)	POISSION-S RATIO	COEFF OF THER EXP (1/K)	HARDNESS (PA)	WEAR COEFFICIENT
SHAFT	7.75037E+03	1.99948E+11	2.50000E-01	1.17000E-05		
HOUSING	7.75037E+03	1.99948E+11	2.50000E-01	1.17000E-05		
ROLL ELE	3.20000E+03	3.10000E+11	2.60000E-01	2.90000E-06	1.00000E+10	2.00000E-06
RACE	7.75037E+03	1.99348E+11	2.50000E-01	1.17000E-05	7.84532E+09	5.00000E-06
CAGE	1.50000E+03	1.73000E+09	3.00000E-01	3.00000E-06	1.00000E+09	1.00000E-05

LISTING OF INPUT DATA RECORDS ---

```
REC 1          1     1   160     1     0   160     5
REC 2       5.0000E-03 5.0000E-04 1.0000E+00 1.0000E+03
REC 3.1    F107 NO. 3 BRG SIN-M50
REC 3.2      2  1  0 17  1  1  0  0  0  0  0  0  0  1  0  0  1
REC 3.3      0  0  0  0  2  0  0  0  2  1 18
REC 4.1     2.9542E-02 4.7000E-02 1.0000E-02 6.0000E-02 0.         0.
REC 4.2     2.9500E+02 2.9500E+02 2.9500E+02 2.9500E+02 2.9500E+02 2.9500E+02 2.9500E+02
REC 5A      5.5560E-03 3.8510E-02 1.8600E+01 5.2000E-01 5.4000E-01
REC 7.1     4.1224E-02 3.7389E-02 8.1910E-03 2.5000E-04 1.0000E-03 0.
REC 7.2.1   4.1224E-02 1.0000E-03 4.0955E-03 2.5000E-04
REC 7.2.2   4.1224E-02 1.0000E-03 4.0955E-03 2.5000E-04
REC 7.3     2.5000E-04 2.5000E-04 0.         1.0000E-04 0.
REC 8.1     3.2000E+03 3.1000E+11 2.6000E-01 2.9000E-06 1.0000E+10 2.0000E-06
REC 8.5     1.5000E+03 1.7300E+09 3.0000E-01 3.0000E-06 1.0000E+09 1.0000E-05
REC 9.1     4.5000E+02 2.2500E+02 0.         0.         0.         0.         0.         6.3500E+04
REC 10.1    0.         2.4000E+01 0.        -6.0000E-01
REC 10.5.1  1.0000E-01 0.         0.        -1.0000E-01 5.0000E-07
REC 10.5.2  6.0000E-01 0.         0.        -6.0000E-01 5.0000E-07
REC 11      0.         0.         9.8100E+00
```

INPUT FROM USER ACCESSIBLE ROUTINES ---

Appendix A

COMPUTER OUTPUT

Appendix A contains the print output generated by ADORE for the Williams International F107 #3 position ball bearing in the initial run for 160 time steps. The nomenclature defining symbols and variables used in the computer program are given in Appendix B. The output describes the bearing geometry, operating conditions and typical interactions at the various interfaces in the bearing. Following this run, the simulation was continued in terms of several successive runs to obtain the bearing performance simulation for approximately 475° rotation of the shaft. The plot output, following the print output, was generated close to the end of the simulation. After examining this output the simulations were further advanced by another 100 time steps to fully simulate the ball/cage collisions observed in the various ball pockets. These solutions are discussed in the main part of this report.

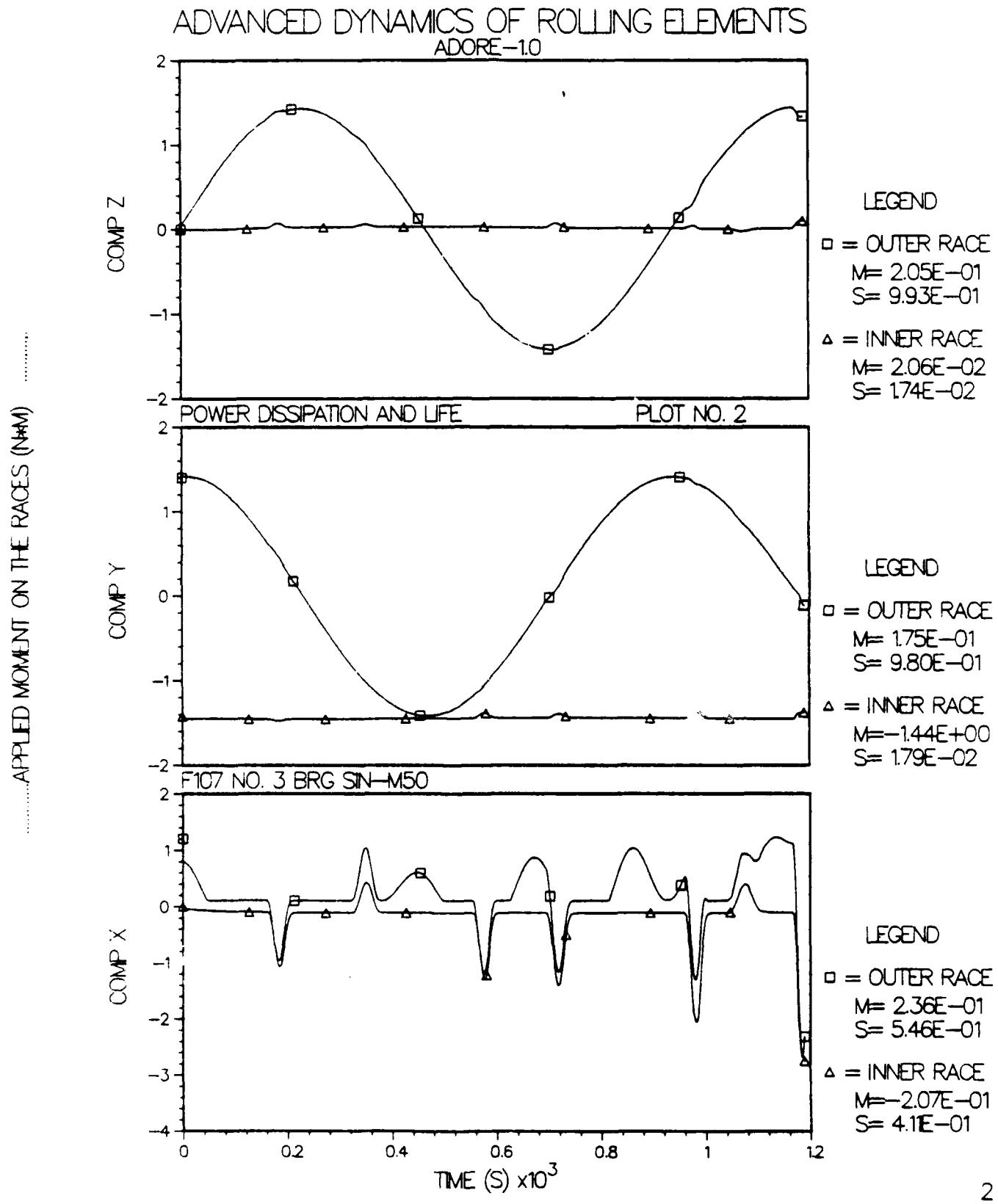
ADVANCED DYNAMICS OF ROLLING ELEMENTS
ADORE-1.0
POWER DISSIPATION AND LIFE
PLOT NO. 2
F107 NO. 3 BRG SIN-M50
APPLIED MOMENT ON THE RACES (N*M)
COMP Z
COMP Y
COMP X
TIME (S) x10^3
LEGEND
□ = OUTER RACE
M= 2.05E-01
S= 9.93E-01
△ = INNER RACE
M= 2.06E-02
S= 1.74E-02
LEGEND
□ = OUTER RACE
M= 1.75E-01
S= 9.80E-01
△ = INNER RACE
M=-1.44E+00
S= 1.79E-02
LEGEND
□ = OUTER RACE
M= 2.36E-01
S= 5.46E-01
△ = INNER RACE
M=-2.07E-01
S= 4.11E-01
2

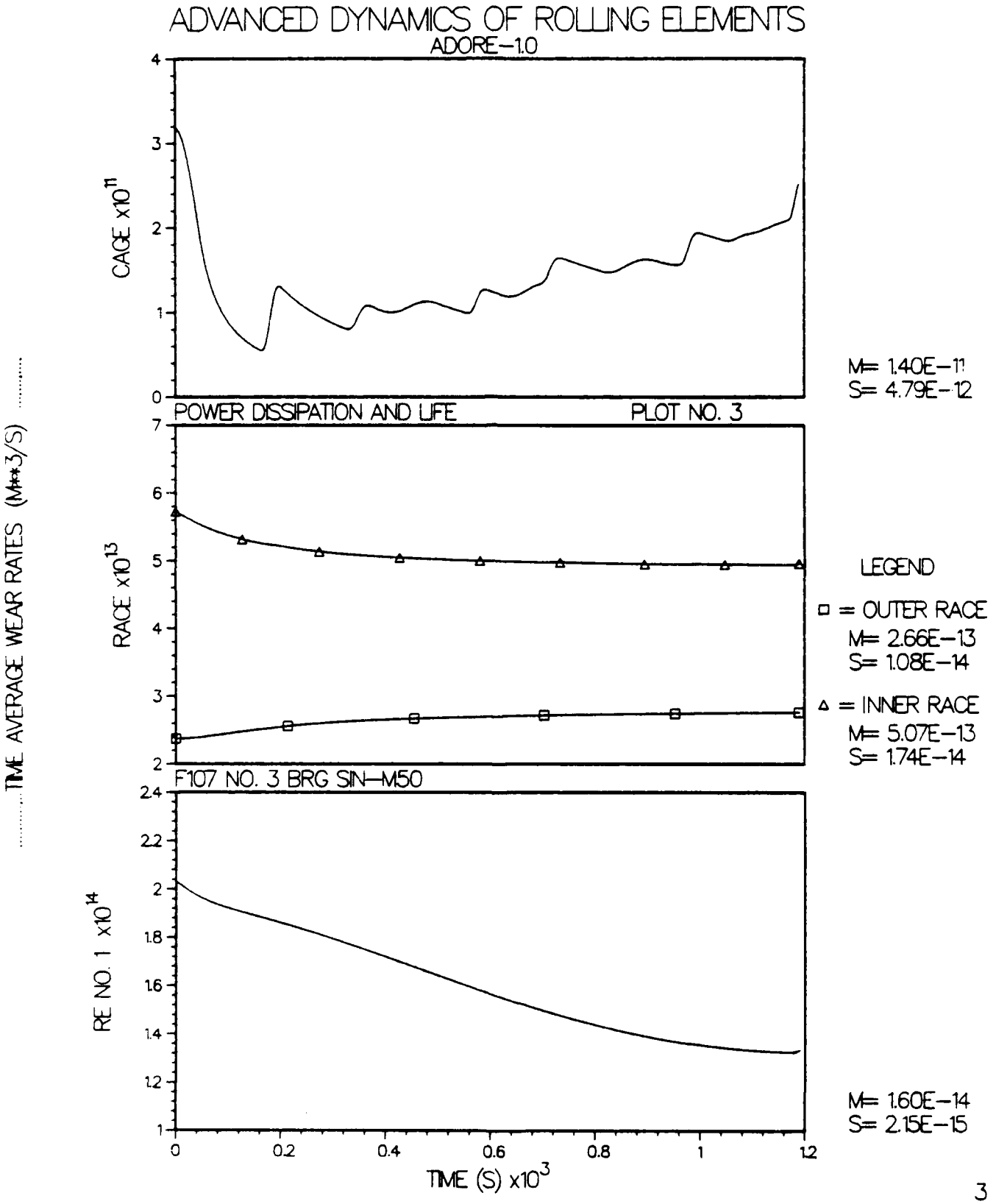
ADVANCED DYNAMICS OF ROLLING ELEMENTS
ADORE-1.0
CAGE x10^11
M= 1.40E-11
S= 4.79E-12
POWER DISSIPATION AND LIFE
PLOT NO. 3
RACE x10^13
LEGEND
□ = OUTER RACE
M= 2.66E-13
S= 1.08E-14
△ = INNER RACE
M= 5.07E-13
S= 1.74E-14
F107 NO. 3 BRG SIN-M50
RE NO. 1 x10^14
M= 1.60E-14
S= 2.15E-15
TIME (S) x10^3
TIME AVERAGE WEAR RATES (M**3/S)

3

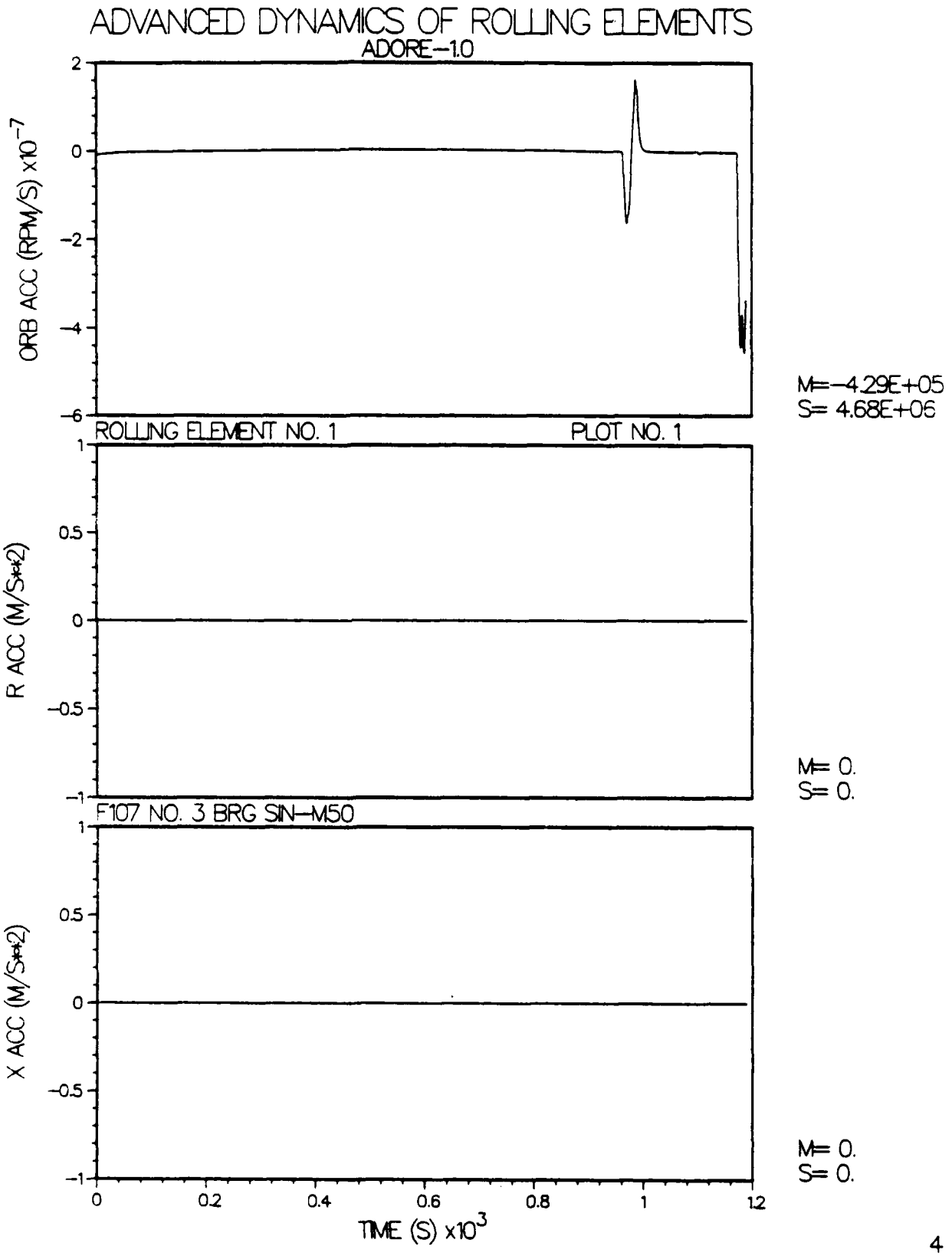
ADVANCED DYNAMICS OF ROLLING ELEMENTS
ADORE-1.0
ORB ACC (RPM/S) x10^-7
M=-4.29E+05
S= 4.68E+06
ROLLING ELEMENT NO. 1
PLOT NO. 1
R ACC (M/S**2)
M= 0.
S= 0.
F107 NO. 3 BRG SIN-M50
X ACC (M/S**2)
M= 0.
S= 0.
TIME (S) x10^3
4

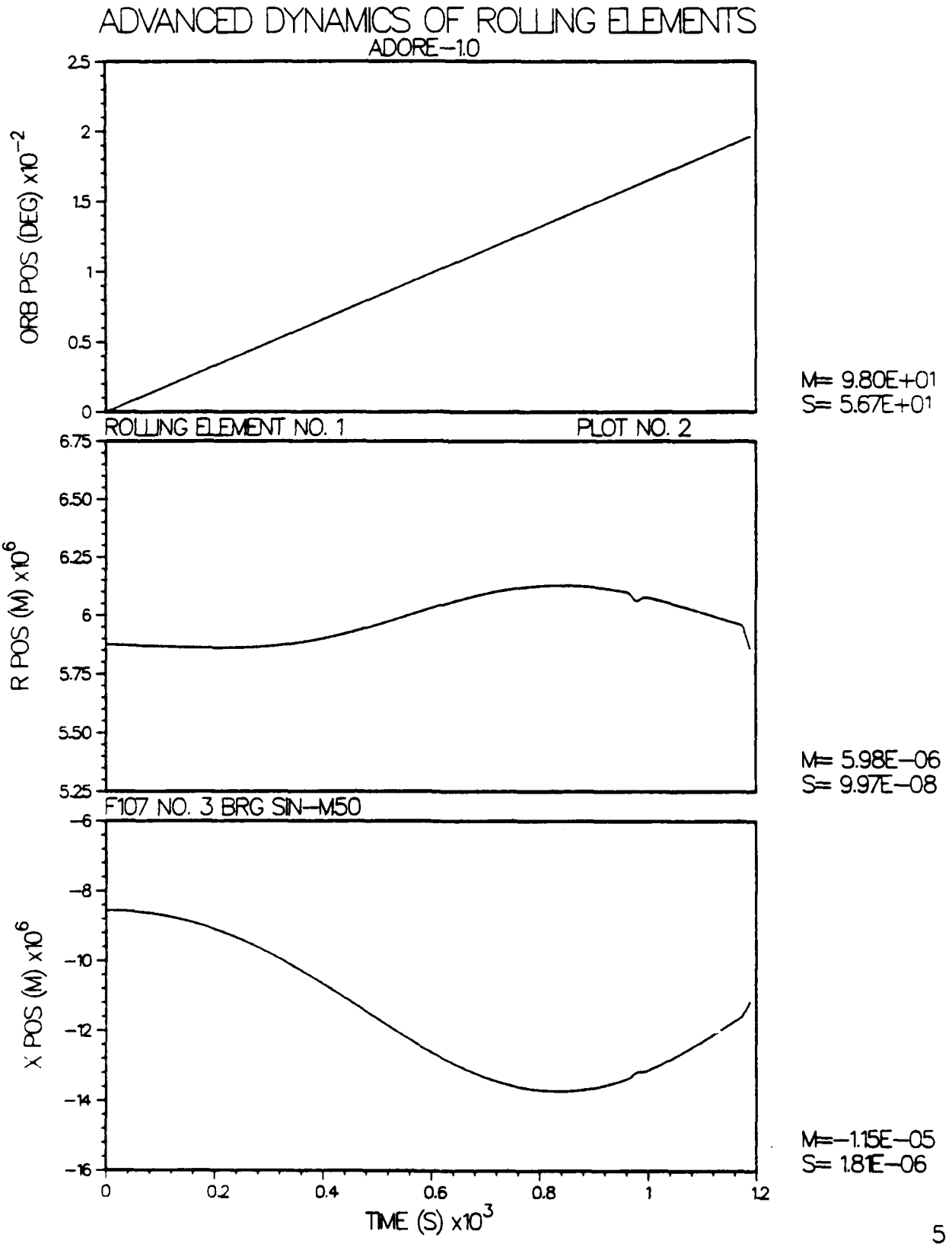
ADVANCED DYNAMICS OF ROLLING ELEMENTS
ADORE-1.0
ORB POS (DEG) x10^-2
2.5
2
1.5
1
0.5
0
M= 9.80E+01
S= 5.67E+01
ROLLING ELEMENT NO. 1
PLOT NO. 2
R POS (M) x10^6
6.75
6.50
6.25
6
5.75
5.50
5.25
M= 5.98E-06
S= 9.97E-08
F107 NO. 3 BRG SIN-M50
X POS (M) x10^6
-6
-8
-10
-12
-14
-16
M=-1.15E-05
S= 1.81E-06
0
0.2
0.4
0.6
0.8
1
1.2
TIME (S) x10^3

5

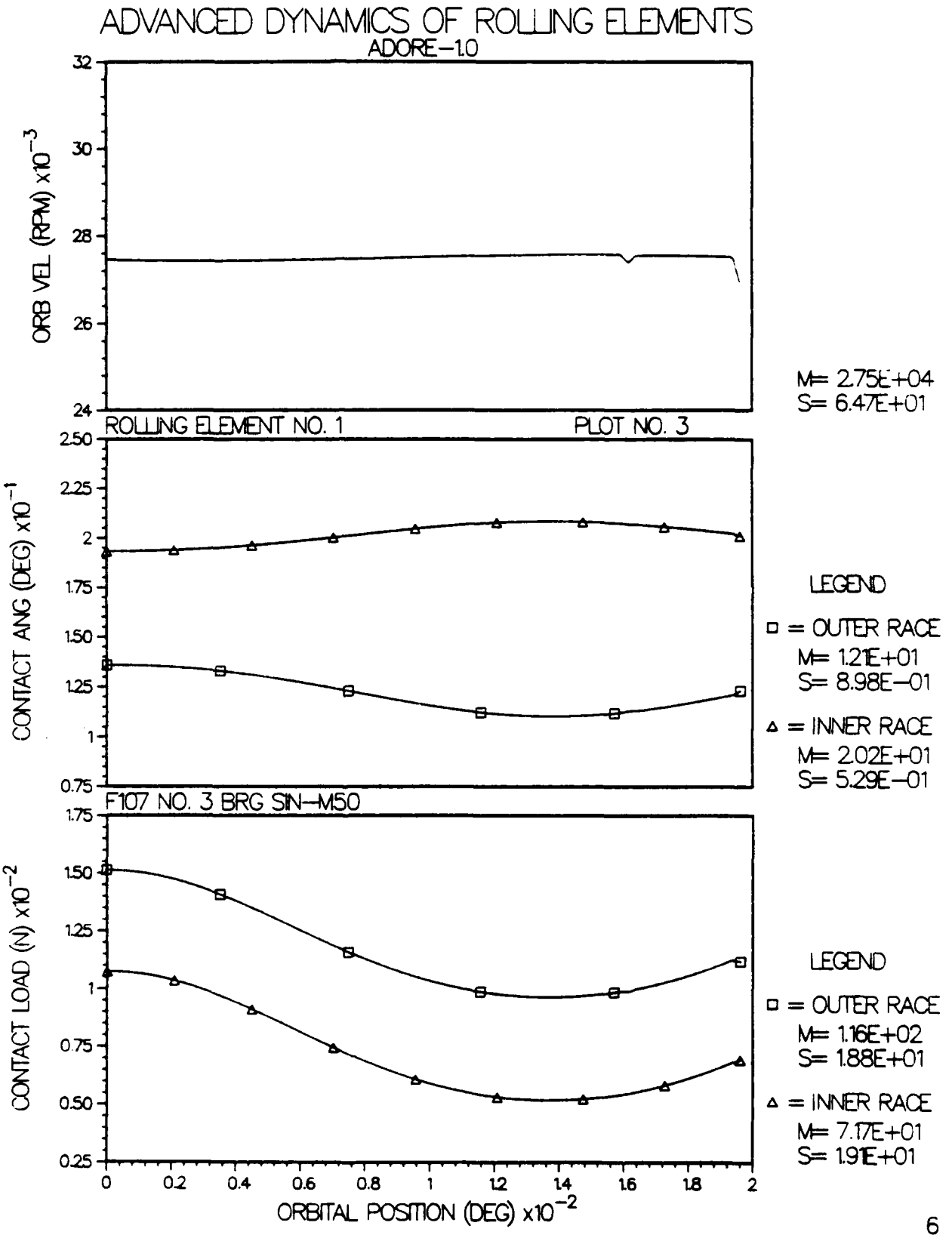
ADVANCED DYNAMICS OF ROLLING ELEMENTS
ADORE-1.0
ORB VEL (RPM) x10^-3
32
30
28
26
24
M= 2.75E+04
S= 6.47E+01
ROLLING ELEMENT NO. 1
PLOT NO. 3
CONTACT ANG (DEG) x10^-1
2.50
2.25
2
1.75
1.50
1.25
1
0.75
LEGEND
□ = OUTER RACE
M= 1.21E+01
S= 8.98E-01
△ = INNER RACE
M= 2.02E+01
S= 5.29E-01
F107 NO. 3 BRG SIN-M50
CONTACT LOAD (N) x10^-2
1.75
1.50
1.25
1
0.75
0.50
0.25
LEGEND
□ = OUTER RACE
M= 1.16E+02
S= 1.88E+01
△ = INNER RACE
M= 7.17E+01
S= 1.91E+01
0
0.2
0.4
0.6
0.8
1
1.2
1.4
1.6
1.8
2
ORBITAL POSITION (DEG) x10^-2
6

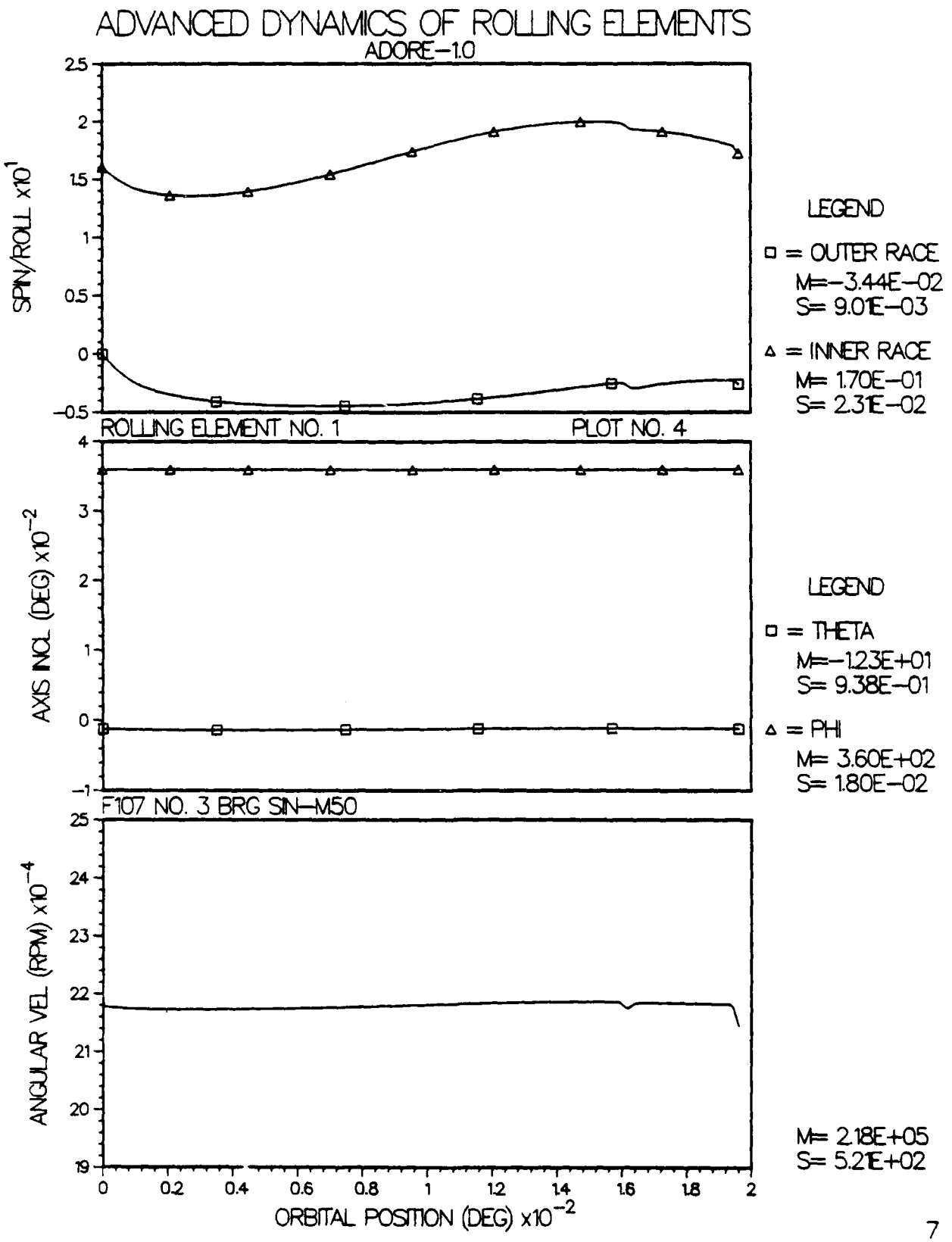
ADVANCED DYNAMICS OF ROLLING ELEMENTS
ADORE-1.0
SPIN/ROLL x10^1
2.5
2
1.5
1
0.5
0
-0.5
LEGEND
□ = OUTER RACE
M=-3.44E-02
S= 9.01E-03
Δ = INNER RACE
M= 1.70E-01
S= 2.31E-02
ROLLING ELEMENT NO. 1
PLOT NO. 4
AXIS INCL (DEG) x10^-2
4
3
2
1
0
-1
LEGEND
□ = THETA
M=-1.23E+01
S= 9.38E-01
Δ = PHI
M= 3.60E+02
S= 1.80E-02
F107 NO. 3 BRG SIN-M50
ANGULAR VEL (RPM) x10^-4
25
24
23
22
21
20
19
M= 2.18E+05
S= 5.21E+02
0
0.2
0.4
0.6
0.8
1
1.2
1.4
1.6
1.8
2
ORBITAL POSITION (DEG) x10^-2

7

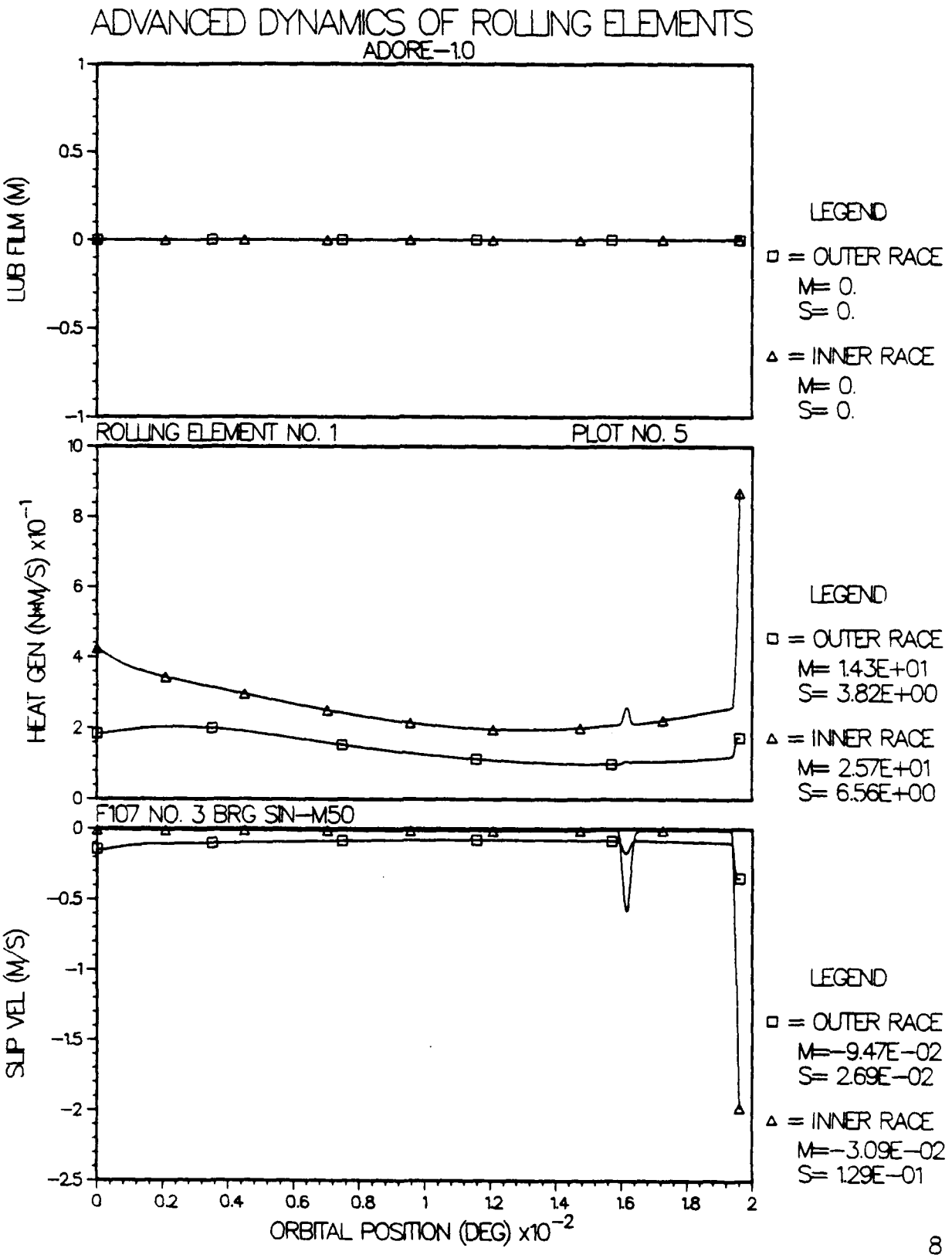
ADVANCED DYNAMICS OF ROLLING ELEMENTS
ADORE-1.0
LUB FILM (M)
ROLLING ELEMENT NO. 1
PLOT NO. 5
HEAT GEN (N*M/S) x10^-1
F107 NO. 3 BRG SIN-M50
SLP VEL (M/S)
ORBITAL POSITION (DEG) x10^-2
LEGEND
□ = OUTER RACE
M= 0.
S= 0.
△ = INNER RACE
M= 0.
S= 0.
LEGEND
□ = OUTER RACE
M= 1.43E+01
S= 3.82E+00
△ = INNER RACE
M= 2.57E+01
S= 6.56E+00
LEGEND
□ = OUTER RACE
M=-9.47E-02
S= 2.69E-02
△ = INNER RACE
M=-3.09E-02
S= 1.29E-01

8

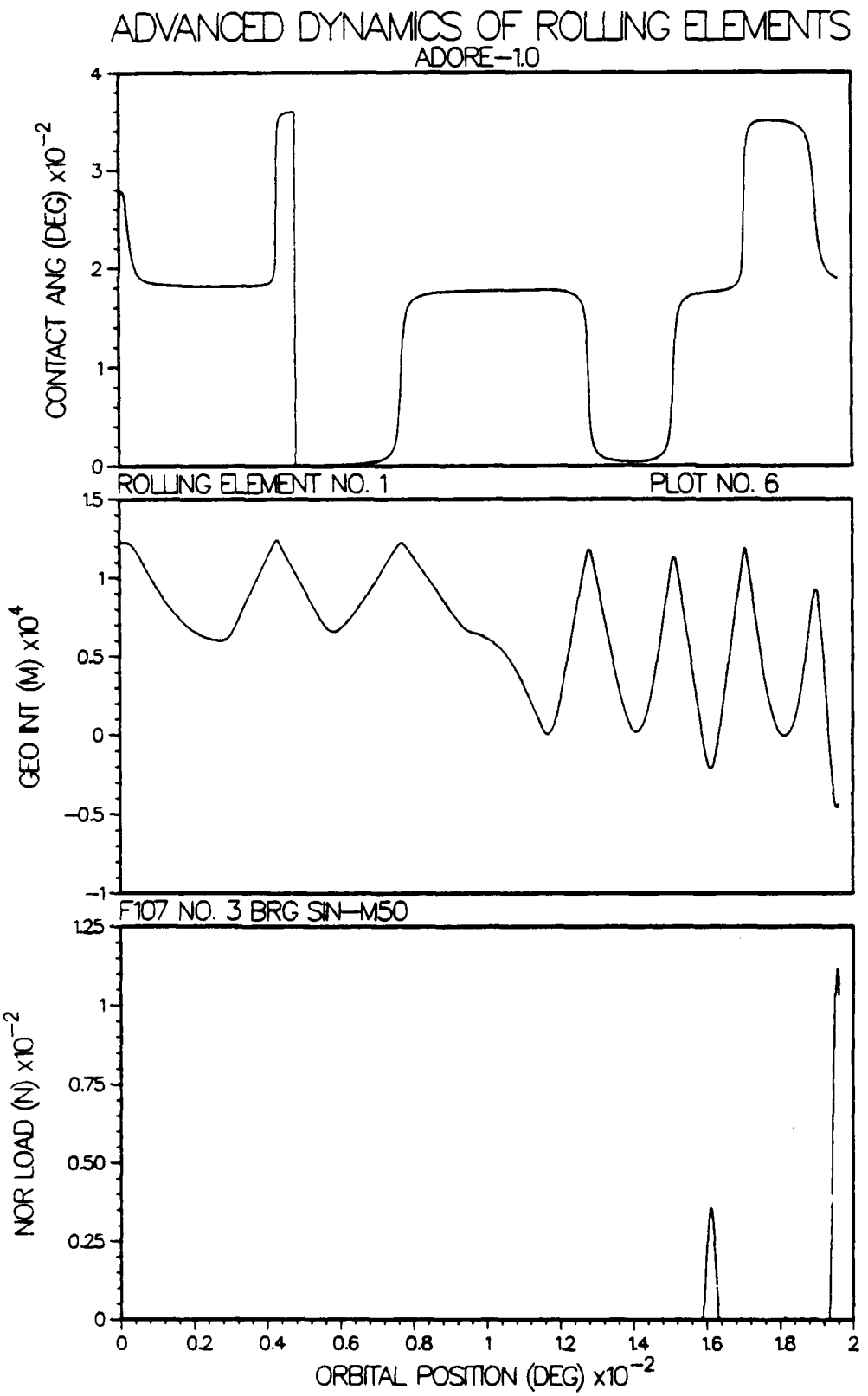

M= 1.56E+02
S= 1.04E+02

M= 6.60E-05
S= 3.81E-05

M= 1.46E+00
S= 1.01E+01

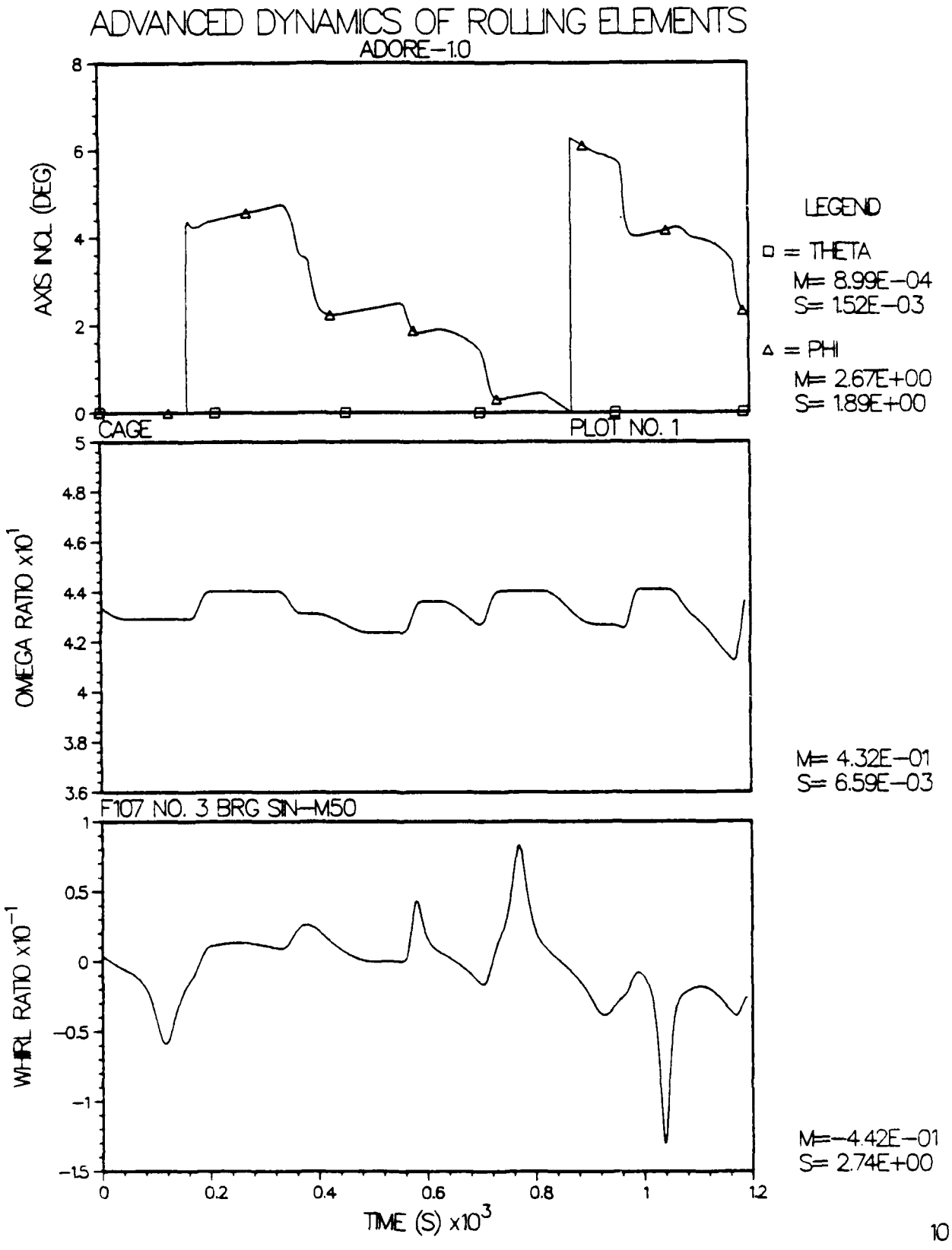
ADVANCED DYNAMICS OF ROLLING ELEMENTS
ADORE-1.0
AXIS INCL (DEG)
8
6
4
2
0
LEGEND
□ = THETA
M= 8.99E-04
S= 1.52E-03
△ = PHI
M= 2.67E+00
S= 1.89E+00
CAGE
PLOT NO. 1
OMEGA RATIO x10^1
5
4.8
4.6
4.4
4.2
4
3.8
3.6
M= 4.32E-01
S= 6.59E-03
F107 NO. 3 BRG SIN-M50
WHIRL RATIO x10^-1
1
0.5
0
-0.5
-1
-1.5
M=-4.42E-01
S= 2.74E+00
0
0.2
0.4
0.6
0.8
1
1.2
TIME (S) x10^3
10

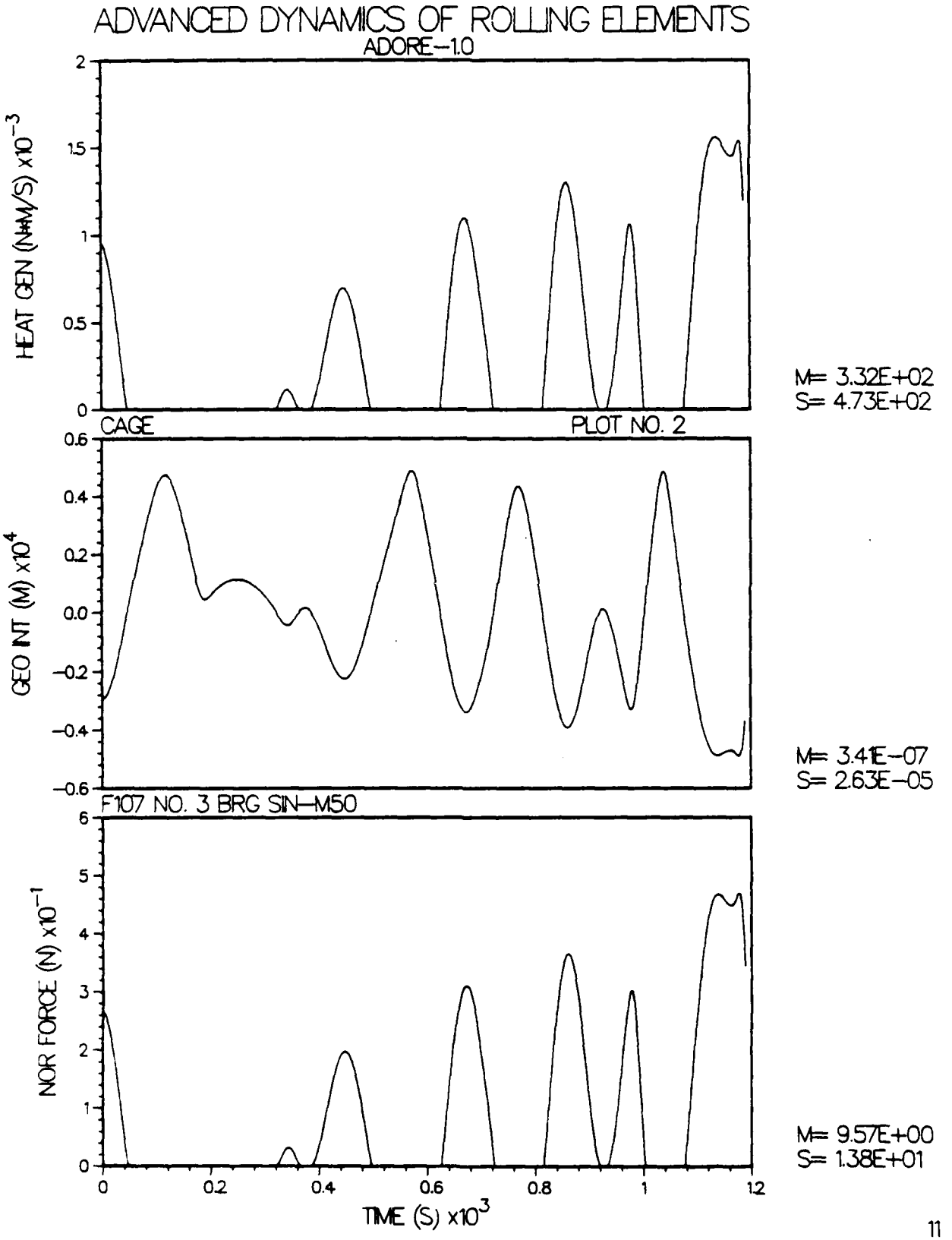
ADVANCED DYNAMICS OF ROLLING ELEMENTS
ADORE-1.0
HEAT GEN (N#M/S) x10^-3
2
1.5
1
0.5
0
M= 3.32E+02
S= 4.73E+02
CAGE
PLOT NO. 2
GEO INT (M) x10^4
0.6
0.4
0.2
0.0
-0.2
-0.4
-0.6
M= 3.41E-07
S= 2.63E-05
F107 NO. 3 BRG SIN-M50
NOR FORCE (N) x10^-1
6
5
4
3
2
1
0
M= 9.57E+00
S= 1.38E+01
0
0.2
0.4
0.6
0.8
1
1.2
TIME (S) x10^3

11

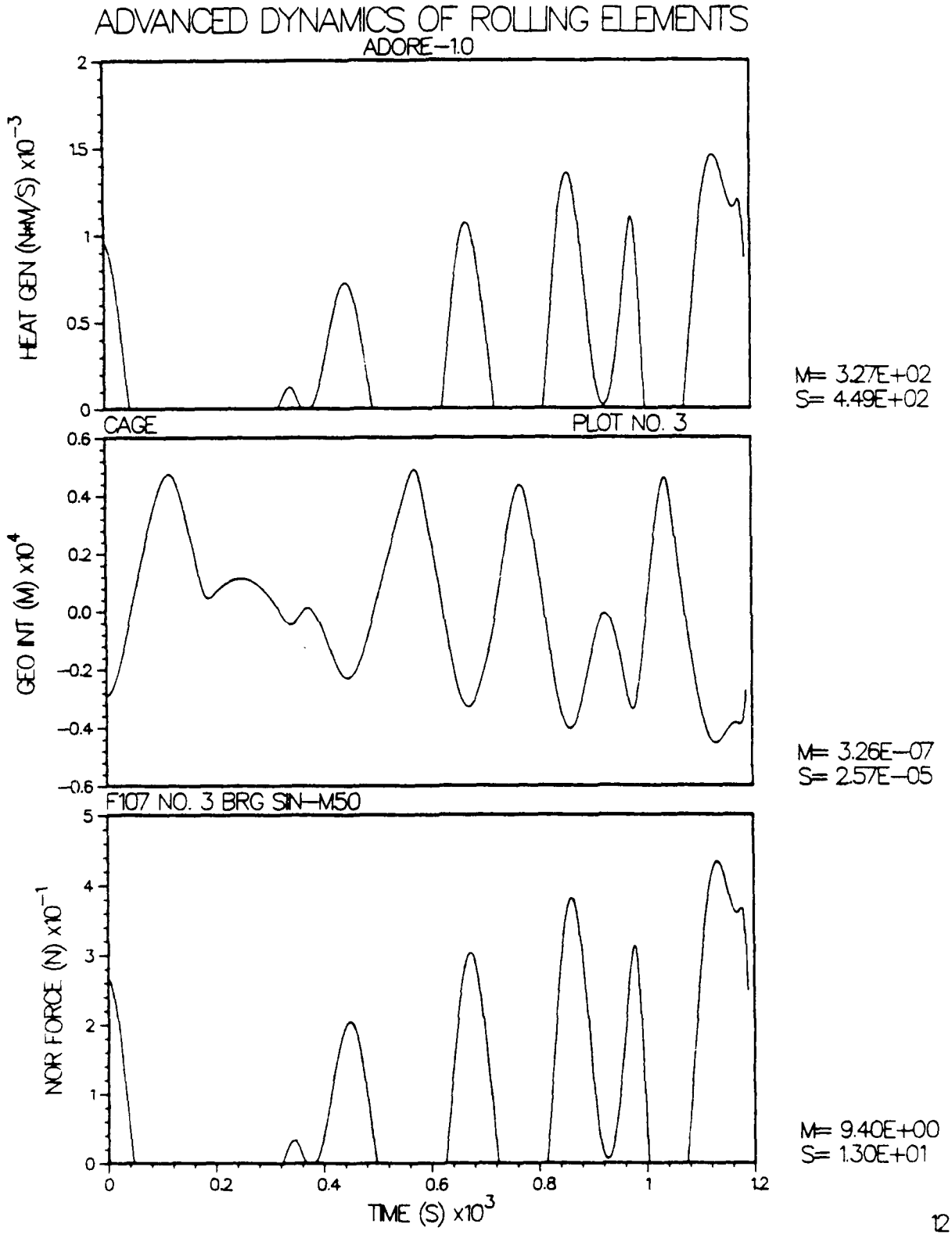
ADVANCED DYNAMICS OF ROLLING ELEMENTS
ADORE-1.0
HEAT GEN (N*M/S) x10^-3
M= 3.27E+02
S= 4.49E+02
CAGE
PLOT NO. 3
GEO NT (M) x10^4
M= 3.26E-07
S= 2.57E-05
F107 NO. 3 BRG SIN-M50
NOR FORCE (N) x10^-1
M= 9.40E+00
S= 1.30E+01
TIME (S) x10^3

12

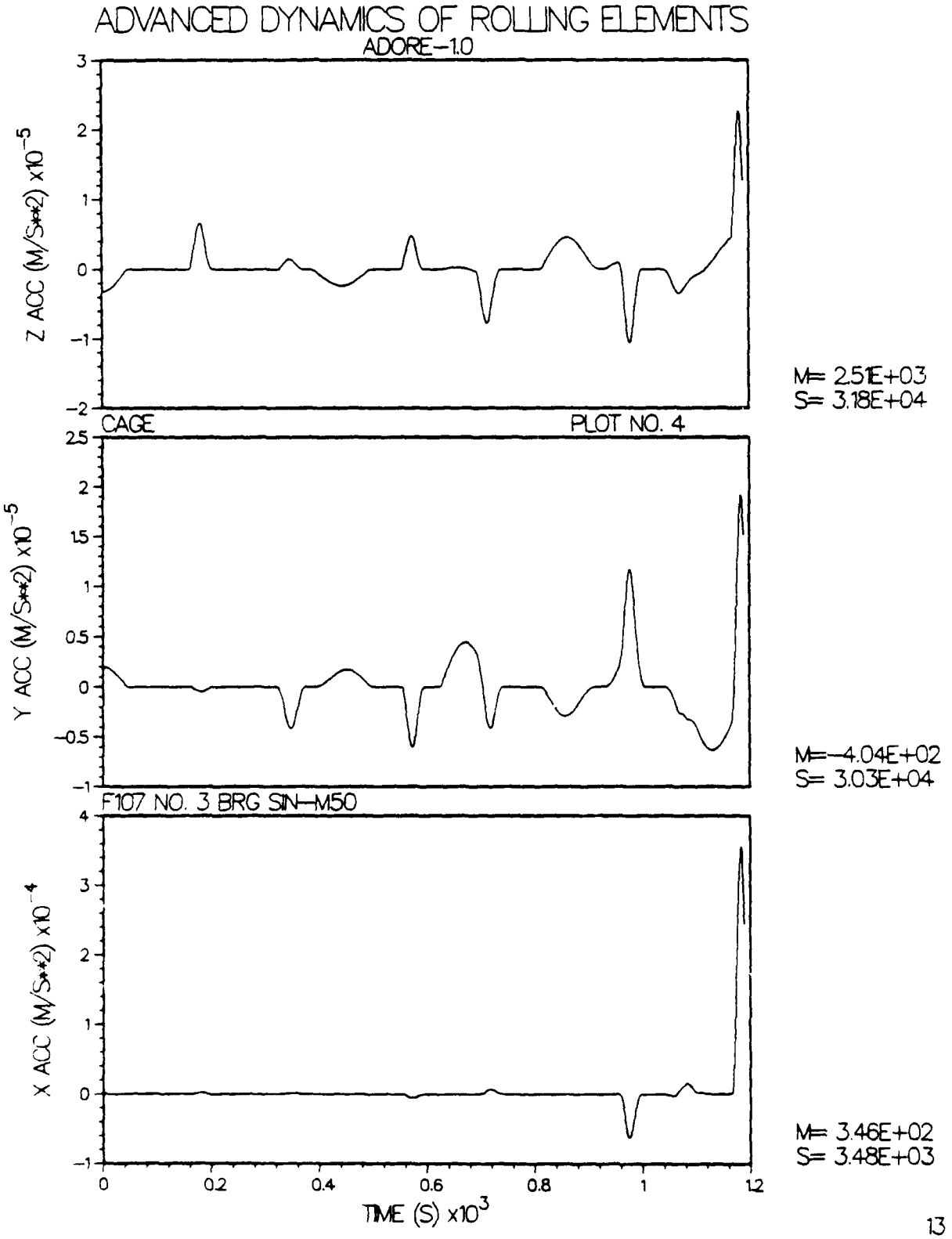
ADVANCED DYNAMICS OF ROLLING ELEMENTS
ADORE-1.0
Z ACC (M/S**2) x10**-5
M= 2.51E+03
S= 3.18E+04
CAGE
PLOT NO. 4
Y ACC (M/S**2) x10**-5
M=-4.04E+02
S= 3.03E+04
F107 NO. 3 BRG SIN-M50
X ACC (M/S**2) x10**-4
M= 3.46E+02
S= 3.48E+03
TIME (S) x10**3
13

ADVANCED DYNAMICS OF ROLLING ELEMENTS

ADORE–1.0

CAGE

PLOT NO. 5

F107 NO. 3 BRG SIN–M50

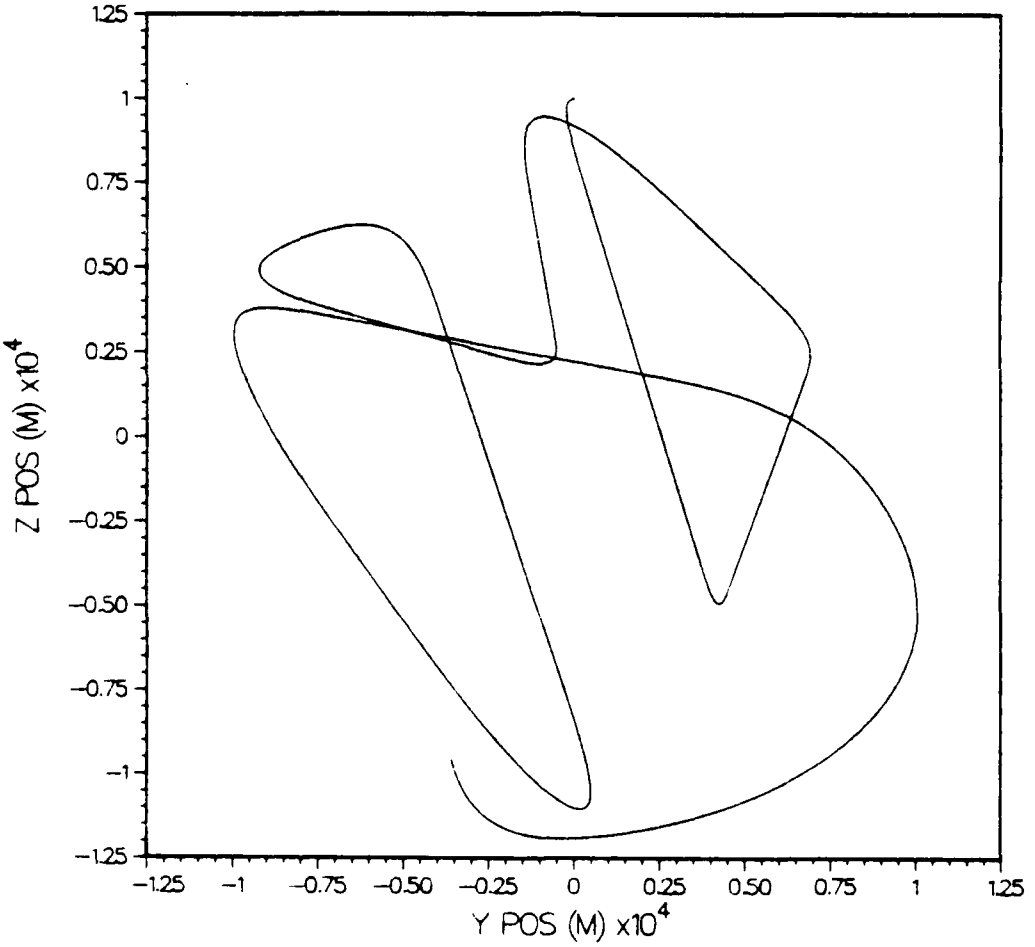

14

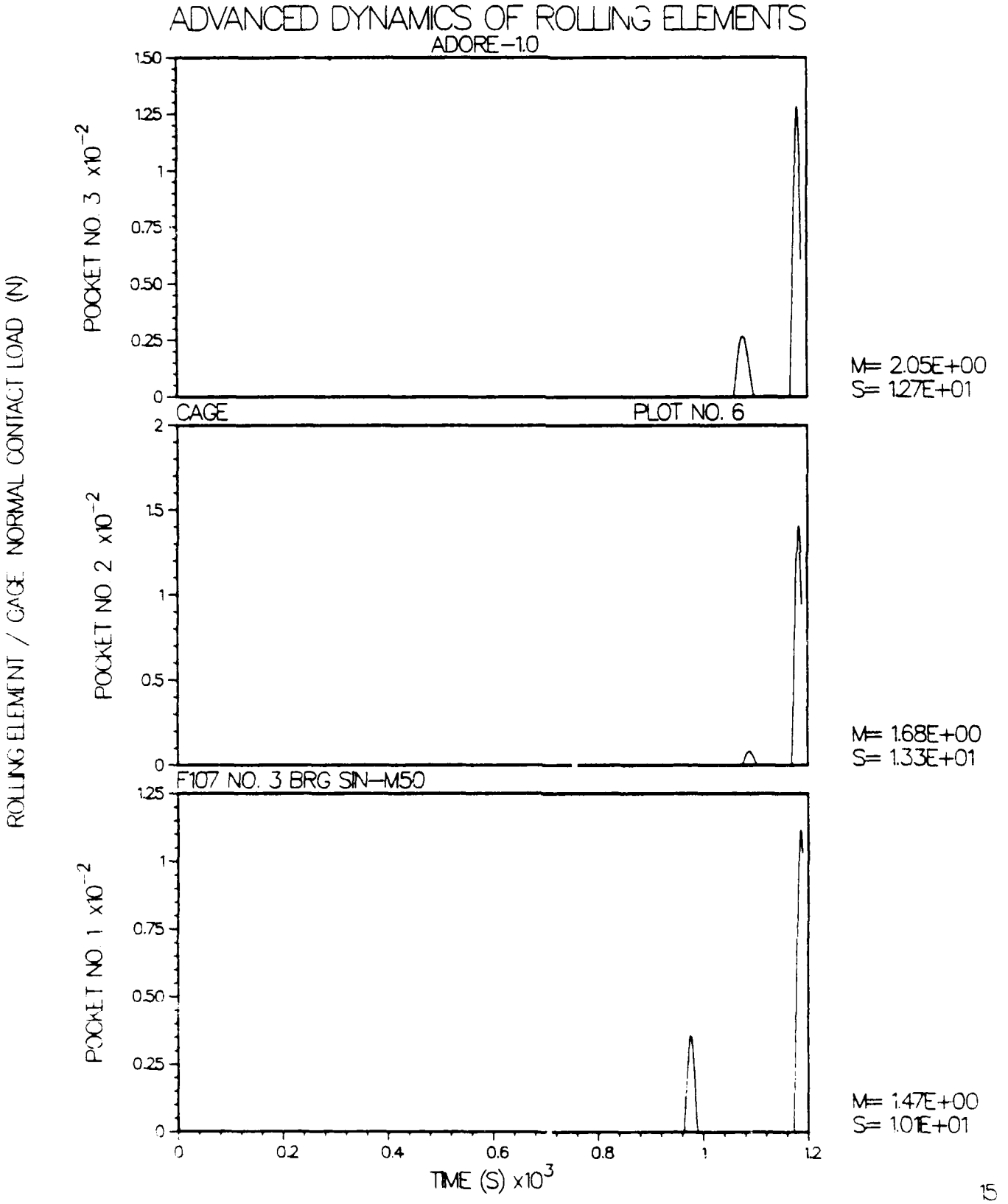
ADVANCED DYNAMICS OF ROLLING ELEMENTS
ADORE-1.0
ROLLING ELEMENT / CAGE NORMAL CONTACT LOAD (N)
POCKET NO. 3 x10^-2
POCKET NO 2 x10^-2
POCKET NO 1 x10^-2
CAGE
PLOT NO. 6
F107 NO. 3 BRG SIN-M50
M= 2.05E+00
S= 1.27E+01
M= 1.68E+00
S= 1.33E+01
M= 1.47E+00
S= 1.01E+01
TIME (S) x10^3

15

AD-A155 042 FRICTION AND WEAR OF SOLID-LUBRICATED CONTACT IN GAS TURBINE ENGINE BEARINGS(U) MECHANICAL TECHNOLOGY INC LATHAM N Y S GRAY ET AL. NOV 84 MTI-84TR72

UNCLASSIFIED AFWAL-TR-84-4143 F33615-83-C-5037 F/G 11/8 NL

END

DATE FILMED

7 85

DT

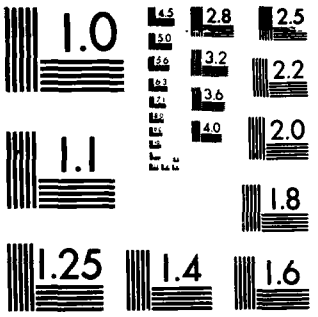

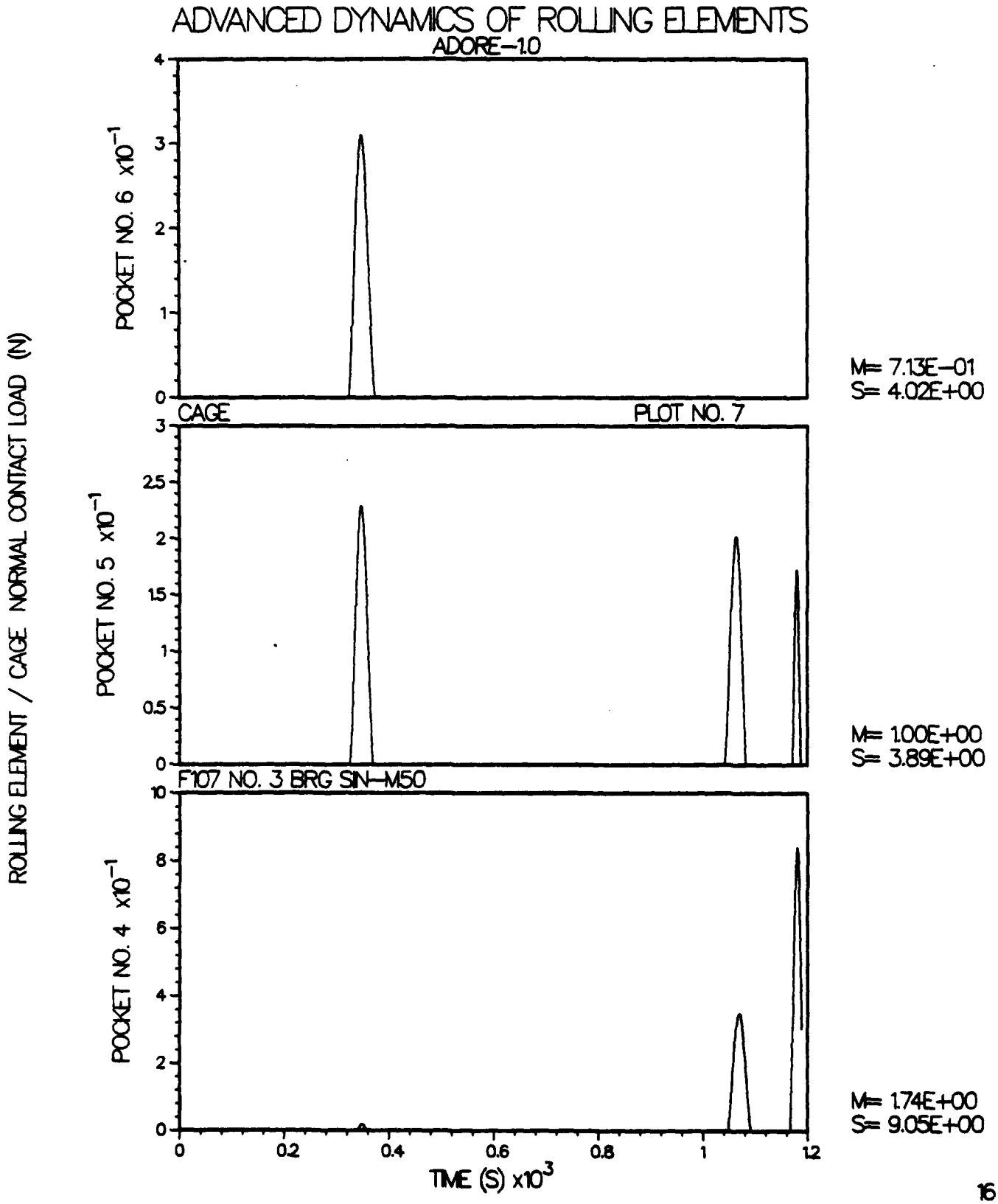
ADVANCED DYNAMICS OF ROLLING ELEMENTS
ADORE-1.0
ROLLING ELEMENT / CAGE NORMAL CONTACT LOAD (N)
POCKET NO. 6 x10⁻¹
M= 7.13E-01
S= 4.02E+00
CAGE
PLOT NO. 7
POCKET NO. 5 x10⁻¹
M= 1.00E+00
S= 3.89E+00
F107 NO. 3 BRG SIN-M50
POCKET NO. 4 x10⁻¹
M= 1.74E+00
S= 9.05E+00
TIME (S) x10³

16

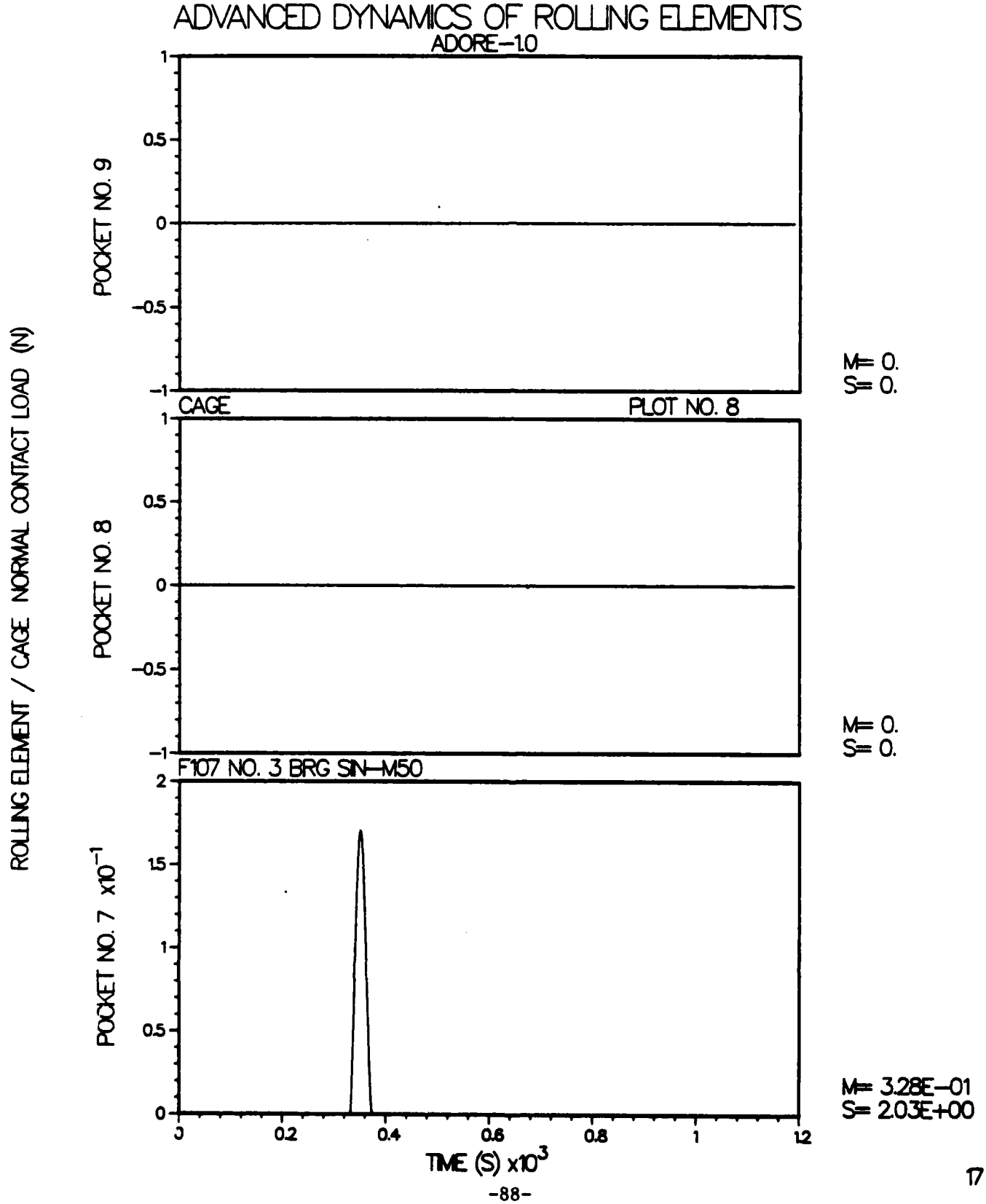
ADVANCED DYNAMICS OF ROLLING ELEMENTS
ADORE-1.0
ROLLING ELEMENT / CAGE NORMAL CONTACT LOAD (N)
POCKET NO. 9
1
0.5
0
-0.5
-1
M= 0.
S= 0.
CAGE
PLOT NO. 8
POCKET NO. 8
1
0.5
0
-0.5
-1
M= 0.
S= 0.
F107 NO. 3 BRG SIN-M50
POCKET NO. 7 x10^-1
2
1.5
1
0.5
0
M= 3.28E-01
S= 2.03E+00
0
0.2
0.4
0.6
0.8
1
1.2
TIME (S) x10^3

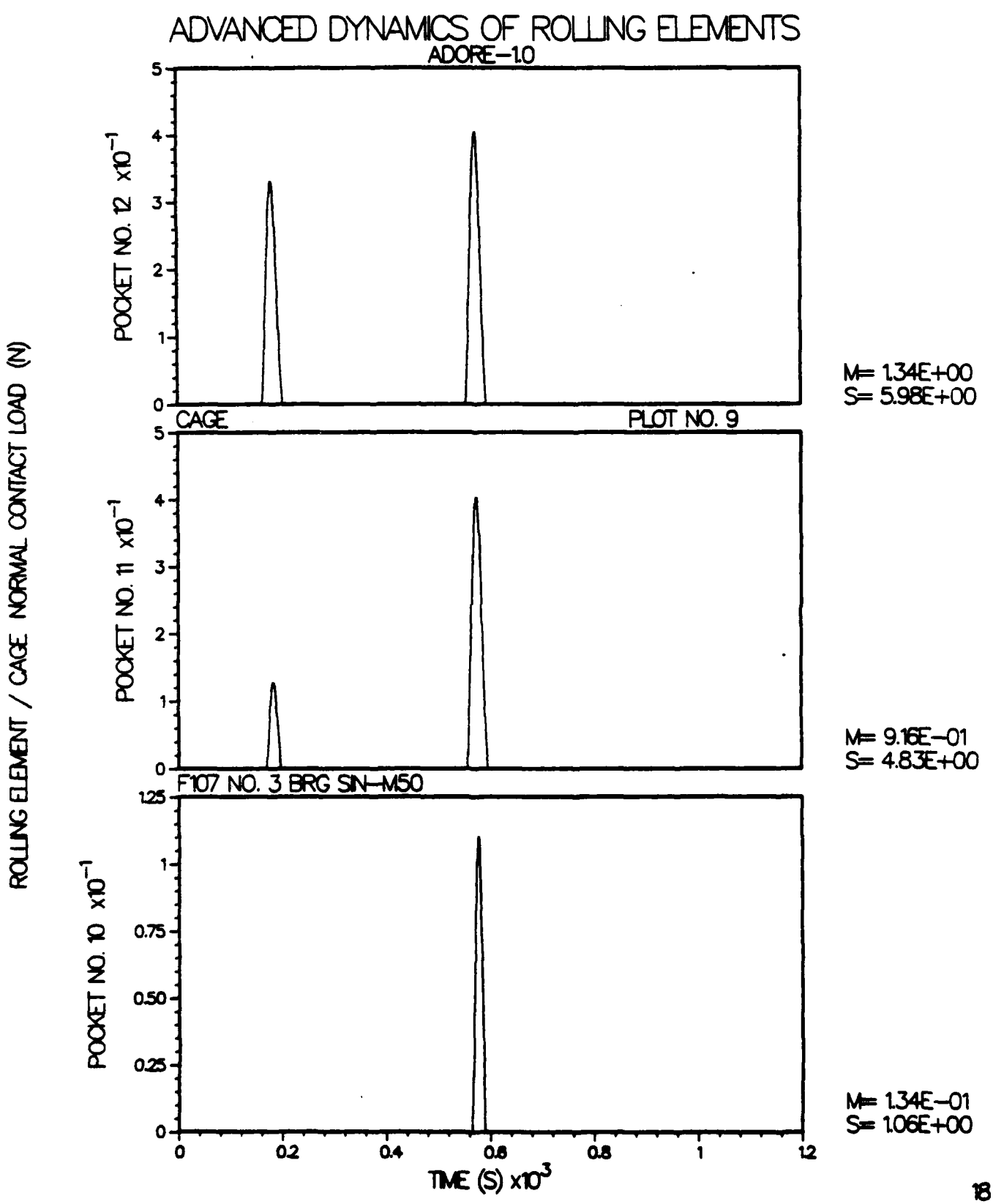
ADVANCED DYNAMICS OF ROLLING ELEMENTS
ADORE-1.0
ROLLING ELEMENT / CAGE NORMAL CONTACT LOAD (N)
POCKET NO. 12 x10⁻¹
M= 1.34E+00
S= 5.98E+00
CAGE
PLOT NO. 9
POCKET NO. 11 x10⁻¹
M= 9.16E-01
S= 4.83E+00
F107 NO. 3 BRG SIN-M50
POCKET NO. 10 x10⁻¹
M= 1.34E-01
S= 1.06E+00
TIME (S) x10³
18

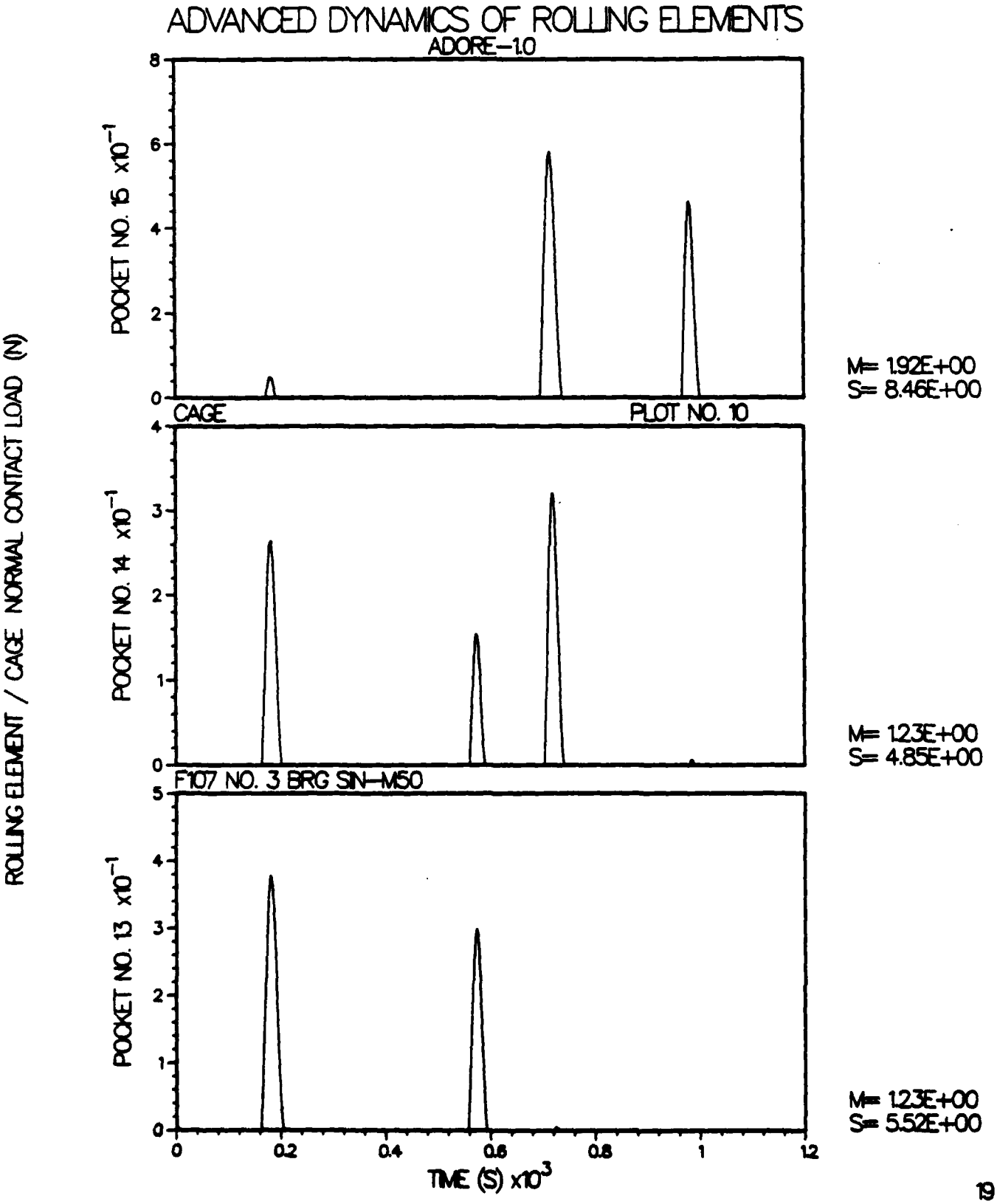
ADVANCED DYNAMICS OF ROLLING ELEMENTS
ADORE-1.0
ROLLING ELEMENT / CAGE NORMAL CONTACT LOAD (N)
POCKET NO. 15 x10⁻¹
M= 1.92E+00
S= 8.46E+00
CAGE
PLOT NO. 10
POCKET NO. 14 x10⁻¹
M= 1.23E+00
S= 4.85E+00
F107 NO. 3 BRG SIN-M50
POCKET NO. 13 x10⁻¹
M= 1.23E+00
S= 5.52E+00
TIME (S) x10³
19

ADVANCED DYNAMICS OF ROLLING ELEMENTS
ADORE–1.0

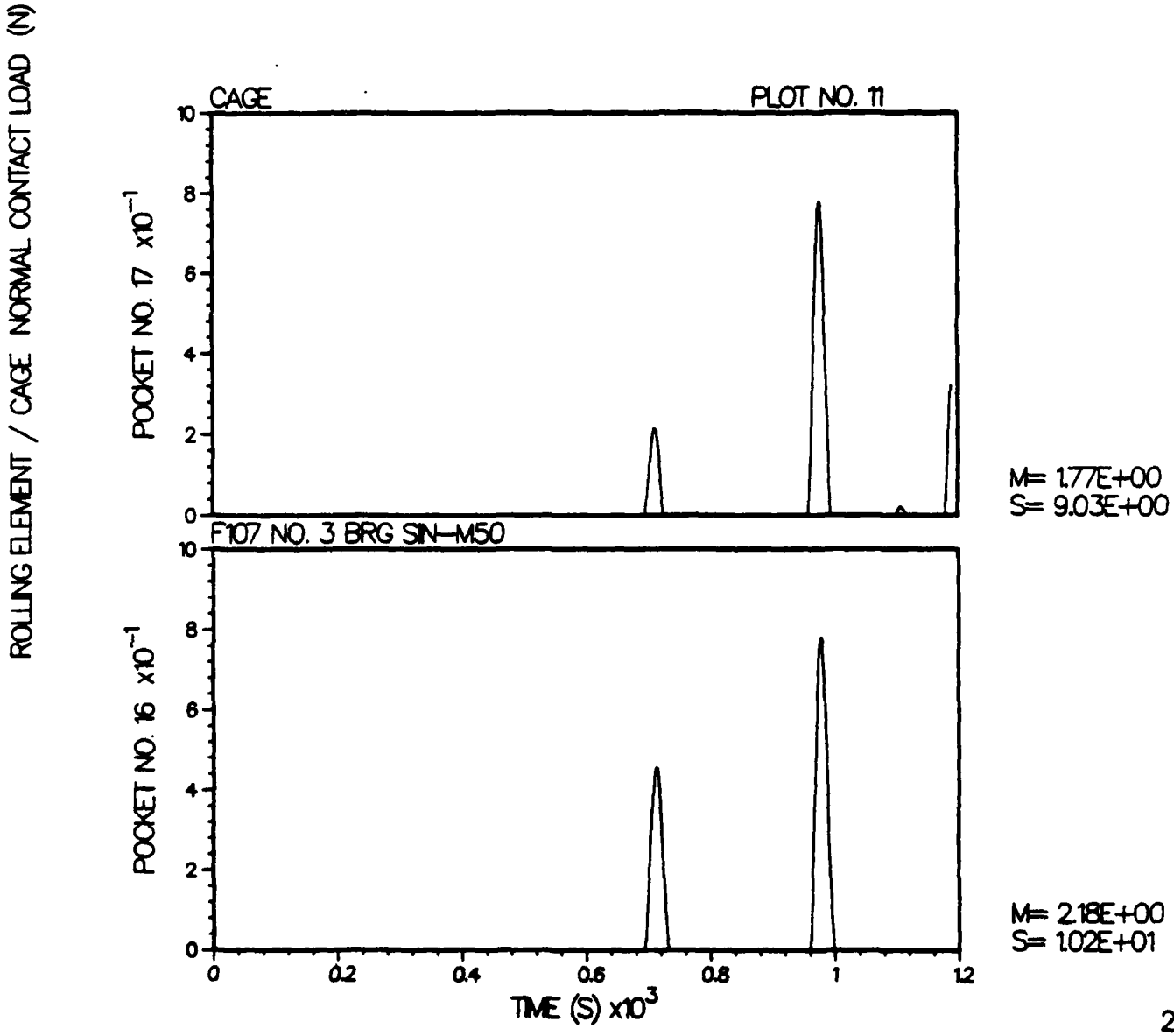

20

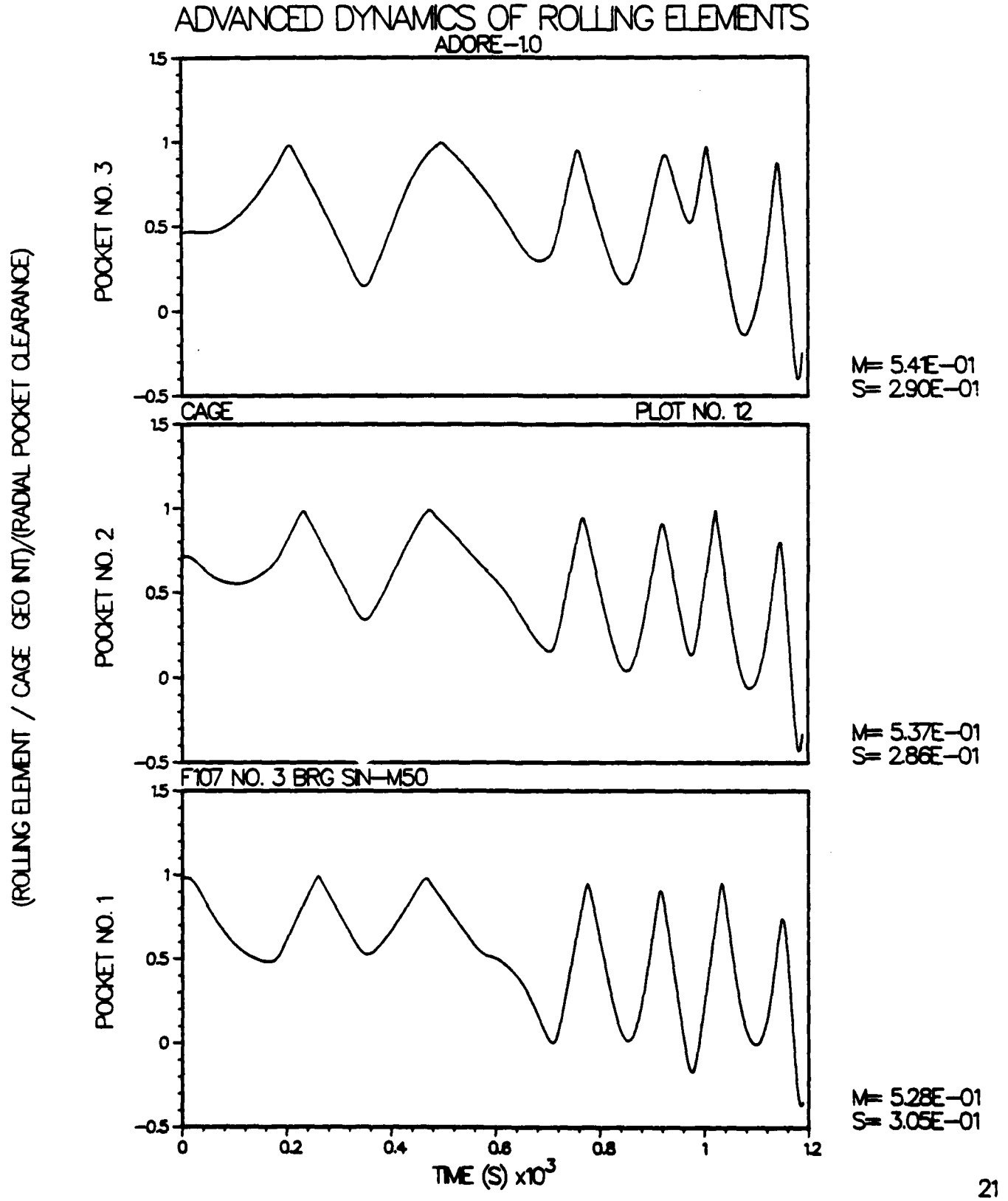
ADVANCED DYNAMICS OF ROLLING ELEMENTS
ADORE-1.0
(ROLLING ELEMENT / CAGE GEO INT)/(RADIAL POCKET CLEARANCE)
POCKET NO. 3
M= 5.41E-01
S= 2.90E-01
CAGE
PLOT NO. 12
POCKET NO. 2
M= 5.37E-01
S= 2.86E-01
F107 NO. 3 BRG SIN-M50
POCKET NO. 1
M= 5.28E-01
S= 3.05E-01
1.5
1
0.5
0
-0.5
0
0.2
0.4
0.6
0.8
1
1.2
TIME (S) x10^3

21

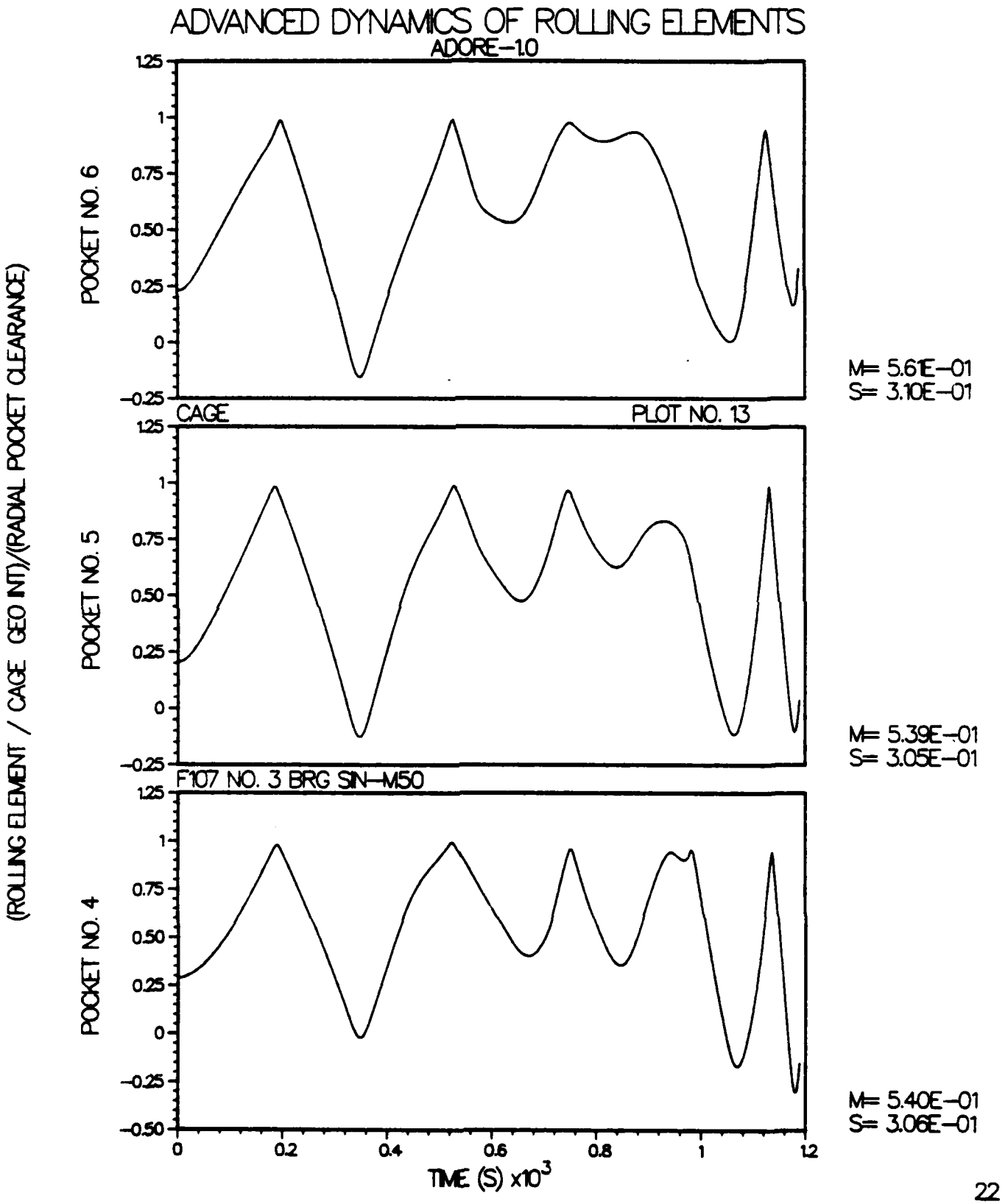
ADVANCED DYNAMICS OF ROLLING ELEMENTS
ADORE-1.0
(ROLLING ELEMENT / CAGE GEO INT)/(RADIAL POCKET CLEARANCE)
POCKET NO. 6
1.25
1
0.75
0.50
0.25
0
-0.25
M= 5.61E-01
S= 3.10E-01
CAGE
PLOT NO. 13
POCKET NO. 5
M= 5.39E-01
S= 3.05E-01
F107 NO. 3 BRG SIN-M50
POCKET NO. 4
-0.50
M= 5.40E-01
S= 3.06E-01
0
0.2
0.4
0.6
0.8
1
1.2
TIME (S) x10^3
22

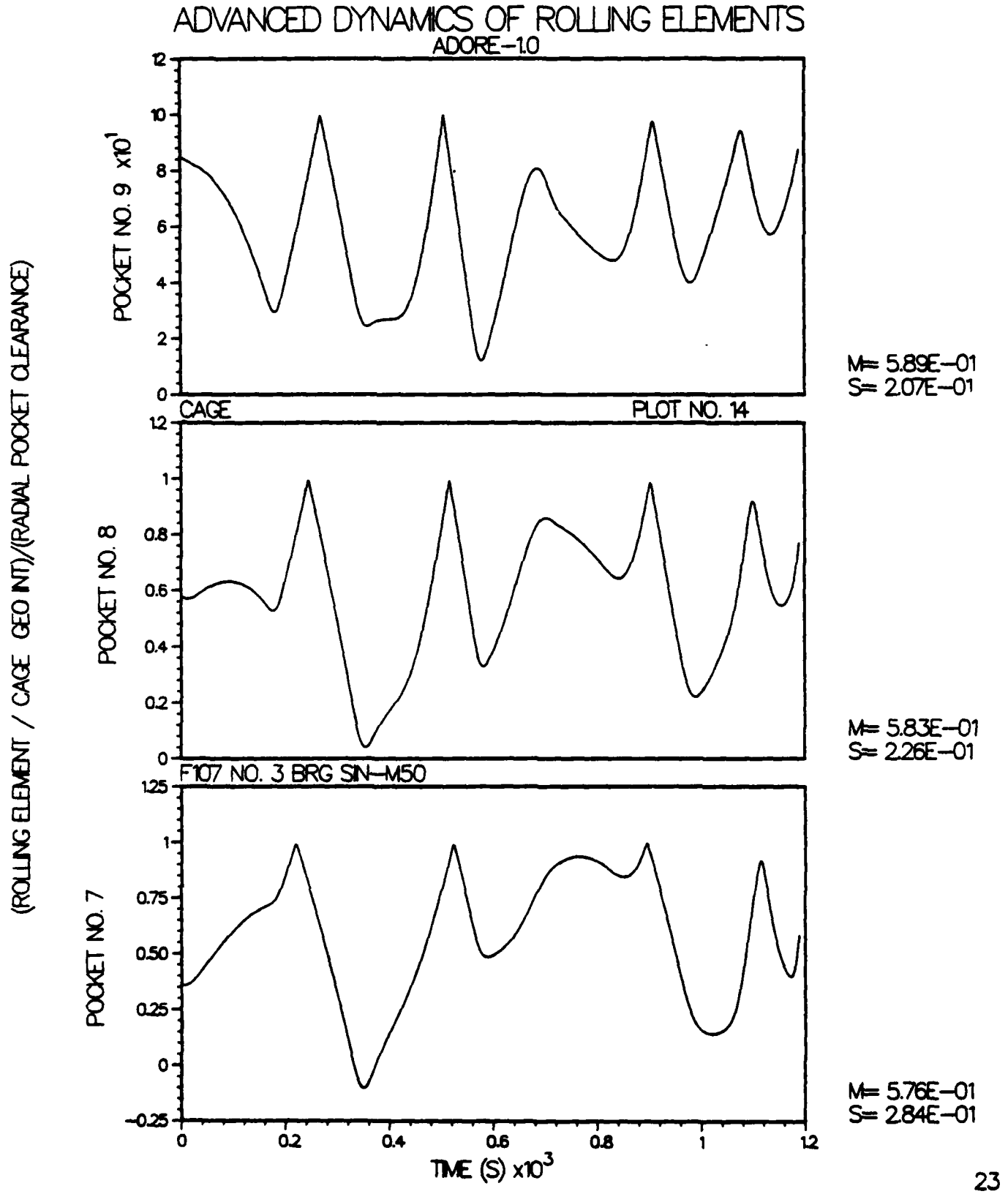
ADVANCED DYNAMICS OF ROLLING ELEMENTS
ADORE-1.0
POCKET NO. 9 x10^1
M= 5.89E-01
S= 2.07E-01
CAGE
PLOT NO. 14
POCKET NO. 8
M= 5.83E-01
S= 2.26E-01
F107 NO. 3 BRG SIN-M50
POCKET NO. 7
M= 5.76E-01
S= 2.84E-01
TIME (S) x10^3
(ROLLING ELEMENT / CAGE GEO INT)/(RADIAL POCKET CLEARANCE)

23

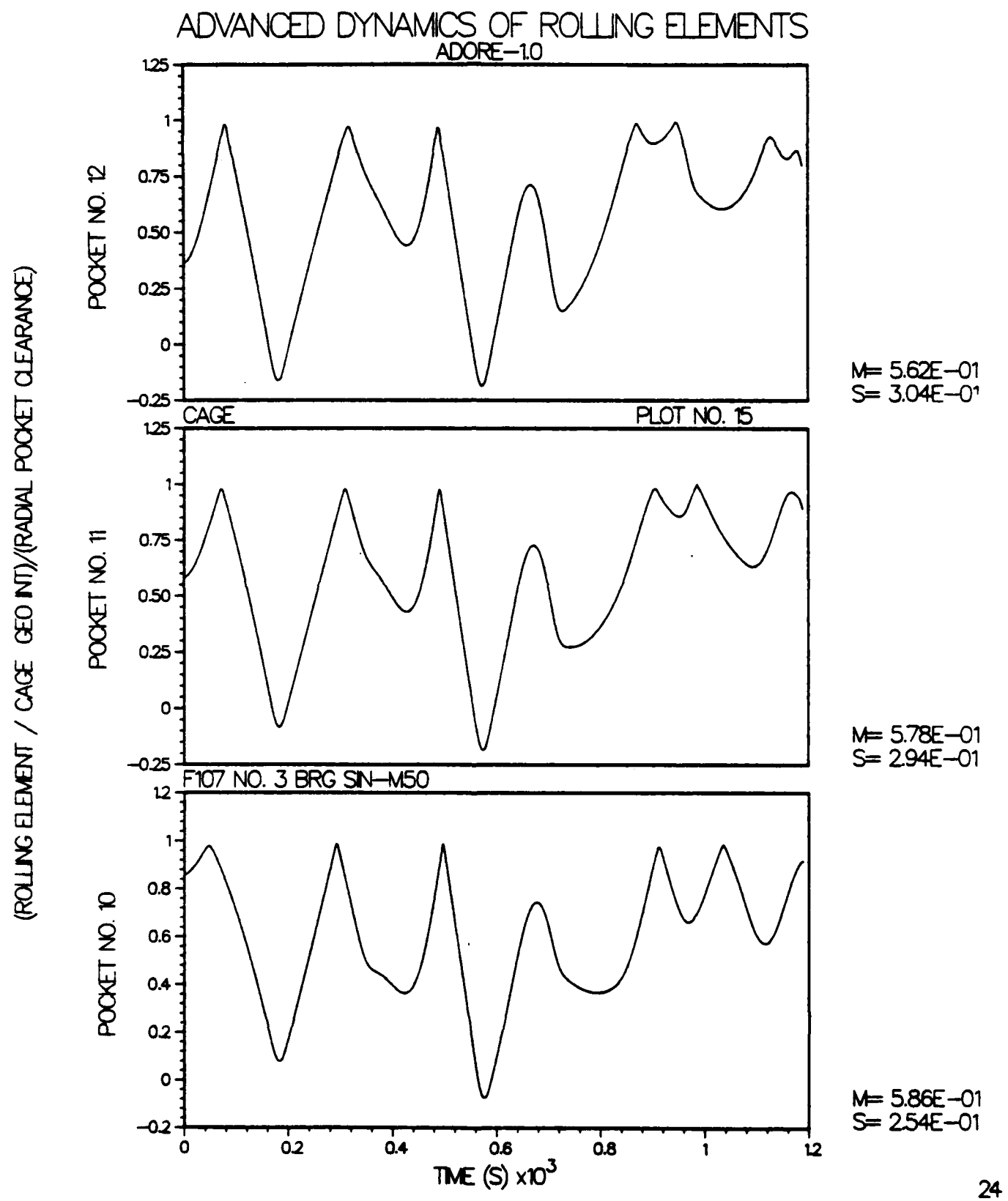
ADVANCED DYNAMICS OF ROLLING ELEMENTS
ADORE-1.0
(ROLLING ELEMENT / CAGE GEO INT)/(RADIAL POCKET CLEARANCE)
POCKET NO. 12
1.25
1
0.75
0.50
0.25
0
-0.25
M= 5.62E-01
S= 3.04E-01
CAGE
PLOT NO. 15
POCKET NO. 11
M= 5.78E-01
S= 2.94E-01
F107 NO. 3 BRG SIN-M50
POCKET NO. 10
1.2
0.8
0.6
0.4
0.2
-0.2
M= 5.86E-01
S= 2.54E-01
0
0.2
0.4
0.6
0.8
1
1.2
TIME (S) x10^3
24

APPENDIX B

NOMENCLATURE USED IN COMPUTER OUTPUT

Appendix B

NOMENCLATURE USED IN COMPUTER OUTPUT

Although most of the computer print and plot output is self explanatory, a few of the variables have been abbreviated as follows:

M	= Mean of the variable plotted on any given axis in the plot output.
S	= Standard Deviation of the variable plotted on any given axis in the plot output.
RE NO. 1	= Rolling Element Number 1.
COMP X	= Component along the X-axis (Bearing axis).
COMP Y	= Component along the transverse Y-axis.
COMP Z	= Component along the transverse Z-axis.
X ACC	= Axial acceleration.
Y ACC	= Acceleration along the transverse Y-axis.
Z ACC	= Acceleration along the transverse Z-axis.
R ACC	= Radial acceleration.
ORB ACC	= Orbital acceleration.
X POS	= Axial position.
Y POS	= Position along the transverse Y-axis.
Z POS	= Position along the transverse Z-axis.
R POS	= Radial position.
ORB POS	= Orbital position.
ORB VEL	= Orbital velocity.
ANGULAR VEL	= Angular Velocity.
AXIS INCL	= Orientation of the angular velocity vector.
THETA	= Inclination of the angular velocity

vector relative to the bearing axis.

PHI	= Angle between the plane containing the bearing axis and the angular velocity vector, and the X-Z plane.
SLIP VEL	= Slip velocity in the center of the ball/race contact.
HEAT GEN	= Heat generation.
NOR LOAD	= Normal contact load.
GEO INT	= Geometrical interaction or minimum clearance between interacting elements.
CONTACT ANG	= Contact angle. The ball/cage contact angle is such that when the contact angle is zero degree, the cage drives the ball, while the ball drives the cage when the contact angles is 180 degrees.
WHIRL RATIO	= Ratio of the cage mass center whirl velocity to the shaft angular velocity.
OMEGA RATIO	= Ratio of the cage angular velocity to the shaft angular velocity.
NOR FORCE	= Normal contact force.

U.S.Government Printing Office: 1985 — 559-065/20761


DAT
FILM